Synthesis, Pharmacological Evaluation, and Docking Studies of Novel Pyridazinone-Based Cannabinoid Receptor Type 2 Ligands

By: Giulio Ragusa, Serena Bencivenni, Paula Morales, Tyra Callaway, Dow P. Hurst, Battistina Asproni, Stefania Merighi, Giovanni Loriga, Gerard A. Pinna, Patricia H. Reggio, Stefania Gessi, and Gabriele Murineddu

This is the peer reviewed version of the following article:

Ragusa, G., Bencivenni, S., Morales, P., Callaway, T., Hurst, D.P., Asproni, B., Merighi, S., Loriga, G., Pinna, G.A., Reggio, P.H., Gessi, S., & Murineddu, G. (2018). Synthesis, Pharmacological Evaluation, and Docking Studies of Novel Pyridazinone-Based Cannabinoid Receptor Type 2 Ligands. *ChemMedChem, 13*(11), 1102-1114.

which has been published in final form at https://doi.org/10.1002/cmdc.201800152. This article may be used for non-commercial purposes in accordance with Wiley Terms and Conditions for Use of Self-Archived Versions.

*****© 2018 Wiley-VCH Verlag GmbH & Co. Reprinted with permission. No further reproduction is authorized without written permission from Wiley. *****

Abstract:

In recent years, cannabinoid type 2 receptors (CB_2R) have emerged as promising therapeutic targets in a wide variety of diseases. Selective ligands of CB_2R are devoid of the psychoactive effects typically observed for CB_1R ligands. Based on our recent studies on a class of pyridazinone 4-carboxamides, further structural modifications of the pyridazinone core were made to better investigate the structure–activity relationships for this promising scaffold with the aim to develop potent CB_2R ligands. In binding assays, two of the new synthesized compounds [6-(3,4-dichlorophenyl)-2-(4-fluorobenzyl)-*cis*-*N*-(4-methylcyclohexyl)-3-oxo-2,3-dihydropyridazine-4-carboxamide (**2**) and 6-(4-chloro-3-methylphenyl)-*cis*-*N*-(4-methylcyclohexyl)-3-oxo-2-pentyl-2,3-dihydropyridazine-4-carboxamide (**22**)] showed high CB_2R affinity, with K_i values of 2.1 and 1.6 nm, respectively. In addition, functional assays of these compounds and other new active related derivatives revealed their pharmacological profiles as CB_2R inverse agonists. Compound **22** displayed the highest CB_2R selectivity and potency, presenting a favorable in silico pharmacokinetic profile. Furthermore, a molecular modeling study revealed how **22** produces inverse agonism through blocking the movement of the toggle-switch residue, W6.48.

Keywords: ADMET calculations | cannabinoid receptors | CB2 inverse agonism | docking studies | synthesis

Article:

Introduction

The cannabinoid subtype 2 receptor (CB_2R) belongs to the rhodopsin-like G-protein-coupled receptor (GPCR) superfamily and constitutes, along with the cannabinoid subtype 1 receptor (CB_1R), the family of cannabinoid receptors (CBRs).[1, 2] CBRs are mainly activated by three types of ligands: endogenous cannabinoids, such as *N*-arachidonoylethanolamine and 2-arachidonoyl glycerol, phytocannabinoids, such as (−)-*trans*-Δ^9-tetrahydrocannabinol, and synthetic cannabinoids.[3] In recent years, significant progress have been made toward understand the role played by CBRs in many physiological and pathophysiological conditions.

CB_1Rs and CB_2Rs show certain common features and they share similar signaling mechanisms; nevertheless they differ in anatomic distribution. The former are expressed in several cell types and tissues, including muscle and liver cells, as well as spleen, pituitary gland, reproductive organs and adipose tissues.[4] Nevertheless, they are predominantly distributed throughout the central nervous system (CNS) in which they are implicated in the control of many neurobiological processes, including nociception, control of movement, emesis, emotional response, motivated behavior, cognitive function and homeostasis.[5, 6] CB_2Rs are mostly expressed in immune cells such as monocytes, macrophages, and natural killer cells, in which they play an important role in mediating the immune-modulatory function.[7, 8] However, it has been reported that CB_2Rs are also localized in other types of cells and tissues such as vascular endothelial cells, cardiomyocytes, bone cells, and tissues of the gastrointestinal tract.[4] Moreover, CB_2Rs have been found in activated microglia or astroglia, and might be also expressed by central neurons, especially under pathological conditions.[9, 10]

CBRs have been proposed as potential therapeutic targets for the treatment of several diseases[4, 11] and some nonselective CB_1R/CB_2R agonists are already approved drugs for use in use in the clinic (i.e., Sativex, Cesamet, Marinol). However, psychotropic side effects are the major limitation related to the therapeutic use of nonselective cannabinoid derivatives. It is well known that the undesirable effects of cannabinoids on the CNS are mediated by CB_1R,[12] and consequently the new goal for medicinal chemists has become the discovery of CB_2R-selective ligands. These ligands are devoid of the central side effects due to their limited distribution in the CNS, although there are a number of potential drawbacks for the immune system (e.g., immunosuppression). Furthermore, there is an increasing amount of evidence for the therapeutic potential of pharmacologically modulating the CB_2R. Preclinical evidence supports that CB_2R-selective ligands could be used for the treatment of various CNS-related neurodegenerative disorders including Alzheimer's, Huntington's and Parkinson's diseases, multiple sclerosis and amyotrophic lateral sclerosis.[10, 13-15] In addition to being a promising target for the treatment of pain and inflammation,[15-17] the CB_2R is also indicated for the treatment of irritable bowel syndrome, myocardial infarction, bone disorders, and different types of cancer.[4, 15, 18, 19] However, none of the CB_2 ligands tested in clinical trials have reached the market, probably due to their lack of efficacy.[20]

Recently, we synthesized a new series of pyridazinone-based derivatives[21] endowed with CB_2R affinity in the nanomolar range and good CB_2R selectivity. Among these novel compounds, the 6-(4-chloro-3-methylphenyl)-2-(4-fluorobenzyl)-*N*-(4-*cis*-methylcyclo-hexyl)-3-oxo-2,3-dihydropyridazine-4-carboxamide (**1**, Figure **1**) showed high CB_2R affinity (K_iCB_2R=2.0±0.8 nm) and notable selectivity (K_iCB_1R/K_iCB_2R >2000). To further explore structure–activity relationships in this new class of CB_2R ligands, we modulated the design of compound **1**,

designated as a lead compound, to obtain derivatives **2**–**24** (Figure **1**). Accordingly, we planned structural modifications at three positions (Ar, R_1 and R_2) of the dihydropyridazinone core, to evaluate the effect of their lipophilicity and steric hindrance on CBR affinity of this series of pyridazinone-based derivatives. In this study, we report the synthesis, the preliminary pharmacological data and docking studies on the new pyridazinones **2**–**24** reported in Table **1**.

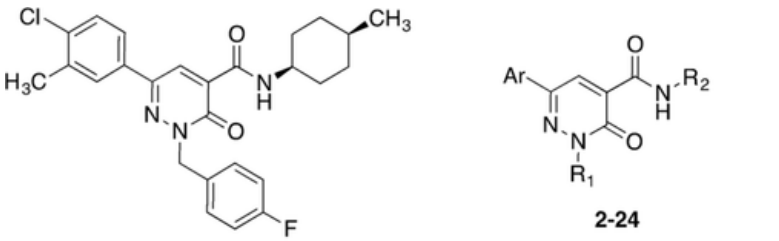

1

K_iCB_2 = 2.0 ± 0.81 nM
K_iCB_1 > 4000 nM
selectivity K_iCB_1/K_iCB_2 > 2000

Figure 1. Structures of pyridazinone compounds **2**–**24**.

Table 1. Structures and binding data for compounds **2**–**24**.

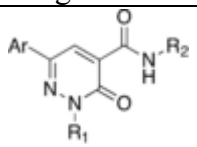

				K_i [nm][a]		Selectivity[b]
Compound	**Ar**	**R_1**	**R_2**	**CB_1R**	**CB_2R**	
2	3,4-dichlorophenyl	4-fluorobenzyl	*4-cis*-methylcyclohexyl	213±18	2.1±0.2	101
3	3,4-dichlorophenyl	4-fluorobenzyl	*4-trans*-methylcyclohexyl	85±7	90±7	0.94
4	3,4-dichlorophenyl	4-fluorobenzyl	cyclohexyl	350±31	6.3±0.5	55
5	3,4-dichlorophenyl	4-fluorobenzyl	cycloheptyl	226±25	7.2±0.9	31
6	3,4-dichlorophenyl	4-fluorobenzyl	adamantyl	1200±123	21±2	57
7	3,4-dichlorophenyl	cyclohexylmethyl	4-*cis*-methylcyclohexyl	3300±315	4.2±0.3	786
8	3,4-dichlorophenyl	cyclohexylmethyl	4-*trans*-methylcyclohexyl	>10 000	10±1	>1000
9	3,4-dichlorophenyl	cyclohexylmethyl	cyclohexyl	6000±578	11±1	545
10	3,4-dichlorophenyl	cyclohexylmethyl	cycloheptyl	>10 000	10±1	>1000
11	3,4-dichlorophenyl	cyclohexylmethyl	adamantyl	93±9	25±3	4
12	3,4-dichlorophenyl	chloropentyl	4-*cis*-methylcyclohexyl	>10 000	9.0±0.8	>1111
13	3,4-dichlorophenyl	chloropentyl	4-*trans*-methylcyclohexyl	4000±395	16±2	250
14	3,4-dichlorophenyl	chloropentyl	cyclohexyl	5300±542	85±8	62
15	3,4-dichlorophenyl	chloropentyl	cycloheptyl	147±16	55±6	3
16	3,4-dichlorophenyl	chloropentyl	adamantyl	>10 000	16±2	>625
17	5-bromothiophene	4-fluorobenzyl	4-*cis*-methylcyclohexyl	1600±146	5.5±0.7	291
18	5-bromothiophene	4-fluorobenzyl	4-*trans*-methylcyclohexyl	200±23	10.5±0.9	19
19	5-bromothiophene	4-fluorobenzyl	cyclohexyl	5600±559	8.4±0.9	667
20	5-bromothiophene	4-fluorobenzyl	cycloheptyl	800±78	110±13	7
21	5-bromothiophene	4-fluorobenzyl	adamantyl	6125±583	3.1±0.3	1976
22	4-chloro-3-methylphenyl	pentyl	4-*cis*-methylcyclohexyl	>10 000	1.6±0.2	>6250
23	4-chloro-3-methylphenyl	pentyl	cyclohexyl	2500±271	7.5±0.9	333
24	4-chloro-3-methylphenyl	pentyl	cycloheptyl	666±68	6.1±0.8	109

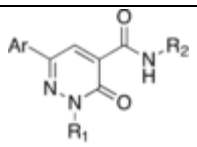

				K_i [nm][a]		Selectivity[b]
Compound	**Ar**	**R_1**	**R_2**	**CB_1R**	**CB_2R**	
WIN 55,212-2	–	–	–	13±2	2.5±0.3	5.2

[a] K_i values for CB_2Rs and CB_1Rs were determined by competitive displacement of the radioligand [^{3}H]CP 55,940. The K_i was calculated from the IC_{50} values determined from the binding curves, using the Cheng–Prusoff equation.[22] Values are the mean±SEM of at least three independent experiments performed in triplicate. [b] (K_i CB_1R)/(K_i CB_2R).

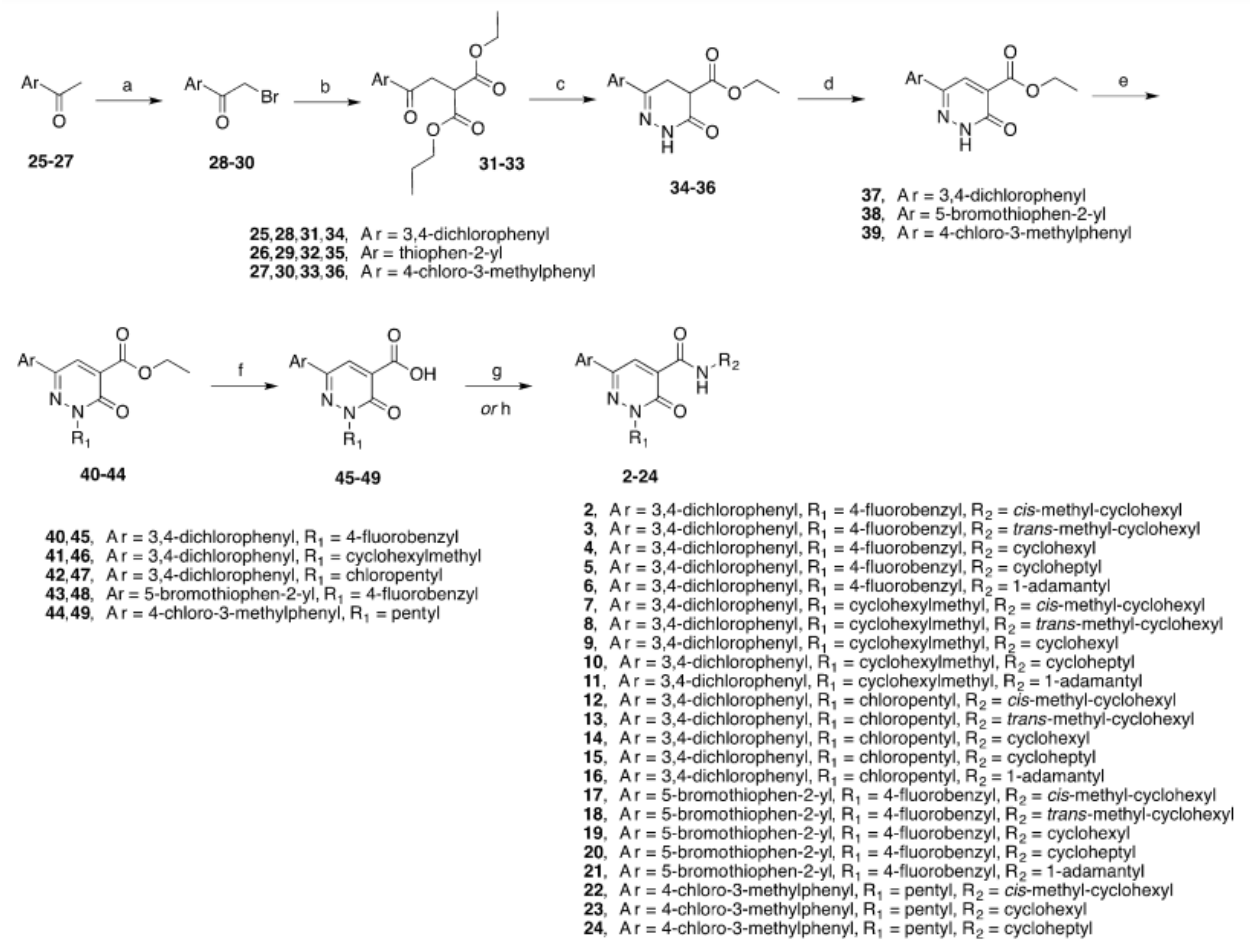

Scheme 1. Reagents and conditions: a) Br_2, AcOH (for **25** and **27**) or CH_2Cl_2 (for **26**), RT, 8 h; b) diethyl malonate, NaH, THF, 0 °C–RT, 20–24 h; c) $NH_2NH_2{\cdot}H_2O$, EtOH, reflux, 24 h; d) Br_2, AcOH, RT, 6 h; e) K_2CO_3, DMF, R_1X, ultrasonic irradiation, RT, 2 h; f) 2 m NaOH, EtOH, reflux, 8 h; g) HOBt, EDC, R_2NH_2, CH_2Cl_2, 0 °C–RT, 12–24 h (for **2**–**16**, **22**–**24**); h) $SOCl_2$, toluene, reflux, 3 h, then Et_3N, R_2NH_2, CH_2Cl_2, 0 °C–RT, 12 h (for **17**–**21**).

EDC–HOBt mediated coupling reaction between acids **45**–**47**, **49** and the appropriate amines afforded the desired carboxamide derivatives **2**–**16** and **22**–**24**. Due to lower reaction yields for the coupling of acid **48** in these conditions, it was previously activated with thionyl chloride, then, treated with the appropriate amines to furnish the desired derivatives **17**–**21**.

Results and Discussion

Chemistry

Target 3-oxo-6-aryl-2,3-dihydropyridazines **2**–**24** were synthesized as outlined in Scheme **1**. α-Halogenation of commercial ketones **25**–**27** with bromine gave acyl halides **28**–**30**. Nucleophilic substitution on the acyl halides with the enolate of diethyl malonate in anhydrous THF furnished diesters **31**–**33**, which were converted into cyclic derivatives **34**–**36** by reaction with hydrazine hydrate in ethanol at reflux. Bromine-assisted oxidation of dihydropyridazinones **34** and **36** in acetic acid provided pyridazinones **37** and **39**. Ring oxidation and bromination of the thiophene moiety at the C5 position of **35** was accomplished by reaction with bromine in acetic acid to afford pyridazinone **38**. N-Alkylation of **37**–**39** in anhydrous DMF with the appropriate alkyl halide or benzyl halide in the presence of K_2CO_3, under ultrasound irradiation, afforded compounds **40**–**44**, which were hydrolyzed with NaOH in ethanol to the corresponding carboxylic acids **45**–**49** in almost quantitative yield.

Biological evaluation

The CB_1R and CB_2R binding affinities of the novel 3-oxo-2,3-dihydropyridazine-4-carboxamides **2**–**24** were evaluated by radioligand binding assays performed by using transfected human CB_1R (*h*CB_1R) and CB_2R (*h*CB_2R) Chinese hamster ovary (CHO) cells. [^{3}H]CP 55,940 was used as the radiolabeled ligand. The experimental data (IC_{50} values) were converted into K_i values.[22] The receptor affinities are shown in Table **1**. For comparison, the K_i value of the mixed CB_1R/CB_2R ligand WIN 55,212-2 is reported.

The substitution of 3-CH_3 group on the benzene ring of the lead compound **1** with a second chlorine atom gave derivative **2**, which retained good CB_2R affinity (K_i=2.1±0.2 nm) with moderate selectivity ($K_i$$CB_1R$/$K_i$$CB_2R$=101), whereas its *trans* isomer **3** showed similar affinity for CB_2R and CB_1R (K_i=90±7 and 85±7 nm, respectively). The elimination of the methyl group from the cyclohexyl ring (compound **4**) and homologation of the aliphatic ring to cycloheptyl (**5**) restored CB_2R affinity (K_i=6.3±0.5 and K_i=7.2±0.9 nm, respectively) and moderate selectivity ($K_i$$CB_1R$/$K_i$$CB_2R$=55 and 31, respectively). Finally, the introduction of a bulky group in the carboxylic portion, such as 1-adamantylamine, gave compound **6** which showed a 10-fold decrease in CB_2R affinity (K_i=21±2 nm) with respect to derivative **2**.

The same trend was observed in the small series of derivatives bearing a methylenecyclohexyl chain on the N2 atom of the pyridazinone ring, derivatives **7**–**11**. All compounds showed a good CB_2R affinity (K_i=4.2–25 nm), resulting the *N*-(4-*cis*-methylcyclohexyl)-carboxamide **7** having the best CB_2R binding profile within this series (K_i=4.2±0.3 nm), similar to that of lead compound **1** and analogue **2**.

Next, we wanted to evaluate the effect of inserting a chloropentyl substituent at the N2 position of pyridazinone, thus we synthesized compounds **12**–**16**. Derivatives of this series maintained good CB_2R affinity (K_i, 9–85 nm), and carboxamide **12** showed high CB_2R selectivity

(K_iCB$_1$R/K_iCB$_2$R>1111) even though its K_iCB$_2$R affinity was 4.5-fold less than lead compound **1**.

Therefore, the double chlorine atom substitution on the aromatic ring at C6, and either keeping the N^2-4-fluorobenzyl group (compound **2**) or introducing an N^2-methylcyclohexyl group (**7**) gave derivatives with similar K_iCB$_2$R values to the lead compound **1**, whereas substitution with cyclopentyl at N2 gave **9** with a lower K_iCB$_2$R affinity.

Having evaluated the effects of the substituent in the N2 position of the pyridazinone, we wanted to investigate replacement of the disubstituted phenyl group at C6 of the pyridazinone ring with a thiophene, thus we synthesized compounds **17**–**21**. Within this series, both the derivative **17**, bioisostere of the lead **1**, and the *N*-(adamantan-1-yl)-carboxamide **21** showed interesting CB$_2$R affinities (K_i=5.5 and 3.1 nm, respectively), and the latter compound was endowed with good selectivity (K_iCB$_1$R/K_iCB$_2$R >1976).

Finally, we synthesized derivatives **22**–**24**, three analogues of lead compound **1** bearing a pentyl chain at the N2 position, to confirm that the *N*-4-*cis*-methylcyclohexyl group was the preferred substituent in the carboxamide moiety, as indicated from data obtained for compound **22** (K_iCB$_2$R=1.6±0.17 nm), which displayed the highest CB$_2$R selectivity (K_iCB$_1$R/K_iCB$_2$R>6250).

CB$_1$R/CB$_2$R-stimulated cAMP binding

Selected compounds characterized by high affinity and selectivity toward the CB$_2$R were studied in functional assays to assess their behavior as agonists, antagonists or inverse agonists at the CB$_2$R. Therefore, their modulation of forskolin-stimulated cAMP levels in human CB$_2$R-expressing CHO cells was investigated and compared with the reference agonist compound WIN 55,212-2. This ligand (0.1 μm) decreased forskolin-stimulated cAMP levels by 78 %, and compounds **2**, **7**, and **22** antagonized this effect in the concentration range 0.01–1 μm, with the **22** and **2** being the most potent molecules according to binding data. However, compounds **12**, **13**, **17** and **21**, despite having high affinities for the CB$_2$R, did not display an antagonistic effect on adenylyl cyclase activity inhibition induced by WIN 55,212-2 (Figure **2**).

In addition, all the ligands tested in the functional assay were also evaluated for their ability to increase forskolin-stimulated cAMP production in the concentration range 1–100 nm. As shown in Figure **3**, the molecules under examination induced an increase in forskolin-stimulated cAMP levels, suggesting their role as inverse agonists at the CB$_2$R.

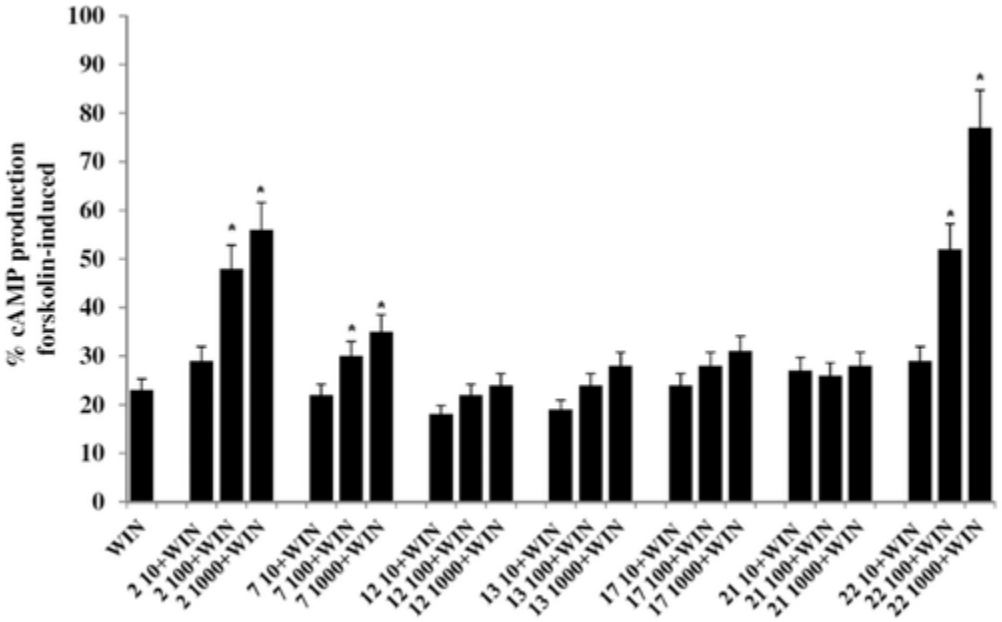

Figure 2. Inhibition of forskolin-stimulated cAMP levels by WIN 55,212-2 (100 nm) and antagonism by **22**, **7**, **2**, **21**, **17**, **12**, and **13** (10–1000 nm) in *h*CB_2R-CHO cells. The effect of forskolin (5 μm) was set to 100 %. Values are the mean±SEM of four independent experiments (*N*=4). **P*<0.05, compared with WIN 55,212-2; analysis was by ANOVA followed by Dunnett's test.

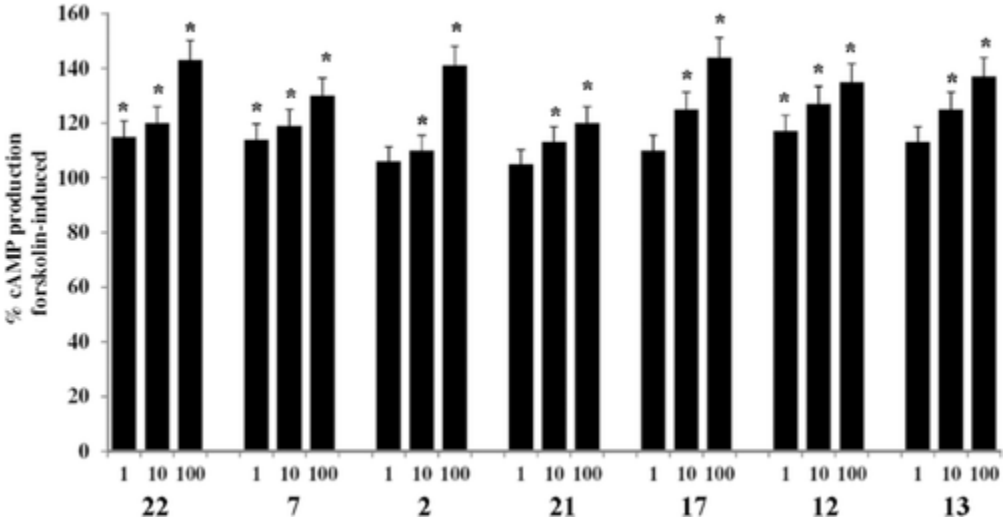

Figure 3. Effect of **22**, **7**, **2**, **21**, **17**, **12**, and **13** (1–100 nm) expressed as % of increase of forskolin-stimulated cAMP accumulation in *h*CB_2R-CHO cells. The effect of forskolin (5 μm) was set to 100 %. Values are the mean±SEM of four independent experiments (*N*=4). **P*<0.05, compared with Forskolin (5 μm); analysis was by ANOVA followed by Dunnett's test.

Molecular modeling

A previous study identified the binding site for the CB_2R antagonist SR144528, using our CB_2R inactive-state (R) homology model.[23] This study suggested that the SR144528 amide functional group is important for interacting with CB_2R. In addition, aromatic stacking interactions in the

transmembrane helix (TMH) 5–6 aromatic cluster were revealed to be crucial to the SR144528–CB_2R complex. Further exploration of the 1,8-naphthyridin-2(1*H*)-one-3-carboxamide scaffold in the CB_2R R model, showed that antagonists from this series bind in the TMH2–3–6–7 region with the C6 naphthyridine substituent directly blocking the W6.48(258) toggle switch.[24]

In the current study, Glide docking studies revealed that the novel pyridazinones reported here bind in a similar orientation as the 1,8-naphthyridin-2(1*H*)-one-3-carboxamides. The most potent and selective CB_2R inverse agonist, **22**, was docked in a previously published CB_2R R-state model.[23-26] This homology model was pre-equilibrated in a stearoyl-docosahexaenoylphosphatidylcholine (SDPC) bilayer for 300 ns to allow it to adjust in a lipidic environment[23] (see the Experimental Section). A complete conformational analysis of **22** was performed to identify the global minimum energy conformer as well as other minimum energy conformations that **22** can adopt. This global minimum energy conformer has an intramolecular hydrogen bond between the pyridazin-3(2*H*)-one carbonyl oxygen and the amide hydrogen atom. This global minimum energy conformer was used in the docking studies. As shown in Figure **4** A, pyridazinone **22** occupies the CB_2R TMH2–3–6–7 region.

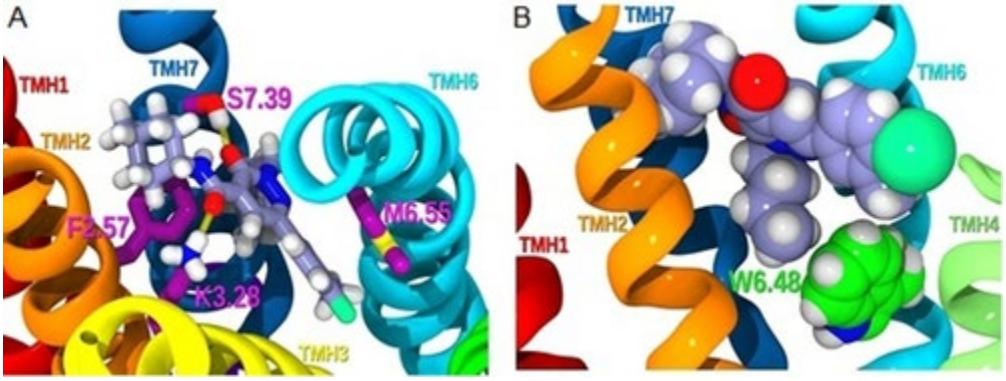

Figure 4. A) An extracellular view of **22** (lavender) docked in the TMH2–3–6–7 region of CB_2R. Carbon atoms of residues with which **22** has direct interactions are shown in purple. B) A side view of **22** (lavender, atoms contoured at their van der Waals radii) docked at CB_2R. It is clear that **22** is adjacent to the toggle-switch residue, W6.48 (green), and blocks the W6.48 χ1 g+→*trans* associated with activation.

The energy-minimized **22**–CB_2R complex (Figure **4** A) displays four main binding site interactions. The carbonyl oxygen atom of the pyridazinone core is engaged in a hydrogen bond with S7.39(285) [hydrogen bond (O−O) distance=2.90 Å and (O−H−O) angle=166°], and the carbonyl oxygen of the 4-*cis*-methylcyclohexyl amide substituent establishes a hydrogen bond with K3.28(109) [hydrogen bond (O−O) distance=2.90 Å and (O−H−O) angle=150°]. In addition, the central pyridazin-3(2*H*)-one ring forms a tilted-T aromatic stack with F2.57(87) (ring centroid to ring centroid distance=5.60 Å, and the angle between the ring planes=63°). Moreover, M6.55(265) establishes a Met–aromatic interaction with the 4-chloro-3-methylphenyl moiety [distances to the central ring centroid from M6.55 side-chain atoms: carbon preceding sulfur atom, CG (3.92 Å); sulfur atom, SD (3.60 Å); and terminal methyl carbon, CE (3.89 Å), see Figure **4** A] The ligand–receptor interaction energies for residues within 5 Å of **22** were also assessed. The ligand conformational cost for **22** was 0.89 kcal mol^{-1}, bringing the total interaction energy to −65.70 kcal mol^{-1} (see Table S1). The Glide score for this dock was −9.50.

The conformational change of W6.48 (χ1 g+→*trans*) is associated with receptor activation in class A GPCRs such as CB_2R. This change can modulate the Pro kink in TMH6 (P6.50), causing an opening at the IC end of the receptor to form for G-protein interaction.[24] W6.48 is therefore considered to be part of the "toggle switch" for activation. As illustrated in Figure **4** B, the 4-chloro-3-methylphenyl pyridazinone substituent of **22** points toward TMH5 and extends deep enough in the binding pocket to block the movement of W6.48(258) and therefore keep its χ1 at g+. This is consistent with **22** acting as an inverse agonist at the CB_2R. Therefore, this docking study provides a rational structural explanation for the ability of ligands such as **22** to prevent G-protein-dependent CB_2R activation.

In silico ADMET parameters

In silico prediction of properties related to absorption, distribution, metabolism, excretion and toxicity (ADMET) can help to efficiently prioritize the most promising molecules to be further developed from the early stages of the drug discovery process. The high predictive potential and the decreased time and cost associated with these in silico approaches have increased its use in the search for novel drug candidates.[27-29]

The pharmacokinetic properties of the newly synthesized pyridazinones and of well-known CB_2R ligands such as SR144528 and HU308 were calculated in silico using QikProp in Maestro (Schrödinger package). This program calculates a set of 34 physicochemical descriptors based on the global minimum energy conformer of each molecule.

According to our drug-likeness prediction studies, the pyridazinones described herein follow the Lipinski and Jorgensen pharmacokinetics rules (Table **2**).[30, 31] As shown in Table **2**, the prediction of blood–brain barrier permeability, human oral absorption, bioavailability, human intestinal permeability or binding to human serum albumin suggest that pyridazinones **2**–**24** have a suitable drug profile. The compounds presented here have solubility values that fall outside the range predicted by QikProp for 95 % of known oral drugs. Solubility issues are widely known in cannabinoid pharmacology because of their lipophilic nature.[32, 33] Within all the structural subsets of pyridazinones, the derivatives bearing an adamantyl group at the R_1 position (**6**, **11**, **16**, **21**) display higher in silico lipophilicity values. 6-(4-Chloro-3-methylphenyl)-3-oxo-2-pentyl-2,3-dihydropyridazine-4-carboxamides (**22**–**24**) display the best solubility among this series of compounds, being better than the widely used CB_2R reference ligands SR144528 and HU308.

Table 2. Physicochemical descriptors of compounds **2**–**24**, SR144528 and HU308 calculated by QikProp integrated in Maestro.

Compound	QPlogP[a]	QlogBB[b]	QPPMDCK[c]	QPlogKhsa[d]	QPPCaco[e]	Absorption [%][f]
2	7.52	−0.01	10 000	1.64	2524	100
3	7.56	−0.07	10 000	1.69	2248	100
4	7.21	−0.10	10 000	1.53	2111	100
5	7.45	−0.04	10 000	1.62	2328	100
6	7.96	−0.13	9996	1.87	2053	100
7	7.50	−0.22	5819	1.81	2149	100
8	7.49	−0.22	5819	1.80	2165	100
9	7.12	−0.04	8058	1.60	2905	100

Compound	QPlogP[a]	QlogBB[b]	QPPMDCK[c]	QPlogKhsa[d]	QPPCaco[e]	Absorption [%][f]
10	7.33	−0.03	7953	1.69	2869	100
11	7.86	−0.14	6590	1.96	2412	100
12	7.15	−0.11	10 000	1.50	1966	100
13	7.26	−0.24	10 000	1.52	1840	100
14	7.40	−0.23	10 000	1.57	1964	100
15	7.70	−0.21	10 000	1.69	2054	100
16	8.12	−0.13	10 000	1.87	2445	100
17	7.09	0.05	10 000	1.52	2629	100
18	7.12	0.11	10 000	1.52	2893	100
19	6.76	0.10	10 000	1.36	2802	100
20	7.02	0.01	9935	1.50	2375	100
21	7.54	0.05	10 000	1.72	2631	100
22	6.69	−0.37	2874	1.30	2494	100
23	6.65	−0.56	2219	1.48	1963	100
24	6.88	−0.52	2357	1.57	2076	100
HU308	7.01	−0.52	2057	1.62	3738	100
SR144528	7.61	0.11	5587	1.91	4606	100

[a] Predicted octanol–water partition coefficient (−2.0–6.5). [b] Predicted log of the brain–blood partition coefficient (−3.0–1.2). [c] Predicted apparent Madin–Darby canine kidney (MDCK) cell permeability [nm s^{-1}, <25 poor, >500 good]. [d] Prediction of binding to human serum albumin (−1.5–1.5). [e] Apparent Caco-2 cell permeability [nm s^{-1}, intestinal drug permeability, <25 poor, >500 excellent]. QikProp predictions are for nonactive transport. [f] Human oral absorption in the GI [<25 % is poor]; [range of 95 % of drugs].

To further explore in silico metabolism and toxicity for these novel compounds, we calculated the parameters summarized in Tables S2 and S3 by using the admetSAR server.[34] Over 70 % of human drug metabolism occurs via cytochrome P450 oxidases (CYP450).[35] The most abundant CYP450 isoenzymes in human liver and intestine are CYP3A4, CYP2C9 and CYP2D6.[36] The pharmacokinetic behavior of drugs can be determined by their interactions with these enzymes, because their inhibition can affect drug clearance, consequently enhancing toxicity. Therefore, it is important to predict whether a new compound is a substrate, an inhibitor or an inducer of these CYP isoforms in early drug discovery phases. As shown in Table S2, compounds **22**–**24** present the best metabolic profiles in that they are substrates but not inhibitors of the most abundant isoform CYP3A4. These compounds will not hamper the biotransformation of drugs metabolized by this cytochrome P450 enzyme, whereas certain inhibitors could trigger adverse side effects. This difference in the metabolism among pyridazinones might be due to the presence of halogens in the molecule (derivatives **22**–**24** have only one halogen, whereas the other derivatives have at least two halogens per structure).[37, 38]

In terms of toxicity, as shown in Table S3, the safety profile of all ligands reported here are favorable, because they present low cardiotoxicity and are nonmutagenic and noncarcinogenic. Low oral toxicity values were found also for the reference compounds SR144528 and HU308. In addition, the predicted median lethal dose (LD_{50} in rat model) for these compounds is in the range of most FDA-approved small-molecule drugs.[39, 40] Therefore, taking the pharmacological and ADMET prediction data into consideration, the highly selective CB_2R inverse agonist **22** might serve as a lead structure for further optimizing this novel class of CB_2R ligands in terms of potency and pharmacokinetic properties.

Conclusions

The modulation of the 6-aryl-3-oxo-2,3-dihydropyridazine-4-carboxamide scaffold in three different positions, the N2 chain, C4 carboxamide moiety and C6-aryl ring, led us to determine the key features of this novel class of CB_2R ligands. In general, the *N*-4-*cis*-methylcyclohexyl group was the preferred substituent in the C4 carboxamide moiety; the derivatives bearing this group had high CB_2R affinity (K_iCB_2R ranging from 1.6 to 9.0 nm) and selectivity (K_iCB_1R/K_iCB_2R from 101 to >6250). Concerning the N2 position, all inserted chains showed a good CB_2R binding profile, especially the 5-chloropentyl and 4-fluorobenzyl groups; however, the presence of a 3,4-disubstituted aromatic system in the C6 position provides a better binding profile for CB_2Rs.

Docking studies on compound **22** provides a rational structural explanation for the ability of these novel derivatives to act as inverse agonists at CB_2R, preventing G-protein-dependent CB_2R activation.

The in silico prediction of the pharmacokinetic properties suggest that novel pyridazinones have a suitable drug-like profile. Compound **22**, and its congeners, display the best solubility values from this series, and have improved solubility over the reference compounds SR144528 and HU308. Finally, calculations to predict toxicity and metabolism showed compound **22** acts as a substrate, but not an inhibitor, for the most abundant CYP450 isoenzymes, and presents the best metabolic profile in this novel class of pyridazinones.

In summary, compound **22**, a very potent and selective CB_2R inverse agonist has been identified with favorable properties that indicate this compound could be a lead for drug development.

Experimental Section

Chemistry

All reactions involving air- or moisture-sensitive compounds were performed under a nitrogen atmosphere. Solvents and reagents were obtained from commercial suppliers and were used without further purification. The starting ketones **25**–**27** and amines for the synthesis of final compounds were purchased from Sigma–Aldrich. Ultrasonic irradiation experiments were carried out in a Bandelin Sonorex RK-100 H ultrasonic bath. Flash column chromatography was performed either on an automated FlashMaster system (Biotage) with pre-packed Biotage SNAP silica gel cartridges or manually on silica gel (Kieselgel 60, 0.040–0.063 mm, Merck). Thin layer chromatography (TLC) was performed with Polygram SIL N-HR/HV_{254} pre-coated plastic sheets (0.2 mm) or aluminum sheets (Kieselgel 60 F_{254}, Merck). Melting points were obtained on a Köfler melting point apparatus and are uncorrected. IR spectra were recorded on nujol mulls on NaCl plates with a Jasco FTIR 460 Plus spectrophotometer and are expressed in ν [cm^{-1}]. NMR experiments were performed on a Bruker Avance III Nanoboy 400 system (400.13 MHz for ^1H, 100.62 MHz for ^{13}C). Spectra were acquired using deuterated chloroform ($CDCl_3$) or deuterated dimethylsulfoxide ([D_6]DMSO) as solvents. Chemical shifts (δ) for ^1H and ^{13}C NMR spectra are reported in parts per million (ppm) using the residual nondeuterated solvent resonance as the internal standard ($CDCl_3$: 7.26 and 77.16 ppm, respectively; [D_6]DMSO: 2.50 and 39.52 ppm,

respectively). Data are reported as follows: chemical shift (listed in descending order), multiplicity (s, singlet; br s, broad singlet; d, doublet; dd, double doublet; t, triplet; q, quadruplet; m, multiplet), coupling constants (*J*) in Hertz (Hz), and integral. LC–MS analyses in positive-ion mode were performed on an Agilent 1100 LC–MSD system consisting of a single quadrupole detector mass spectrometer equipped with an electrospray ionization (ESI) interface and a photodiode array detector, the range of which was 120–550 nm. LC analysis was performed at room temperature with MeCN/H_2O (8:2) as the mobile phase at a flow rate of 0.9 mL min^{-1}. All final compounds were of ≥95 % purity as determined by elemental analysis on a PerkinElmer 240-B analyzer for C, H, and N.

Synthesis of acyl bromides 28–30

General method A: Bromine (3.02 mL, 59.3 mmol, 1 equiv) was dropwise added to a stirred solution of the ketone (59.3 mmol, 1 equiv) in glacial AcOH (65 mL), and the resulting solution was stirred at room temperature for 8 h. Then, ice-water was poured into reaction flask and the resulting precipitate was filtered, washed with H_2O, and air-dried. The resulting crude product was purified by column flash chromatography using appropriate eluents.

General method B: A solution of bromine (4.0 mL, 79.2 mmol, 1 equiv) in CH_2Cl_2 (40 mL) was dropwise added to a stirred solution of the ketone (79.2 mmol, 1 equiv) in CH_2Cl_2 (48 mL). The resulting mixture was stirred at room temperature for 1 h, then neutralized with saturated $NaHCO_3$ aqueous solution. The organic layer was separated in a separating funnel and washed with brine. The organic solution was dried (Na_2SO_4) and the solvent removed under reduced pressure. The resulting residue was purified by column flash chromatography using appropriate eluents.

Bromo-1-(3,4-dichlorophenyl)ethan-1-one (28): Reaction of ketone **25** according to method A afforded a yellow solid, which was purified by flash chromatography (petroleum ether/EtOAc 95:5) to give **28** as a white solid (14.9 g, 94 %). R_f=0.45 (petroleum ether/EtOAc 95:5); m.p.: 44–45 °C; ^{1}H NMR (400 MHz, $CDCl_3$): δ=8.07 (s, 1 H), 7.81 (d, *J*=8.3 Hz, 1 H), 7.58 (d, *J*=8.3 Hz, 1 H), 4.38 ppm (s, 2 H).

Bromo-1-(thiophen-2-yl)ethan-1-one (29): Reaction of ketone **26** according to method B afforded a dark oil, which was purified by flash chromatography (petroleum ether/EtOAc 95:5) to give **29** as a yellow oil (14.9 g, 92 %). R_f=0.33 (petroleum ether/EtOAc 95:5); ^{1}H NMR (400 MHz, $CDCl_3$): δ=7.81 (t, *J*=2.9 Hz, 1 H), 7.72 (d, *J*=4.5 Hz, 1 H), 7.17 (d, *J*=2.4 Hz, 1 H), 4.36 ppm (s, 2 H).

See the Supporting Information for compound **30**.

General procedure for the preparation of ketodiester derivatives 31–33

A solution of diethyl malonate (1.83 mL, 12 mmol, 1.2 equiv) in anhydrous THF (6.5 mL) was added to a suspension of NaH (60 % dispersion in mineral oil, 0.480 g, 20 mmol, 2 equiv) in anhydrous THF (26 mL) under N_2 flow at 0 °C, and the mixture was stirred for 1 h. Then, a solution of bromoketone (10 mmol, 1 equiv) in anhydrous THF (4 mL) was added dropwise and

the resulting mixture was stirred at room temperature until complete conversion of the starting materials (monitored by TLC). The reaction was quenched with saturated NH_4Cl aqueous solution, and the aqueous layer extracted with EtOAc. The combined organic layers were washed with H_2O and brine, then dried over Na_2SO_4. The solvent was removed under reduced pressure and the resulting residue was purified by column flash chromatography with appropriate eluents.

Diethyl 2-[2-(3,4-dichlorophenyl)-2-oxoethyl]malonate (31): A mixture of diethyl malonate, NaH and **28** was stirred at room temperature for 20 h. The crude product of the reaction was purified by flash chromatography (petroleum ether/EtOAc 9:1) to afford **31** as a yellow oil (2.7 g, 77 %). R_f=0.30 (petroleum ether/EtOAc 9:1); ^{1}H NMR (400 MHz, $CDCl_3$): δ=8.05 (s, 1 H), 7.79 (d, J=8.4 Hz, 1 H), 7.55 (d, J=8.4 Hz, 1 H), 4.11 (q, J=7.1 Hz, 4 H), 4.03 (t, J=6.9 Hz, 1 H), 3.55 (d, J=7.0 Hz, 2 H), 1.28 ppm (t, J=7.1 Hz, 6 H).

See the Supporting Information for compounds **32** and **33**.

General procedure for the preparation of dihydropyridazinone derivatives 34–36

Hydrazine monohydrate (64–65 %, 0.79 mL, 16.5 mmol, 1.1 equiv) was added dropwise to an ice-bath-cooled solution of malonate derivatives **31**–**33** (15 mmol, 1 equiv) in absolute ethanol (75 mL). The resulting solution was warmed to room temperature, then heated at reflux for 24 h. The solution was allowed to stand at room temperature and the resulting precipitate was isolated by vacuum filtration, washed with cold water, and dried in air. The obtained solid was purified by column flash chromatography using appropriate eluents.

Ethyl 5-(3,4-dichlorophenyl)-2-oxo-1,2,3,4-tetrahydropyridine-3-carboxylate (34): From reaction of **31** was obtained a solid, which was purified by flash chromatography (petroleum ether/EtOAc 6:4) to give **34** as a pale yellow solid (2.79 g, 59 %). R_f=0.51 (petroleum ether/EtOAc 6:4); m.p.: 166–168 °C; ^{1}H NMR (400 MHz, CDCl3): δ=8.96 (s, 1 H; NH, exchanged with D_2O), 7.84 (s, 1 H), 7.56 (d, J=8.5 Hz, 1 H), 7.48 (d, J=8.4 Hz, 1 H), 4.25 (q, J=7.2 Hz, 2 H), 3.61 (t, J=7.5 Hz, 1 H), 3.39 (dd, J=17.0, 7.9 Hz, 1 H), 3.05 (dd, J=17.0, 6.9 Hz, 1 H), 1.28 ppm (t, J=7.2 Hz, 3 H).

See the Supporting Information for compounds **35** and **36**.

General procedure for the preparation of pyridazinone derivatives 37–39

A solution of bromine (0.51 mL, 10 mmol, 2 equiv) in glacial AcOH (8 mL) was added dropwise over 30 min to a stirred solution of dihydropyridazinone **34**–**36** (5 mmol, 1 equiv) in glacial AcOH (30 mL). The resulting mixture was stirred at room temperature for 6–8 h. Then, the solution was poured into ice-water, and the aqueous solution was extracted into EtOAc using a separating funnel. The collected organic phases were washed with H_2O, saturated $NaHCO_3$ solution and brine, then dried (Na_2SO_4) and concentrated under reduced pressure to yield a residue, which was purified by column flash chromatography using appropriate eluents.

Ethyl 6-(3,4-dichlorophenyl)-3-oxo-2,3-dihydropyridazine-4-carboxylate (37): The general procedure for the preparation of pyridazinones was used to oxidize **34**. The reaction mixture was

stirred for 8 h and the obtained crude product purified by flash chromatography (petroleum ether/EtOAc 1:1) to afford **37** as a pale yellow solid (0.85 g, 54 %). R_f=0.47 (petroleum ether/EtOAc 1:1); m.p.: 188–190 °C; ^{1}H NMR (400 MHz, $CDCl_3$): δ=8.26 (s, 1 H), 7.94 (s, 1 H), 7.66 (d, J=8.3 Hz, 1 H), 7.55 (d, J=8.3 Hz, 1 H), 4.47 (q, J=7.1 Hz, 2 H), 1.44 ppm (t, J=7.0 Hz, 3 H); ^{13}C NMR (101 MHz, $CDCl_3$): δ=162.79 (C), 158.25 (C), 143.09 (C), 134.31 (C), 133.65 (C), 133.63 (CH), 132.71 (CH), 131.08 (C), 130.75 (C), 127.76 (CH), 124.93 (CH), 62.60 (CH_2), 14.22 ppm (CH_3).

See the Supporting Information for compounds **38** and **39**.

General procedure for the preparation of *N*-alkylpyridazinone derivatives 40–44

K_2CO_3 (1.65 g, 12 mmol, 3 equiv) then the appropriate alkyl or benzyl halide (12 mmol, 3 equiv) were added to a solution of pyridazinone **37**–**39** (4 mmol, 1 equiv) in anhydrous DMF (18 mL). The resulting suspension was subjected to ultrasound irradiation for 2 h at room temperature. Then the reaction mixture was poured into ice-water, filtered, and extracted with EtOAc in a separating funnel. The collected organic phases were washed with H_2O, 5 % LiCl solution and brine, then dried (Na_2SO_4) and concentrated under reduced pressure. The resulting residue was purified by column flash chromatography using appropriate eluents.

Ethyl 6-(3,4-dichlorophenyl)-2-(4-fluorobenzyl)-3-oxo-2,3-dihydropyridazine-4-carboxylate (40): From the reaction between pyridazinone **37** and 4-fluorobenzyl bromide was obtained a residue, which was purified by flash chromatography (petroleum ether/EtOAc 8:2) to obtain **40** as a pale yellow solid (1.3 g, 78 %). R_f=0.47 (petroleum ether/EtOAc 7:3); m.p.: 139–140 °C; ^{1}H NMR (400 MHz, $CDCl_3$): δ=8.15 (s, 1 H), 7.90 (s, 1 H), 7.62 (d, J=8.3 Hz, 1 H), 7.57–7.48 (m, 3 H), 7.02 (t, J=8.0 Hz, 2 H), 5.40 (s, 2 H), 4.43 (q, J=6.9 Hz, 2 H), 1.41 ppm (t, J=7.0 Hz, 3 H); ^{13}C NMR (101 MHz, $CDCl_3$): δ=163.93 (C), 163.30 (CF), 161.28 (CF), 156.24 (C), 141.39 (C), 134.10 (C), 133.94 (C), 133.59 (C), 131.41 (CH), 131.18 (C), 131.13 (CH), 131.04 (2×CH), 130.60 (C), 127.63 (CH), 124.84 (CH), 115.71 (CH), 115.50 (CH), 62.49 (CH_2), 55.82 (CH_2), 14.21 ppm (CH_3).

See the Supporting Information for compounds **41**–**44**.

General procedure for the preparation of pyridazinone carboxylic acid derivatives 45–49

NaOH (2 m, 50 mL) was added to a stirred solution of pyridazinone ethyl ester (3 mmol) in EtOH (50 mL). The resulting mixture was heated at reflux and stirred overnight. Then, the solution was allowed to cool to room temperature and acidified with HCl (6 m). The resulting precipitate was filtered under vacuum, washed with H_2O and air-dried to yield the analytically pure acid.

6-(3,4-Dichlorophenyl)-2-(4-fluorobenzyl)-3-oxo-2,3-dihydropyridazine-4-carboxylic acid (45): Alkaline saponification in hydroalcoholic NaOH of pyridazinone ethyl ester **40** furnished acid **45** as a pink solid (1.1 g, 92 %). R_f=0.46 ($CHCl_3$/MeOH 9:1); m.p.: 200–201 °C; ^{1}H NMR (400 MHz, $CDCl_3$): δ=8.60 (s, 1 H), 7.97 (s, 1 H), 7.67 (d, J=8.5 Hz, 1 H), 7.60 (d, J=8.4 Hz, 1 H), 7.54–7.48 (m, 2 H), 7.07 (t, J=8.1 Hz, 2 H), 5.49 ppm (s, 2 H); ^{13}C NMR (101 MHz,

$CDCl_3$): δ=164.24 (CF), 162.72 (C), 161.78 (CF), 160.41 (C), 144.63 (C), 135.19 (C), 133.98 (C), 132.99 (CH), 132.96 (C), 131.32 (CH), 131.21 (CH), 131.13 (CH), 129.93 (C), 127.99 (CH), 126.72 (C), 125.14 (CH), 116.10 (CH), 115.88 (CH), 56.32 ppm (CH_2).

See the Supporting Information for compounds **46**–**49**.

Synthesis of carboxamide derivatives 2–24

General procedure A: HOBt (0.20 g, 1.5 mmol, 1.5 equiv) and EDC (0.38 g, 2 mmol, 2 equiv) were added to a stirred solution of acids **45**–**47**, or **49** (1 mmol, 1 equiv) in CH_2Cl_2 (10 mL). The resulting mixture was stirred at room temperature for 30 min. Next, a solution of the appropriate amine in CH_2Cl_2 (10 mL) was added dropwise at 0 °C. The reaction mixture was allowed to stand at room temperature, and then stirred for 12–24 h. The solution was then poured into a separating funnel and H_2O was added. The aqueous phase was separated, and extracted with CH_2Cl_2. The combined organic phases were washed with H_2O and brine, dried (Na_2SO_4) and concentrated under reduced pressure. The analytically pure product was isolated by flash column chromatography using appropriate eluents.

General procedure B: A solution of acid **48** (410 mg, 1.0 mmol, 1 equiv) and thionyl chloride (0.22 mL, 3 mmol, 3 equiv) in toluene (9 mL) was heated at reflux for 3 h. Then, the excess thionyl chloride was removed under reduced pressure and the resulting dark solid was dissolved in CH_2Cl_2 (15 mL). The appropriate amine (1.5 equiv) and Et_3N (1.5 equiv) in CH_2Cl_2 (15 mL) was added dropwise at 0 °C to the solution. The reaction mixture was allowed to stand at room temperature and stirred for 12 h. Then the mixture was poured into a separating funnel and H_2O was added. The aqueous phase was separated and extracted with CH_2Cl_2. The combined organic phases were washed with H_2O, dried (Na_2SO_4) and concentrated under reduced pressure. The analytically pure product was isolated by flash column chromatography using appropriate eluents.

6-(3,4-Dichlorophenyl)-2-(4-fluorobenzyl)-*cis*-*N*-(4-methylcyclohexyl)-3-oxo-2,3-dihydropyridazine-4-carboxamide (2) and 6-(3,4-dichlorophenyl)-2-(4-fluorobenzyl)-*trans*-*N*-(-4-methylcyclohexyl)-3-oxo-2,3-dihydropyridazine-4-carboxamide (3): 4-Methylcyclohexylamine and **45** were reacted according to general procedure A to afford the title products. The reaction mixture was stirred for 18 h, then the *cis*/*trans* isomers were separated by flash chromatography (petroleum ether/EtOAc 9:1).

Compound 2 (111 mg, 23 %), white solid. R_f=0.41 (petroleum ether/EtOAc 85:15); m.p.: 130–132 °C; ^{1}H NMR (400 MHz, $CDCl_3$): δ=9.80 (d, J=7.9 Hz, 1 H; NH, exchanged with D_2O), 8.63 (s, 1 H), 7.98 (d, J=2.1 Hz, 1 H), 7.68 (dd, J=8.5, 2.2 Hz, 1 H), 7.55 (d, J=8.4 Hz, 1 H), 7.49 (dd, J=8.5, 5.5 Hz, 2 H), 7.05 (t, J=8.6 Hz, 2 H), 5.45 (s, 2 H), 4.26–4.18 (m, 1 H), 1.86–1.77 (m, 2 H), 1.71–1.56 (m, 5 H), 1.33–1.20 (m, 2 H), 0.98 ppm (d, J=6.5 Hz, 3 H); ^{13}C NMR (101 MHz, $CDCl_3$): δ=163.96 (CF), 161.50 (CF), 160.43 (C), 159.74 (C), 143.14 (C), 134.22 (C), 134.00 (C), 133.59 (C), 131.09 (C), 131.03 (CH), 130.91 (CH), 130.87 (CH), 130.79 (CH), 130.39 (C) 127.86 (CH), 125.06 (CH), 115.80 (CH), 115.59 (CH), 55.54 (CH_2), 49.95 (CH), 30.98 (CH), 30.06 (2×CH_2), 29.45 (2×CH_2), 21.49 ppm (CH_3); IR: $\tilde{\nu}$ =1681 (C=O), 3274 cm^{-1} (NH); MS

(ESI): *m*/*z*: calcd for $C_{25}H_{24}FCl_2N_3O_2$: 487.1; found: 488.1 $[M+H]^+$; elemental analysis calcd (%) for $C_{25}H_{24}FCl_2N_3O_2$: C 61.48, H 4.95, N 8.60; found: C 61.59, H 4.94, N 8.61.

Compound 3 (58 mg, 12 %), white solid. R_f=0.50 (petroleum ether/EtOAc 85:15); m.p.: 136–138 °C; ^{1}H NMR (400 MHz, $CDCl_3$): δ=9.40 (d, *J*=8.0 Hz, 1 H; NH, exchanged with D_2O), 8.63 (s, 1 H), 7.98 (s, 1 H), 7.68 (d, *J*=8.4 Hz, 1 H), 7.55 (d, *J*=8.4 Hz, 1 H), 7.47 (t, *J*=6.9 Hz, 2 H), 7.04 (t, *J*=8.5 Hz, 2 H), 5.43 (s, 2 H), 3.97–3.75 (m, 1 H), 2.09–1.98 (m, 2 H), 1.83–1.71 (m, 2 H), 1.64 (s, 1 H), 1.39–1.23 (m, 2 H), 1.17–1.03 (m, 2 H), 0.91 ppm (d, *J*=6.5 Hz, 3 H); ^{13}C NMR (101 MHz, $CDCl_3$): δ=162.93 (CF), 160.47 (CF), 159.39 (C), 158.61 (C), 142.18 (C), 133.23 (C), 132.96 (C), 132.58 (C), 130.06 (C), 130.02 (CH), 129.96 (C), 129.74 (CH), 129.66 (CH), 129.29 (CH), 126.86 (CH), 124.06 (CH), 114.82 (CH), 114.60 (CH), 54.79 (CH_2), 48.10 (CH), 32.76 (2×CH_2), 31.76 (2×CH_2), 30.90 (CH), 21.16 ppm (CH_3); IR: $\tilde{\nu}$ =1677 (C=O), 3280 cm^{-1} (NH); MS (ESI): *m*/*z*: calcd for $C_{25}H_{24}FCl_2N_3O_2$: 487.1; found: 488.1 $[M+H]^+$; elemental analysis calcd (%) for $C_{25}H_{24}FCl_2N_3O_2$: C 61.48, H 4.95, N 8.60; found: C 61.55, H 4.96, N 8.59.

See the Supporting Information for compounds **4**–**6**.

2-(Cyclohexylmethyl)-6-(3,4-dichlorophenyl)-*cis*-*N*-(4-methylcyclohexyl)-3-oxo-2,3-dihydropyridazine-4-carboxamide (7) and 2-(cyclohexylmethyl)-6-(3,4-dichlorophenyl)-*trans*-*N*-(4-methylcyclohexyl)-3-oxo-2,3-dihydropyridazine-4-carboxamide (8): 4-Methylcyclohexylamine and **46** were reacted according to general procedure A to afford the title products. The reaction mixture was stirred for 18 h, then the *cis*/*trans* isomers were separated by flash chromatography (petroleum ether/EtOAc 95:5).

Compound 7 (90 mg, 19 %), white solid. R_f=0.38 (petroleum ether/EtOAc 9:1); m.p.: 131–132 °C; ^{1}H NMR (400 MHz, $CDCl_3$): δ=9.88 (d, *J*=7.8 Hz, 1 H; NH, exchanged with D_2O), 8.63 (s, 1 H), 7.98 (s, 1 H), 7.69 (d, *J*=8.3 Hz, 1 H), 7.55 (d, *J*=8.3 Hz, 1 H), 4.25–4.21 (m, 1 H), 4.19 (d, *J*=7.5 Hz, 2 H), 2.10–2.00 (m, 1 H), 1.89–1.57 (m, 11 H), 1.34–1.04 (m, 8 H), 0.97 ppm (d, *J*=6.4 Hz, 3 H); ^{13}C NMR (101 MHz, $CDCl_3$): δ=159.73 (C), 159.17 (C), 141.36 (C), 133.27 (C), 132.95 (C), 132.51 (C), 129.96 (CH), 129.36 (CH), 128.70 (C), 126.79 (CH), 124.00 (CH), 57.72 (CH_2), 44.95 (CH), 35.91 (CH), 29.99 (CH), 29.52 (2×CH_2), 29.09 (2×CH_2), 28.44 (2×CH_2), 25.24 (CH_2), 24.62 (2×CH_2), 20.44 ppm (CH_3); IR: $\tilde{\nu}$ =1688 (C=O), 3273 cm^{-1} (NH); MS (ESI): *m*/*z*: calcd for $C_{25}H_{31}Cl_2N_3O_2$: 475.2; found: 476.2 $[M+H]^+$; elemental analysis calcd (%) for $C_{25}H_{31}Cl_2N_3O_2$: C 63.02, H 6.56, N 8.82; found: C 62.88, H 6.55, N 8.80.

Compound 8 (47 mg, 10 %), white solid. R_f=0.55 (petroleum ether/EtOAc 9:1); m.p.: 133–135 °C; ^{1}H NMR (400 MHz, $CDCl_3$): δ=9.52 (d, *J*=8.0 Hz, 1 H; NH, exchanged with D_2O), 8.63 (s, 1 H), 7.98 (s, 1 H), 7.69 (d, *J*=8.5 Hz, 1 H), 7.55 (d, *J*=8.5 Hz, 1 H), 4.42 (d, *J*=7.3 Hz, 1 H), 4.17 (d, *J*=7.4 Hz, 2 H), 3.93–3.83 (m, 1 H), 2.12–2.02 (m, 3 H), 1.82–1.55 (m, 9 H), 1.40–1.03 (m, 7 H), 0.92 ppm (d, *J*=6.5 Hz, 3 H); ^{13}C NMR (101 MHz, $CDCl_3$): δ=160.12 (C), 142.49 (C), 134.23 (C), 134.00 (C), 133.53 (C), 132.97 (C), 130.98 (CH), 130.54 (CH), 129.69 (C), 127.82 (CH), 125.04 (CH), 58.99 (CH_2), 49.06 (CH), 36.95 (CH), 33.80 (2×CH_2), 32.81 (2×CH_2), 31.94 (CH), 30.59 (2×CH_2), 26.23 (CH_2), 25.62 (2×CH_2), 22.18 ppm (CH_3); IR: $\tilde{\nu}$ =1690 (C=O), 3275 cm^{-1} (NH); MS (ESI): *m*/*z*: calcd for $C_{25}H_{31}Cl_2N_3O_2$: 475.2; found: 476.2 $[M+H]^+$; elemental analysis calcd (%) for $C_{25}H_{31}Cl_2N_3O_2$: C 63.02, H 6.56, N 8.82; found: C 63.10, H 6.58, N 8.83.

See the Supporting Information for compounds **9**–**11**.

2-(5-Chloropentyl)-6-(3,4-dichlorophenyl)-*cis*-*N*-(4-methylcyclohexyl)-3-oxo-2,3-dihydropyridazine-4-carboxamide (12) and 2-(5-chloropentyl)-6-(3,4-dichlorophenyl)-*trans*-*N*-(4-methylcyclohexyl)-3-oxo-2,3-dihydropyridazine-4-carboxamide (13): General procedure A for the synthesis of carboxamides was used to convert acid **47** and 4-methylcyclohexylamine into the title products. The reaction mixture was stirred for 18 h, then the *cis*/*trans* isomers were separated by flash chromatography (petroleum ether/EtOAc 87:13).

Compound 12 (82 mg, 17 %), colorless oil. R_f=0.42 (petroleum ether/EtOAc 85:15); ^{1}H NMR (400 MHz, $CDCl_3$): δ=9.90 (d, J=7.8 Hz, 1 H; NH, exchanged with D_2O), 8.64 (s, 1 H), 7.99 (s, 1 H), 7.69 (dd, J=8.4, 2.2 Hz, 1 H), 7.55 (d, J=8.4 Hz, 1 H), 4.34 (t, J=7.4 Hz, 2 H), 4.28–4.21 (m, 1 H), 3.47 (t, J=7.0 Hz, 2 H), 1.99–1.79 (m, 4 H), 1.72–1.59 (m, 9 H), 1.56–1.44 (m, 2 H), 0.97 ppm (d, J=6.5 Hz, 3 H); ^{13}C NMR (101 MHz, $CDCl_3$): δ=159.64 (C), 158.90 (C), 141.75 (C), 133.20 (C), 133.00 (C), 132.53 (C), 129.97 (CH), 129.51 (CH), 128.79 (C), 126.81 (CH), 124.00 (CH), 69.25 (CH_2) 51.94 (CH_2), 44.80 (CH), 30.12 (CH), 29.06 (2×CH_2), 28.53 (2×CH_2), 28.39 (CH_2), 27.31 (CH_2), 22.41 (CH_2), 20.56 ppm (CH_3); IR: $\tilde{\nu}$ =1678 (C=O), 3301 cm^{-1} (NH); MS (ESI): *m*/*z*: calcd for $C_{23}H_{28}Cl_3N_3O_2$: 483.1; found: 484.1 [M+H]$^+$; elemental analysis calcd (%) for $C_{23}H_{28}Cl_3N_3O_2$: C 56.99, H 5.80, N 8.64; found: C 56.90, H 5.82, N 8.67.

Compound 13 (48 mg, 10 %), colorless oil. R_f=0.53 (petroleum ether/EtOAc 85:15); ^{1}H NMR (400 MHz, CDCl3): δ=9.52 (d, J=8.0 Hz, 1 H; NH, exchanged with D_2O), 8.63 (d, J=5.3 Hz, 1 H), 7.99 (s, 1 H), 7.69–7.67 (m, 1 H), 7.46–7.40 (m, 1 H), 4.33 (dd, J=13.1, 5.7 Hz, 2 H), 3.94–3.83 (m, 1 H), 3.51–3.40 (m, 2 H), 2.09–1.88 (m, 4 H), 1.80–1.72 (m, 2 H), 1.70–1.58 (m, 6 H), 1.35–1.23 (m, 3 H), 0.91 ppm (d, J=6.5 Hz, 3 H); ^{13}C NMR (101 MHz, $CDCl_3$): δ=159.44 (C), 158.92 (C), 141.68 (C), 133.11 (C), 133.05 (C), 132.22 (C), 129.79 (CH), 129.22 (CH), 128.80 (C), 126.69 (CH), 124.03 (CH), 69.26 (CH_2), 51.90 (CH_2), 42.72 (CH), 29.00 (2×CH_2), 28.30 (2×CH_2), 28.25 (CH), 28.09 (CH_2), 27.33 (CH_2), 22.42 (CH_2), 13.52 ppm (CH_3); IR: $\tilde{\nu}$ =1673 (C=O), 3298 cm^{-1} (NH); MS (ESI): *m*/*z*: calcd for $C_{23}H_{28}Cl_3N_3O_2$: 483.1; found: 484.2 [M+H]$^+$; elemental analysis calcd (%) for $C_{23}H_{28}Cl_3N_3O_2$: C 56.98, H 5.82, N 8.67; found: C 57.05, H 5.83, N 8.65.

See the Supporting Information for compounds **14**–**16**.

6-(5-Bromothiophen-2-yl)-2-(4-fluorobenzyl)-*cis*-*N*-(4-methylcyclohexyl)-3-oxo-2,3-dihydropyridazine-4-carboxamide (17) and 6-(5-bromothiophen-2-yl)-2-(4-fluorobenzyl)-*trans*-*N*-(4-methylcyclohexyl)-3-oxo-2,3-dihydropyridazine-4-carboxamide (18): 4-Methylcyclohexylamine and **48** were reacted according to general procedure B to afford the title products. The *cis*/*trans* isomers were separated by flash chromatography (petroleum ether/EtOAc 85:15).

Compound 17 (90 mg, 19 %), yellow solid. R_f=0.30 (petroleum ether/EtOAc 85:15); m.p.: 158–159 °C; ^{1}H NMR (400 MHz, $CDCl_3$): δ=9.81 (d, J=7.7 Hz, 1 H; NH, exchanged with D_2O), 8.50 (s, 1 H), 7.52–7.44 (m, 2 H), 7.23 (d, J=4.0 Hz, 1 H), 7.04 (t, J=6.5 Hz, 3 H), 5.36 (s, 2 H), 4.33–4.13 (m, 1 H), 1.86–1.76 (m, 2 H), 1.70–1.56 (m, 4 H), 1.32–1.20 (m, 3 H), 0.97 ppm (d, J=6.5

Hz, 3 H); ^{13}C NMR (101 MHz, $CDCl_3$): δ=162.94 (CF), 160.48 (CF), 159.32 (C), 158.48 (C), 140.00 (C), 138.99 (C), 130.07 (C), 129.98 (CH), 129.91 (CH), 129.90 (CH), 129.21 (C), 128.90 (CH), 125.42 (CH), 115.07 (C), 114.73 (CH), 114.52 (CH), 53.96 (CH_2), 44.94 (CH), 29.96 (CH), 29.04 (2×CH_2), 28.42 (2×CH_2), 20.48 ppm (CH_3); IR: $\tilde{\nu}$ =1683 (C=O), 3308 cm^{-1} (NH); MS (ESI): *m*/*z*: calcd for $C_{23}H_{23}BrFN_3O_2S$: 503.1; found: 504.2 [*M*+H]$^+$; elemental analysis calcd (%) for $C_{23}H_{23}BrFN_3O_2S$: C 54.77, H 4.60, N 8.33; found: C 54.88, H 4.61, N 8.34.

Compound 18 (55 mg, 11 %), yellow solid. R_f=0.48 (petroleum ether/EtOAc 85:15); m.p.: 140–412 °C; ^{1}H NMR (400 MHz, CDCl3): δ=9.42 (d, *J*=8.1 Hz, 1 H; NH, exchanged with D_2O), 8.50 (s, 1 H), 7.51–7.43 (m, 2 H), 7.24 (d, *J*=4.0 Hz, 1 H), 7.09–7.00 (m, 3 H), 5.34 (s, 2 H), 3.94–3.75 (m, 1 H), 2.07–2.00 (m, 2 H), 1.80–1.71 (m, 2 H), 1.62–1.58 (m, 1 H), 1.41–1.23 (m, 2 H), 1.15–1.01 (m, 2 H), 0.91 ppm (d, *J*=6.6 Hz, 3 H); ^{13}C NMR (101 MHz, $CDCl_3$): δ=162.93 (CF), 160.47 (CF), 159.32 (C), 158.38 (C), 140.06 (C), 138.94 (C), 129.98 (C), 129.92 (CH), 129.85 (CH), 129.77 (CH), 129.15 (C), 129.07 (CH), 125.47 (CH), 115.12 (C), 114.77 (CH), 114.55 (CH), 54.23 (CH_2), 48.09 (CH), 32.76 (2×CH_2), 31.74 (2×CH_2), 30.89 (CH), 21.16 ppm (CH_3); IR: $\tilde{\nu}$ =1681 (C=O), 3305 cm^{-1} (NH); MS (ESI): *m*/*z*: calcd for $C_{23}H_{23}BrFN_3O_2S$: 503.1; found: 504.2 [*M*+H]$^+$; elemental analysis calcd (%) for $C_{23}H_{23}BrFN_3O_2S$: C 54.77, H 4.60, N 8.33; found: C 54.85, H 4.59, N 8.34.

See the Supporting Information for compounds **19**–**21**.

6-(4-Chloro-3-methylphenyl)-*cis*-*N*-(4-methylcyclohexyl)-3-oxo-2-pentyl-2,3-dihydropyridazine-4-carboxamide (22): 4-Methylcyclohexylamine and **44** were reacted according to general procedure A to afford the title products. The reaction mixture was stirred for 18 h, then the crude material was purified by flash chromatography (petroleum ether/EtOAc 95:5) to afford **22** (98 mg, 23 %) as a colorless oil. R_f=0.22 (petroleum ether/EtOAc 95:5); ^{1}H NMR (400 MHz, $CDCl_3$): δ=9.96 (d, *J*=7.8 Hz, 1 H; NH, exchanged with D_2O), 8.65 (s, 1 H), 7.73 (s, 1 H), 7.64 (d, *J*=8.3, 2.3 Hz, 1 H), 7.43 (d, *J*=8.3 Hz, 1 H), 4.33 (t, *J*=7.6 Hz, 2 H), 4.27–4.19 (m, 1 H), 2.45 (s, 3 H), 2.19–2.02 (m, 1 H), 1.98–1.79 (m, 3 H), 1.80–1.55 (m, 4 H), 1.51–1.22 (m, 7 H), 0.97 (d, *J*=6.5 Hz, 3 H), 0.92 ppm (t, *J*=6.3 Hz, 3 H); ^{13}C NMR (101 MHz, $CDCl_3$): δ=159.91 (C), 158.95 (C), 143.16 (C), 135.83 (C), 135.04 (C), 131.81 (C), 129.88 (CH), 128.67 (CH), 128.50 (C), 127.35 (CH), 123.61 (CH), 51.88 (CH_2), 44.79 (CH), 30.10 (CH), 29.08 (2×CH_2), 28.51 (2×CH_2), 27.77 (CH_2), 27.18 (CH_2), 21.31 (CH_2), 19.19 (2×CH_3), 12.94 ppm (CH_3); IR: $\tilde{\nu}$ =1683 (C=O), 3261 cm^{-1} (NH); MS (ESI): *m*/*z*: calcd for $C_{24}H_{32}ClN_3O_2$: 429.2; found: 430.1 [*M*+H]$^+$; elemental analysis calcd (%) for $C_{24}H_{32}ClN_3O_2$: C 67.04, H 7.50, N 9.77; found: C 66.93, H 7.48, N 9.80.

See the Supporting Information for compounds **23** and **24**.

Biological assays

Radioligand binding assays at *h*CB$_1$Rs and *h*CB$_2$Rs: [^{3}H]CP 55,940 (specific activity, 180 Ci mmol^{-1}) and CHO cells transfected with *h*CB_1R and *h*CB_2R were purchased from PerkinElmer Life and Analytical Sciences. All other reagents were obtained from Sigma (Milan, Italy). CHO cells expressing CB_1R and CB_2R were cultured in Ham's F12 supplemented with 10 % fetal bovine serum, penicillin (100 U mL^{-1}), streptomycin (100 μg mL^{-1}), and geneticin

(G418, 0.4 mg mL^{-1}) at 37 °C in air containing 5 % CO_2.[41] Membranes from transfected cells to be used in binding experiments were obtained as previously reported.[41] In brief, the cells were detached in ice-cold hypotonic buffer (5 mm Tris-HCl, 2 mm EDTA, pH 7.4), triturated with a Polytron and centrifuged for 10 min at 1000 *g*. Then the supernatant was centrifuged for 30 min at 100 000 *g* and the membrane pellet was diluted in 50 mm Tris-HCl buffer, 0.5 % BSA (pH 7.4) containing 5 mm $MgCl_2$, 2.5 mm EDTA or 1 mm EDTA for *h*CB_1R or *h*CB_2R, respectively. Competition binding experiments were carried out with [^{3}H]CP 55,940 in the presence of ligands under examination in the concentration range 1 nm to 10 μm or WIN 55,212-2, the CB_1R/CB_2R standard agonist. Incubation times were 90 or 60 min at 30 °C for CB_1Rs or CB_2Rs, respectively. Bound and free radioactivities were separated by filtering the assay mixture through Whatman GF/C glass fiber filters using a Brandel cell harvester (Brandel Instruments, Unterföhring, Germany). The filter-bound radioactivity was counted on a PerkinElmer 2810 TR scintillation counter (PerkinElmer Life and Analytical Sciences).

cAMP assays for *h*CB_2Rs: CHO cells expressing *h*CB_2Rs were preincubated with the phosphodiesterase inhibitor 4-(3-butoxy-4-methoxybenzyl)-2-imidazolidinone (Ro 20–1724, 0.5 mm). Then, the effect of a selection of compounds characterized by high affinity and selectivity toward CB_2Rs was tested at increasing concentrations (0.001–1 μm) with or without WIN 55,212-2 (0.1 μm) in the presence of forskolin (5 μm), by using the fluorimetric cAMP kit (AlphaScreen cAMP assay kit, PerkinElmer) according to the manufacturer's instructions.

Data analysis: The protein concentration was measured by a Bio-Rad method[42] with bovine albumin as reference standard. Inhibitory binding constants K_i were obtained from the IC_{50} values following the Cheng and Prusoff equation: $K_i=IC_{50}/(1+[C]/K_D)$, where [C] is the concentration of the radioligand and K_D its dissociation constant (Cheng–Prusoff).[22] A weighted nonlinear least-squares curve fitting program, LIGAND, was used for computer analysis of the inhibition experiments.[43] All the data are presented as the mean±SEM of n=4 independent experiments. Statistical analysis of the data was performed using ANOVA followed by Dunnett's test.

Computational studies

Conformational analysis: The Ballesteros–Weinstein numbering system for GPCR amino acid residues is used. In this numbering system, the label 0.50 is assigned to the most highly conserved residue in class A GPCRs in each transmembrane helix (TMH).[44] This is preceded by the TMH number. In this system, for example, the most highly conserved residue in TMH6 is P6.50. The residue immediately before this would be labeled 6.49, and the residue immediately after this would be labeled 6.51. In reference to a specific CB_2R residue, the Ballesteros–Weinstein name is followed by the absolute sequence number given in parentheses [e.g., K3.28(109)]; however, if referring to a highly conserved residue among class A GPCRs (and not a specific residue in CB_2R), only the Ballesteros–Weinstein name is given.

A complete conformational analysis of **22** was performed using the Mixed Torsional/Low-Mode Sampling technique as encoded in Macromodel (version 11.6, Schrödinger, LLC, New York, NY). Torsional moves of 30° or greater were set for all rotatable bonds within **22**, including full exploration of the 4-*cis*-cyclohexyl ring. The search was comprised of 20 000 Monte Carlo steps

using the OPLS3 force field with a distance-dependent dielectric and a dielectric base constant of 2. An 8.0 Å nonbonded cutoff (updated every 10 steps), a 20.0 Å electrostatic cutoff, and a 4.0 Å hydrogen-bond cutoff were applied to the minimization of each conformation with a gradient of 0.01 kcal mol^{-1} Å. Duplicate conformations identified at an RMSD≤0.7 were removed. To calculate the energy difference between the global minimal energy conformer of **22** and its final docked conformation, the single-point energy of each was calculated in OPLS3 and the difference was calculated.

Model development: Complete details on the generation of the CB_2R inactive-state model used here are available in our previous publication.[25] In brief, the crystal structure of the class A GPCR rhodopsin in the dark state was used as the template for the creation of our CB_2R inactive-state model.[45] This template was chosen because no mutations or modifications were made to its structure for crystallization and there are no structural distortions due to crystal packing for this structure. In addition, the cannabinoid receptors and rhodopsin share some unusual sequence motifs. For example, these receptors share a TMH4 GWNC motif at their extracellular ends. Here a Trp residue forms an aromatic stacking interaction with Y5.39, influencing the extracellular positions of TMH3–4–5. The initial CB_2R homology model was refined by calculating the low-free-energy conformations for any TMH with an important sequence divergence from rhodopsin and replacing the corresponding helix from the initial model with one that more accurately reflects the sequence-dictated TMH geometries in CB_2R. This includes TMH2 (a GG helix-distorting motif in rhodopsin vs. no Pro or GG in CB_2R) and TMH5 (Pro at 5.50 in rhodopsin vs. no Pro at 5.50 in CB_2R). This CB_2R model has been tested using results from substituted cysteine-accessibility studies to identify binding-pocket-facing residues,[46, 47] from mutation studies of key ligand interactions sites,[46-49] and from covalent labeling studies of CB_2R that support a lipid-entry pathway for CB_2R ligands.[50] To allow adjustment to a lipid bilayer environment, the resultant model was pre-equilibrated in an SDPC bilayer for 300 ns.[25] Although the toggle-switch residue W6.48(258) remained in its inactive-state g+ $\chi 1$ dihedral angle after the equilibration in SDPC, some notable changes did occur during this equilibration. The R3.50(131)–D6.30(240) salt bridge at the intracellular ends of TMH3 and TMH6 (analogous to the R3.50(135)–E6.30(247) salt bridge in the dark state of rhodopsin) rearranged quickly to form a salt bridge between R3.55(136) and D6.30(240), with Y3.51(132) supporting the salt bridge by hydrogen bonding to the exposed backbone carbonyl of L6.29(239). A second notable change was the development of additional helical turns in the IC-3 (TMH5–TMH6) loop after the original end of TMH5.[25]

Docking study in the CB_2R inactive-state model: Compound **22** was docked into the SR144528–CB_2R binding site previously identified by Glide docking studies.[23, 24, 26] Compound **22** was flexibly docked using Glide (version 7.5, Schrödinger) and the dock with the best Glide score, as ranked by Emodel, was chosen. Glide was used to generate a grid based on the centroid of select residues in the binding pocket. The box size was set to the default value of 24×24×24 Å, with the inner box size set to 10×10×10 Å. This box size encompasses the entire CB_2R binding pocket both in width and depth. No scaling of van der Waals radii was used. S7.39(285) was defined to be a required interaction during the docking procedure, by analogy to literature mutation studies for binding of HU243 at the CB_2R.[51] Extra precision (XP) and flexible docking with 50 K maximum initial poses to be retained for the initial phase of docking were selected for the docking setup. During docking only *trans* amides

were allowed, aromatic protons were set as donors and halogens as acceptors. After docking, a 800-step conjugate gradient minimization was performed on the ligand pose by Glide using OPLS3 (distance-dependent dielectric with a base constant of 2). The resulting ligand–receptor complex with the best Glide score was minimized using the OPLS3 all-atom force field in Macromodel. An 8.0 Å nonbonded cutoff (updated every 10 steps), a 20.0 Å electrostatic cutoff, and a 4.0 Å hydrogen-bond cutoff were used in each stage of the calculation. The first stage consisted of 4000 steps of Polak–Ribier conjugate gradient minimization using a distance-dependent dielectric function with a base constant of 2. No harmonic constraints were placed on the side chains, but 100 kJ mol^{-1} torsional constraints were applied to hold all the backbone φ/ψ torsion angles. During the second stage of 1000 steps, all torsional constraints were released. To relax the loops, an additional 1000-step Polak–Ribier conjugate gradient minimization of the loop regions was performed. The loop and termini regions were left free, whereas the transmembrane regions were not allowed to move during this final minimization. An 8.0 Å extended nonbonded cutoff (updated every 10 steps), 20.0 Å electrostatic cutoff, and 4.0 Å hydrogen-bond cutoff were used in this calculation, and the generalized Born/surface area (GB/SA) continuum solvation model for water available in Macromodel was used.

Assessment of pairwise interaction energies: After the atoms of **22** had been defined as one group (group 1) and the atoms corresponding to a residue that lines the binding site in the final ligand–CB_2R complex as another group (group 2), Macromodel was used to output the pairwise interaction energies (coulombic and van der Waals) for a given pair of atoms. The pairs corresponding to group 1 (ligand) and group 2 (residue of interest) were then summed to yield the energy of interaction between the ligand and that residue. The **22**–CB_2R complex was found to have interaction energies totaling −66.59 kcal mol^{-1}. Taking the conformational energy cost for **22** in the final complex (0.89 kcal mol^{-1}) into account, we found the final total energy for the **22**–CB_2R complex to be −65.70 kcal mol^{-1}. A breakdown of interaction energies is provided in Table S1.

In silico ADMET calculations: A set of 34 physicochemical descriptors were computed using QikProp version 3.5 integrated in Maestro (Schrödinger). The QikProp descriptors are shown in Table **2**. The 3D conformations used in the calculation of QikProp descriptors were generated using the OPLS3 force field and the Mixed Torsional Low Mode Sampling Monte Carlo Conformational Search method in Macromodel 11.3 (Schrödinger, 2016). Possible tautomerization and ionization states were calculated using Epik integrated in the Maestro software. No tautomers were found for pyridazinones **2**–**24**. Toxicity and metabolism predictions were performed by using the admetSAR prediction tool (**http://lmmd.ecust.edu.cn/admetsar1/**).[34] Tables S2 and S3 summarize the parameters calculated and classify the compounds according to previously reported methods (see the Supporting Information).

Acknowledgements. This work was supported by US National Institutes of Health (NIH) grants RO1 DA003934 and KO5 DA021358 (to P.H.R.).

Conflict of interest. The authors declare no conflict of interest.

References

1 S. Munro, K. L. Thomas, M. Abu-Shaar, *Nature* 1993, **365**, 61– 65.

2 P. H. Reggio, *Curr. Med. Chem.* 2010, **17**, 1468– 1486.

3 R. G. Pertwee, R. A. Ross, *Prostaglandins Leukotrienes Essent. Fatty Acids* 2002, **66**, 101– 121.

4 M. Maccarrone, I. Bab, T. Bíró, G. A. Cabral, S. K. Dey, V. Di Marzo, J. C. Konje, G. Kunos, R. Mechoulam, P. Pacher, K. A. Sharkey, A. Zimmer, *Trends Pharmacol. Sci.* 2015, **36**, 277– 296.

5 R. G. Pertwee, *Int. J. Obes.* 2006, **30**, S 13–S 18.

6 D. Piomelli, *Nat. Rev. Neurosci.* 2003, **4**, 873– 884.

7 A. B. Lynn, M. Herkenham, *J. Pharmacol. Exp. Ther.* 1994, **268**, 1612– 1623.

8 R. G. Pertwee, *Br. J. Pharmacol.* 2009, **156**, 397– 411.

9 I. Svízenská, P. Dubový, A. Sulcová, *Pharmacol. Biochem. Behav.* 2008, **90**, 501– 511.

10 G. Navarro, P. Morales, C. Rodriguez-Cueto, J. Fernandez-Ruiz, N. Jagerovic, R. Franco, *Front. Neurosci.* 2016, **10**, 406.

11 V. Di Marzo, M. Bifulco, L. De Petrocellis, *Nat. Rev. Drug Discovery* 2004, **3**, 771– 784.

12 D. R. Compton, K. C. Rice, B. R. De Costa, R. K. Razdan, L. S. Melvin, M. R. Johnson, B. R. Martin, *J. Pharmacol. Exp. Ther.* 1993, **265**, 218– 226.

13 T. Bisogno, V. Di Marzo, *CNS Neurol. Disord. Drug Targets* 2010, **9**, 564– 573.

14 J. L. Shoemaker, K. A. Seely, R. L. Reed, J. P. Crown, P. L. Prather, *J. Neurochem.* 2007, **101**, 87– 98.

15 M. Aghazadeh Tabrizi, P. G. Baraldi, P. A. Borea, K. Varani, *Chem. Rev.* 2016, **116**, 519– 560.

16 F. Vincenzi, M. Targa, C. Corciulo, M. A. Tabrizi, S. Merighi, S. Gessi, G. Saponaro, P. G. Baraldi, P. A. Borea, K. Varani, *Pain* 2013, **154**, 864– 873.

17 A. Quartilho, H. Mata, M. Ibrahim, T. Vanderah, P. Porreca, A. Makriyannis, T. Malan, *Anesthesiology* 2003, **99**, 955– 960.

18 C. Blázquez, L. Gonzalez-Feria, L. Alvarez, A. Haro, M. L. Casanova, M. Guzmán, *Cancer Res.* 2004, **64**, 5617– 5623.

19 S. Pisanti, P. Picardi, A. D′Alessandro, C. Laezza, M. Bifulco, *Trends Pharmacol. Sci.* 2013, **34**, 273– 282.

20 P. Morales, L. Hernandez-Folgado, P. Goya, N. Jagerovic, *Expert Opin. Ther. Pat.* 2016, **26**, 843– 856.

21 G. Ragusa, M. Gómez-Cañas, P. Morales, C. Rodríguez-Cueto, M. R. Pazos, B. Asproni, E. Cichero, P. Fossa, G. A. Pinna, N. Jagerovic, J. Fernández-Ruiz, G. Murineddu, *Eur. J. Med. Chem.* 2017, **127**, 398– 412.

22 Y. Cheng, W. H. Prusoff, *Biochem. Pharmacol.* 1973, **22**, 3099– 3108.

23 E. Kotsikorou, F. Navas, M. Roche, A. Gilliam, B. F. Thomas, H. H. Seltzman, P. Kumar, Z.-H. Song, D. P. Hurst, D. L. Lynch, P. H. Reggio, *J. Med. Chem.* 2013, **56**, 6593– 6612.

24 V. Lucchesi, D. P. Hurst, D. M. Shore, S. Bertini, B. M. Ehrmann, M. Allarà, L. Lawrence, A. Ligresti, F. Minutolo, G. Saccomanni, H. Sharir, M. Macchia, V. Di Marzo, M. E. Abood, P. H. Reggio, C. Manera, *J. Med. Chem.* 2014, **57**, 8777– 8791.

25 D. P. Hurst, A. Grossfield, D. L. Lynch, S. Feller, T. D. Romo, K. Gawrisch, M. C. Pitman, P. H. Reggio, *J. Biol. Chem.* 2010, **285**, 17954– 17964.

26 G. Ragusa, M. Gómez-Cañas, P. Morales, D. P. Hurst, F. Deligia, R. Pazos, G. A. Pinna, J. Fernández-Ruiz, P. Goya, P. H. Reggio, N. Jagerovic, M. García-Arencibia, G. Murineddu, *Eur. J. Med. Chem.* 2015, **101**, 651– 667.

27 H. van de Waterbeemd, E. Gifford, *Nat. Rev. Drug Discovery* 2003, **2**, 192– 204.

28 J. M. Sanders, D. C. Beshore, J. C. Culberson, J. I. Fells, J. E. Imbriglio, H. Gunaydin, A. M. Haidle, M. Labroli, B. E. Mattioni, N. Sciammetta, W. D. Shipe, R. P. Sheridan, L. M. Suen, A. Verras, A. M. Walji, E. M. Joshi, T. Bueters, *J. Med. Chem.* 2017, **60**, 6771– 6780.

29 S. Ekins, C. L. Waller, P. W. Swaan, G. Cruciani, S. A. Wrighton, J. H. Wikel, *J. Pharmacol. Toxicol. Methods* 2000, **44**, 251– 272.

30 C. A. Lipinski, *J. Pharmacol. Toxicol. Methods* 2000, **44**, 235– 249.

31 W. L. Jorgensen, E. M. Duffy, *Adv. Drug Delivery Rev.* 2002, **54**, 355– 366.

32 M. A. Huestis, *Chem. Biodiversity* 2007, **4**, 1770– 1804.

33 F. Grotenhermen, *Clin. Pharmacokinet.* 2003, **42**, 327– 360.

34 F. Cheng, W. Li, Y. Zhou, J. Shen, Z. Wu, G. Liu, P. W. Lee, Y. Tang, *J. Chem. Inf. Model.* 2012, **52**, 3099– 3105.

35 F. P. Guengerich, *Chem. Res. Toxicol.* 2008, **21**, 70– 83.

36 U. M. Zanger, M. Schwab, *Pharmacol. Ther.* 2013, **138**, 103– 141.

37 Z. Xu, Z. Yang, Y. Liu, Y. Lu, K. Chen, W. Zhu, *J. Chem. Inf. Model.* 2014, **54**, 69– 78.

38 M. Hernandes, S. M. Cavalcanti, D. R. Moreira, W. de Azevedo Junior, A. C. Leite, *Curr. Drug Targets* 2010, **11**, 303– 314.

39 H. Zhu, T. M. Martin, L. Ye, A. Sedykh, D. M. Young, A. Tropsha, *Chem. Res. Toxicol.* 2009, **22**, 1913– 1921.

40 X. Li, L. Chen, F. Cheng, Z. Wu, H. Bian, C. Xu, W. Li, G. Liu, X. Shen, Y. Tang, *J. Chem. Inf. Model.* 2014, **54**, 1061– 1069.

41 S. Merighi, C. Simioni, S. Gessi, K. Varani, P. A. Borea, *Biochem. Pharmacol.* 2010, **79**, 471– 477.

42 M. M. Bradford, *Anal. Biochem.* 1976, **72**, 248– 254.

43 P. J. Munson, D. Rodbard, *Anal. Biochem.* 1980, **107**, 220– 239.

44 J. A. Ballesteros, H. Weinstein, *Methods Neurosci.* 1995, **25**, 366– 428.

45 K. Palczewski, T. Kumasaka, T. Hori, C. A. Behnke, H. Motoshima, B. A. Fox, I. Le Trong, D. C. Teller, T. Okada, R. E. Stenkamp, M. Yamamoto, M. Miyano, *Science* 2000, **289**, 739– 745.

46 R. Zhang, D. P. Hurst, J. Barnett-Norris, P. H. Reggio, Z. H. Song, *Mol. Pharmacol.* 2005, **68**, 69– 83.

47 N. M. Nebane, D. P. Hurst, C. A. Carrasquer, Z. Qiao, P. H. Reggio, Z. H. Song, *Biochemistry* 2008, **47**, 13811– 13821.

48 Z. H. Song, C. A. Slowey, D. P. Hurst, P. H. Reggio, *Mol. Pharmacol.* 1999, **56**, 834– 840.

49 Q. Tao, S. D. McAllister, J. Andreassi, K. W. Nowell, G. A. Cabral, D. P. Hurst, K. Bachtel, M. C. Ekman, P. H. Reggio, M. E. Abood, *Mol. Pharmacol.* 1999, **55**, 605– 613.

50 Y. Pei, R. W. Mercier, J. K. Anday, G. A. Thakur, A. M. Zvonok, D. Hurst, P. H. Reggio, D. R. Janero, A. Makriyannis, *Chem. Biol.* 2008, **15**, 1207– 1219.

51 M. H. Rhee, *J. Vet. Sci.* 2002, **3**, 185– 191.

CHEMMEDCHEM
Chemistry & Drug Discovery

Supporting Information

Synthesis, Pharmacological Evaluation, and Docking Studies of Novel Pyridazinone-Based Cannabinoid Receptor Type 2 Ligands

Giulio Ragusa,[a] Serena Bencivenni,[b] Paula Morales,[c] Tyra Callaway,[c] Dow P. Hurst,[c] Battistina Asproni,[a] Stefania Merighi,[b] Giovanni Loriga,[d] Gerard A. Pinna,[a] Patricia H. Reggio,[c] Stefania Gessi,*[b] and Gabriele Murineddu*[a]

cmdc_201800152_sm_miscellaneous_information.pdf

TABLE OF CONTENTS

Synthetic procedures and data for compounds **30**, **32**, **33, 35**, **36**, **38**, **39**, **41**-**44**, **46** – **49**, **4** – **6**, **9** – **11**, **14** – **16**, **19** – **21**, **23** and **24**.

General Procedure for the preparation of acyl bromides (28-30)

Method A: Bromine (3.02 mL, 59,3 mmol, 1 eq) was dropwise added to a stirred solution of appropriate ketone (59.3 mmol, 1 eq) in glacial AcOH (65 mL), the resulting solution was stirred at room temperature for 8 h. Then ice-water was poured into reaction flask and the resulting precipitate was filtered off, washed with H_2O, and air-dried. The resulting crude product was purified by column flash chromatography using the appropriate eluents.

Bromo-1-(4-chloro-3-methylphenyl)ethan-1-one (30): Following method A, ketone **27** led to obtain a yellow solid which was purified by flash chromatography (petroleum ether/EtOAc 95:5) to afford **30** as a white solid (14.6 g, 95%), R_f =0.71 (petroleum ether/EtOAc 9:1); mp 60-61 °C; ^{1}H NMR (400 MHz, Chloroform-*d*) δ 7.61 (s, 1H), 7.49 (d, *J* = 8.2 Hz, 1H), 7.38 (d, *J* = 8.3 Hz, 1H), 4.56 (s, 2H), 2.40 (s, 3H).

General Procedure for the preparation of ketodiester derivatives (31-33). To a suspension of NaH (60% dispersion in mineral oil, 0.480 g, 20 mmol, 2 eq) in anhydrous THF (26 mL) was added dropwiswe a solution of diethylmalonate (1.83 mL, 12 mmol, 1.2 eq) in anhydrous THF (6.5 mL) under N_2 flow at 0 °C, and the mixture was stirred for 1 h. Then a solution of bromoketone (10 mmol, 1eq) in anhydrous THF (4 mL) was added dropwise and the resulting mixture of reaction was stirred at room temperature until complete conversion of the starting materials (TLC). The reaction was quenched with saturated NH_4Cl aqueous solution, and the aqueous layer extracted with EtOAc. The combined organic layers were washed with H_2O and brine, then dried over Na_2SO_4. The solvent was removed under reduced pressure and the resulting residue was purified by column flash chromatography with the appropriate eluents.

Diethyl 2-[2-oxo-2-(thiophen-2-yl)ethyl]malonate (32): A mixture of diethylmalonate, NaH and **29** was stirred at room temperature for 24 h. The crude product of reaction was purified by flash chromatography (petroleum ether/EtOAc 8:2) to afford **32** as an orange oil (1.90 g, 67%), R_f = 0.21 (petroleum ether/EtOAc 9:1); ^{1}H NMR (400 MHz, Chloroform-*d*) δ 7.76 (t, *J* = 2.8 Hz, 1H), 7.64 (d, *J* = 4.4 Hz, 1H), 7.14 – 7.10 (m, 1H), 4.25 – 4.16 (m, 4H), 4.02 (t, *J* = 7.0 Hz, 1H), 3.54 (d, *J* = 7.4 Hz, 2H), 1.26 (t, *J* = 6.8 Hz, 6H).

Diethyl 2-(2-(4-chloro-3-methylphenyl)-2-oxoethyl)malonate (33): A mixture of diethylmalonate, NaH and **30** was stirred at room temperature for 24 h. The crude product of reaction was purified by flash chromatography (petroleum ether/EtOAc 95:5) to afford **33** as a light yellow oil (1.79 g, 55%), R_f = 0.43 (petroleum ether/EtOAc 9:1);^{1}H NMR (400 MHz, Chloroform-*d*) δ 7.61 (s, 1H), 7.49 (d, *J* = 8.2 Hz, 1H), 7.38 (d, *J* = 8.3 Hz, 1H), 4.28 – 4.19 (m, 4H), 4.09 – 4.01 (m, 1H), 3.63 (d, *J* = 7.1 Hz, 2H), 2.40 (s, 3H), 1.34 – 1.22 (m, 9H).

General procedure for the preparation of dihydropyridazinone derivatives (34-36). To an ice-bath cooled solution of malonate derivatives **31**-**33** (15 mmol, 1 eq) in absolute ethanol (75 mL), hydrazine monohydrate 64-65% (0.79 mL, 16.5 mmol, 1.1 eq) was added

dropwise. The resulting solution was warmed to room temperature, then refluxed for 24 h. The solution was allowed to stand at room temperature and the resulting precipitate was isolated by filtration in vacuum, washed with cold water, and dried to air. The obtained solid was purified by column flash chromatography using the appropriate eluents.

Ethyl 3-oxo-6-(thiophen-2-yl)-2,3,4,5-tetrahydropyridazine-4-carboxylate (35): From **32** was obtained a solid which was purified by flash chromatography (petroleum ether/EtOAc 6:4) to give **35** as a white solid (2.6 g, 70%). R_f = 0.43 (petroleum ether/EtOAc 6:4); mp 150-151 °C; ^{1}H NMR (400 MHz, Chloroform-*d*) δ 8.65 (s, 1H, NH, exch. with D_2O), 7.40 (d, J = 4.9 Hz, 1H), 7.31 (t, J = 2.7 Hz, 1H), 7.10 – 7.03 (m, 1H), 4.26 (q, J = 7.0 Hz, 2H), 3.61 (t, J = 7.8 Hz, 1H), 3.42 (dd, J = 16.8, 8.8 Hz, 1H), 3.12 (dd, J = 16.8, 6.9 Hz, 1H), 1.28 (t, J = 7.1 Hz, 3H).

Ethyl 5-(4-chloro-3-methylphenyl)-2-oxo-1,2,3,4-tetrahydropyridine-3-carboxylate (36): From **33** was obtained a solid which was purified by flash chromatography (petroleum ether/EtOAc 7:3) to give **36** as a pale yellow solid (2.24 g, 52%). R_f = 0.32 (petroleum ether/EtOAc 7:3); mp 164-165 °C; ^{1}H NMR (400 MHz, Chloroform-*d*) δ 8.90 (s, 1H, NH, exch. with D_2O), 7.61 (s, 1H), 7.49 (d, *J* = 8.2 Hz, 1H), 7.38 (d, *J* = 8.3 Hz, 1H), 4.25 (q, *J* = 7.0 Hz, 2H), 3.60 (t, *J* = 7.6 Hz, 1H), 3.41 (dd, *J* = 16.9, 8.2 Hz, 1H), 3.07 (dd, *J* = 17.0, 6.9 Hz, 1H), 2.41 (s, 3H), 1.28 (t, *J* = 7.2 Hz, 3H).

General procedure for the preparation of pyridazinone derivatives (37-39). To a stirred solution of dihydropyridazinone **34**-**36** (5 mmol, 1 eq) in glacial AcOH (30 mL) was added dropwise (30 min) a solution of bromine (0.51 mL, 10 mmol, 2 eq) in glacial AcOH (8 mL). The resulting mixture was stirred at room temperature for 6-8 h. Then the solution was poured into ice-water, and aqueous solution was extracted with a separatory funnel with EtOAc. The collected organic phases were washed with H_2O, saturated $NaHCO_3$ solution and brine. Then, dried (Na_2SO_4) and concentrated under reduced pressure to yield a residue which was purified by column flash chromatography using the appropriate eluents.

Ethyl 6-(5-bromothiophen-2-yl)-3-oxo-2,3-dihydropyridazine-4-carboxylate (38): General procedure for the preparation of pyridazinones was used to oxidize **35.** . The reaction mixture was stirred for 8 h and the obtained crude product purified by flash chromatography (petroleum ether/EtOAc 6:4) to afford **38** as a yellow solid (0.72 g, 44%). R_f = 0.26 (petroleum ether/EtOAc 6:4); mp 179-182 °C; ^{1}H NMR (400 MHz, Chloroform-*d*) δ 11.55 (s, 1H, NH, exch. with D_2O), 8.13 (s, 1H), 7.18 (t, *J* = 3.0 Hz, 1H), 7.06 (t, *J* = 3.1 Hz, 1H), 4.46 (q, *J* = 6.9 Hz, 2H), 1.43 (t, *J* = 7.0 Hz, 3H); ^{13}C NMR (101 MHz, $CDCl_3$) δ 162.75 (C), 157.72 (C), 140.94 (C), 140.78 (C), 139.58 (C), 131.85 (CH), 130.79 (CH), 126.13 (CH), 116.26 (C), 62.58 (CH_2), 14.19 (CH_3).

Ethyl 6-(4-chloro-3-methylphenyl)-3-oxo-2,3-dihydropyridazine-4-carboxylate (39): General procedure for the preparation of pyridazinones was used to oxidize **36.** . The reaction mixture was stirred for 8 h and the obtained crude product purified by flash chromatography (petroleum ether/EtOAc 4:6) to afford **39** as a pale yellow solid (0.8 g, 55%). R_f = 0.33 (petroleum ether/EtOAc 1:1); mp 183-185 °C; ^{1}H NMR (400 MHz,

Chloroform-*d*) δ 8.27 (s, 1H), 7.70 (s, 1H), 7.57 (d, *J* = 8.4 Hz, 1H), 7.44 (d, *J* = 8.3 Hz, 1H), 4.47 (q, *J* = 7.1 Hz, 2H), 2.45 (s, 3H), 1.44 (t, *J* = 7.1 Hz, 3H); ^{13}C NMR (101 MHz, Chloroform-*d*) δ 163.06 (C), 158.53 (C), 144.50 (C), 137.02 (C), 136.33 (C), 133.15 (CH), 132.26 (C), 130.53 (C), 129.76 (CH), 128.29 (CH), 124.52 (CH), 62.48 (CH_2), 20.22 (CH_3), 14.23 (CH_3).

General procedure for the preparation of *N*-alkyl pyridazinone derivatives (40-44). To a solution of pyridazinones **37-39** (4 mmol, 1 eq) in anhydrous DMF (18 mL) was added K_2CO_3 (1.65 g, 12 mmol, 3 eq) and then the suitable alkyl/benzyl halide (12 mmol, 3 eq). The resulting suspension was underwent to ultrasound irradiation for 2 h at room temperature. Then the mixture of reaction was poured into ice-water, filtered off, and extracted with EtOAc in a separatory funnel. The collected organic phases were washed with H_2O, LiCl 5% solution and brine, then dried (Na_2SO_4) and concentrated under reduced pressure. Resulting residue was purified by column flash chromatography using the appropriate eluents.

Ethyl 2-(cyclohexylmethyl)-6-(3,4-dichlorophenyl)-3-oxo-2,3-dihydropyridazine-4-carboxylate (41): From pyridazinone **37** and (bromomethyl)cyclohexane was obtained a residue wihich was purified by flash chromatography (petroleum ether/EtOAc 8:2) to obtain **41** as a pale yellow solid (1.3 g, 77%), R_f = 0.38 (petroleum ether/EtOAc 8:2), mp 94-95 °C; ^{1}H NMR (400 MHz, Chloroform-*d*) δ 8.15 (s, 1H), 7.90 (s, 1H), 7.63 (d, *J* = 8.3 Hz, 1H), 7.54 (d, *J* = 8.3 Hz, 1H), 4.44 (q, *J* = 7.0 Hz, 2H), 4.14 (d, *J* = 7.1 Hz, 2H), 2.09 – 1.99 (m, 1H), 1.85 – 1.56 (m, 5H), 1.42 (t, *J* = 7.0 Hz, 3H), 1.33 – 1.02 (m, 5H); ^{13}C NMR (101 MHz, $CDCl_3$) δ 163.71 (C), 156.71 (C), 140.61 (C), 134.22 (C), 133.82 (C), 133.51 (C), 130.98 (CH), 130.90 (CH), 130.05 (C), 127.57 (CH), 124.79 (CH), 62.42 (CH_2), 59.05 (CH_2), 36.88 (CH), 30.61 (CH_2 x2), 26.27 (CH_2), 25.65 (CH_2 x2), 14.21 (CH_3).

Ethyl 2-(5-chloropentyl)-6-(3,4-dichlorophenyl)-3-oxo-2,3-dihydropyridazine-4-carboxylate (42): From pyridazinone **37** and 1,5-dichloropentane was obtained a residue which was purified by flash chromatography (petroleum ether/EtOAc 8:2) to obtain **42** as an orange oil (1.0 g, 53%), R_f = 0.50 (petroleum ether/EtOAc 7:3); ^{1}H NMR (400 MHz, Chloroform-*d*) δ 8.15 (s, 1H), 7.91 (s, 1H), 7.63 (d, *J* = 8.4 Hz, 1H), 7.54 (d, *J* = 8.1 Hz, 1H), 4.44 (q, *J* = 6.7 Hz, 2H), 4.30 (t, *J* = 7.0 Hz, 2H), 3.54 (t, *J* = 6.1 Hz, 2H), 1.98 – 1.78 (m, 4H), 1.62 – 1.51 (m, 2H), 1.42 (t, *J* = 6.7 Hz, 3H); ^{13}C NMR (101 MHz, $CDCl_3$) δ 163.54 (C), 156.42 (C), 141.11 (C), 134.07 (C), 133.95 (C), 133.55 (C), 131.08, 131.00 (CH), 130.21 (C), 127.60 (CH), 127.60 (CH), 124.80 (CH), 62.44 (CH_2), 52.78 (CH_2), 44.67 (CH_2), 32.04 (CH_2), 27.60 (CH_2), 23.91 (CH_2), 14.20 (CH_3).

Ethyl 6-(5-bromothiophen-2-yl)-2-(4-fluorobenzyl)-3-oxo-2,3-dihydropyridazine-4-carboxylate (43): From pyridazinone **38** and 4-fluorobenzylbromide was obtained a residue which was purified by flash chromatography (petroleum ether/EtOAc 7:3) to obtain **43** as a yellow solid (1.39 g, 80%), R_f = 0.44 (petroleum ether/EtOAc 7:3), mp 123-125 °C; ^{1}H NMR (400 MHz, Chloroform-*d*) δ 8.02 (s, 1H), 7.49 (t, *J* = 8.1, 5.5 Hz, 2H), 7.13 (d, *J* = 3.9 Hz, 1H), 7.05 – 6.98 (m, 3H), 5.31 (s, 2H), 4.42 (q, *J* = 7.1 Hz, 2H), 1.40 (t, *J* = 7.1 Hz, 3H); ^{13}C NMR (101 MHz, $CDCl_3$) δ 163.92 (C), 163.23 (CF), 161.26 (CF), 156.02 (C), 139.95 (C), 139.27 (C), 138.31 (C) 131.21 (CH), 131.13 (CH), 130.79 (CH), 130.60 (C),

130.38 (CH), 125.72 (CH), 115.92 (C), 115.66 (CH), 115.45 (CH), 62.47 (CH_2), 55.24 (CH_2), 14.19 (CH_3).

Ethyl 6-(4-chloro-3-methylphenyl)-3-oxo-2-pentyl-2,3-dihydropyridazine-4-carboxylate (44): From pyridazinone **39** and pentylchloride was obtained a residue which was purified by flash chromatography (petroleum ether/EtOAc 8:2) to obtain **44** as a yellow oil (1.2 g, 85%), R_f = 0.36 (petroleum ether/EtOAc 8:2); ^{1}H NMR (400 MHz, Chloroform-*d*) δ 8.16 (s, 1H), 7.67 (s, 1H), 7.56 (d, *J* = 8.2 Hz, 1H), 7.43 (d, *J* = 8.3 Hz, 1H), 4.45 (q, *J* = 7.1 Hz, 2H), 4.29 (t, *J* = 7.4 Hz, 2H), 2.46 (s, 3H), 1.95 – 1.82 (m, 2H), 1.49 – 1.34 (m, 7H), 0.91 (t, *J* = 6.2 Hz, 3H); ^{13}C NMR (101 MHz, Chloroform-*d*) δ 163.94 (C), 156.54 (C), 142.41 (C), 136.88 (C), 135.92 (C), 132.79 (C), 131.41 (CH), 129.97 (C), 129.68 (CH), 128.11 (CH), 124.41 (CH), 62.32 (CH_2), 53.02 (CH_2), 28.79 (CH_2), 28.10 (CH_2), 20.24 (CH_3), 14.22 (CH_3), 13.95 (CH_3).

General procedure for the preparation of pyridazinone carboxilic acid derivatives 45-49. To a stirred solution of pyridazinone ethyl ester (3 mmol) in EtOH (50 mL), a solution of NaOH 2 M (50 mL) was added. The resulting mixture was heated to reflux and stirred for overnight. Then the solution was allowed to cool at room temperature and acidified with HCl 6M. The resulting precipitate was filtered under vacuum, washed with H_2O and air-dried to yield the analytically pure acid.

2-(Cyclohexylmethyl)-6-(3,4-dichlorophenyl)-3-oxo-2,3-dihydropyridazine-4-carboxylic acid (46): alkaline saponification in hydroalcoholic NaOH of pyridazinone ethyl ester **41** furnished acid **46** as a white solid (1.0 g, 89%), R_f = 0.47 ($CHCl_3$/MeOH 95:5); mp 199-201 °C; ^{1}H NMR (400 MHz, Chloroform-*d*) δ 14.01 (s, 1H), 8.61 (s, 1H), 7.98 (s, 1H), 7.68 (d, *J* = 8.2 Hz, 1H), 7.59 (d, *J* = 8.3 Hz, 1H), 4.24 (d, *J* = 7.0 Hz, 2H), 2.10 – 1.98 (m, 1H), 1.81 – 1.63 (m, 6H), 1.32 – 1.06 (m, 4H); ^{13}C NMR (101 MHz, $CDCl_3$) δ 163.15 (C), 161.94 (C), 144.00 (C), 134.96 (C), 133.91 (C), 133.18 (C), 132.35 (CH), 131.26 (CH), 127.95 (CH), 126.10 (C), 125.10 (CH), 59.20 (CH_2), 37.19 (CH), 30.47 (CH_2 x2), 26.10 (CH_2), 25.54 (CH_2 x2).

2-(5-Chloropentyl)-6-(3,4-dichlorophenyl)-3-oxo-2,3-dihydropyridazine-4-carboxylic acid (47): alkaline saponification in hydroalcoholic NaOH of pyridazinone ethyl ester **42** furnished acid **47** as a light yellow solid (0.99 g, 85%), R_f = 0.44 ($CHCl_3$/MeOH 9:1); mp 102-104 °C; ^{1}H NMR (400 MHz, Chloroform-*d*) δ 8.61 (s, 1H), 7.98 (s, 1H), 7.68 (d, *J* = 8.5 Hz, 1H), 7.58 (d, *J* = 8.3 Hz, 1H), 4.40 (q, *J* = 6.5 Hz, 2H), 3.50 – 3.39 (m, 2H), 1.96 (h, *J* = 7.3 Hz, 2H), 1.67 (p, *J* = 6.9 Hz, 2H), 1.50 (h, *J* = 8.0 Hz, 2H); ^{13}C NMR (101 MHz, $CDCl_3$) δ 163.09 (C), 161.65 (C), 144.30 (C), 134.99 (C), 133.90 (C), 133.11 (C), 132.51 (CH), 131.26 (CH), 127.96 (CH), 126.16 (C), 125.12 (CH), 70.11 (CH_2), 53.39 (CH_2), 29.30 (CH_2), 28.25 (CH_2), 23.36 (CH_2).

6-(5-Bromothiophen-2-yl)-2-(4-fluorobenzyl)-3-oxo-2,3-dihydropyridazine-4-carboxylic acid (48): alkaline saponification in hydroalcoholic NaOH of pyridazinone ethyl ester **43** furnished acid **48** as a yellow solid (1.1 g, 93%), R_f = 0.27 ($CHCl_3$/MeOH 95:5); mp 214-216 °C; ^{1}H NMR (400 MHz, Chloroform-*d*) δ 8.47 (s, 1H), 7.58 – 7.44 (m, 2H), 7.19 – 6.96 (m, 4H), 5.40 (s, 2H); ^{13}C NMR (101 MHz, $CDCl_3$) δ 164.22 (CF), 162.70 (C), 161.76 (CF),

161.11 (C), 142.30 (C), 138.80 (C), 129.97 (C) 131.91 (CH), 131.28 (CH), 131.19 (CH x2), 127.35 (CH), 126.56 (C), 117.48 (C), 116.04 (CH), 115.82 (CH), 55.7 (CH_2).

6-(4-Chloro-3-methylphenyl)-3-oxo-2-pentyl-2,3-dihydropyridazine-4-carboxylic acid (49): alkaline saponification in hydroalcoholic NaOH of pyridazinone ethyl ester **44** furnished acid **49** as a pink solid (0.95 g, 94%), R_f = 0.59 ($CHCl_3$/MeOH 9:1); mp 128-129 °C; ^{1}H NMR (400 MHz, Chloroform-*d*) δ 8.64 (s, 1H), 7.72 (s, 1H), 7.63 (d, *J* = 8.0 Hz, 1H), 7.47 (d, *J* = 7.8 Hz, 1H), 4.37 (t, *J* = 7.6 Hz, 2H), 2.47 (s, 3H), 1.93 (s, 2H), 1.41-1.33 (m, 4H), 0.93 (t, *J* = 6.2 Hz, 3H). ^{13}C NMR (101 MHz Chloroform-*d*) δ 163.43 (C=O), 161.68 (C=O), 145.74 (C), 137.26 (C), 136.97 (C), 132.88 (CH), 131.78 (C), 129.98 (CH), 128.47 (CH), 125.92 (C), 124.75 (CH), 53.40 (CH_2), 28.63 (CH_2), 28.11 (CH_2), 22.23 (CH_2), 20.26 (CH_3), 13.90 (CH_3).

General procedures for the synthesis of carboxamide derivatives (2-24).

Procedure A: To a stirred solution of acids **45-47**, **49** (1 mmol, 1 eq) in DCM (10 mL), HOBt (0.20 g, 1.5 mmol, 1.5 eq) and EDC (0.38 g, 2 mmol, 2 eq) were added. The resulting mixture was stirred at room temperature for 30 min. Afterward a solution of suitable amine in DCM (10 mL) was added dropwise at 0 °C. The mixture of reaction was allowed to stand at room temperature, and then stirred for 12-24 h. The solution was then poured into a separatory funnel and H_2O was added. The aqueous phase was separated, and extracted with DCM. The combined organic phases were washed with H_2O and brine, dried (Na_2SO_4) and concentrated under reduced pressure. The analytically pure product was isolated by column flash chromatography purification using the appropriate eluents.

Procedure B: A solution of acid **48** (410 mg, 1.0 mmol, 1 eq) and thionyl chloride (0.22 mL, 3 mmol, 3 eq) in toluene (9 mL) was refluxed for 3 h. Then, the excess of thionyl chloride was removed under reduced pressure and the resulting dark solid was dissolved in DCM (15 mL). To a resulting solution was added dropwise at 0 °C a solution of appropriate amine (1.5 eq) and Et_3N (1.5 eq) in DCM (15 mL). The mixture of reaction was allowed to stand at room temperature and stirred for 12 h. Then the mixture was poured into a separatory funnel and H_2O was added. The aqueous phase was separated and extracted with DCM. The combined organic phases were washed with H_2O, dried (Na_2SO_4) and concentrated under reduced pressure. The analytically pure product was isolated by column flash chromatography purification using the appropriate eluents.

N*-Cyclohexyl-6-(3,4-dichlorophenyl)-2-(4-fluorobenzyl)-3-oxo-2,3-dihydropyridazine-4-carboxamide (4)*: General procedure A for the synthesis of carboxamides was used to convert acid **45** and cyclohexylamine into the title products. The mixture of reaction was stirred for 16 h then the crude of reaction was purified by flash chromatography (petroleum ether/EtOAc 85:15) to afford **4** (137 mg, 29%), as an orange solid, R_f = 0.29 (petroleum ether/EtOAc 9:1); mp 125-127 °C; IR 1669 (C=O), 3380 (NH); ^{1}H NMR (400 MHz, Chloroform-*d*) δ 9.50 (d, *J* = 8.0 Hz, 1H, NH, exch with D_2O), 8.63 (s, 1H), 7.98 (s, 1H), 7.68 (d, J = 8.4 Hz, 1H), 7.55 (d, J = 8.4 Hz, 1H), 7.47 (t, J = 6.8 Hz, 2H), 7.05 (t, J = 8.4 Hz, 2H), 5.43 (s, 2H), 4.09 – 3.84 (m, 1H), 2.03 – 1.94 (m, 2H), 1.80 – 1.71 (m, 2H), 1.67 – 1.58 (m, 2H), 1.50 – 1.20 (m, 4H); ^{13}C NMR (101 MHz, $CDCl_3$) δ 163.95 (CF), 161.49 (CF),

160.27 (C), 159.65 (C), 143.19 (C), 134.24 (C), 133.98 (C), 133.59 (C), 131.08 (CH), 131.04 (CH), 130.99 (C) 130.78 (CH), 130.70 (CH), 130.33 (C), 127.87 (CH), 125.09 (CH), 115.83 (CH), 115.62 (CH), 55.76 (CH_2), 48.64 (CH), 32.65 (CH_2 x2), 25.58 (CH_2), 24.63 (CH_2 x2); MS (ESI): $C_{24}H_{22}FCl_2N_3O_2$ requires m/z 473.1, found 474.2 $[M + 1]^+$; Anal. calcd for $C_{24}H_{22}FCl_2N_3O_2$: C, 60.77; H, 4.67; N, 8.86; Found: C, 60.89; H, 4.68; N, 8.83.

N*-Cycloheptyl-6-(3,4-dichlorophenyl)-2-(4-fluorobenzyl)-3-oxo-2,3-dihydropyridazine-4-carboxamide (5):* General procedure A for the synthesis of carboxamides was used to convert acid **45** and cycloheptylamine into the title products. The mixture of reaction was stirred for 16 h then the crude of reaction was purified by flash chromatography (petroleum ether/EtOAc 8:2) to afford **5** (240 mg, 50%), as an orange solid, R_f = 0.27 (petroleum ether/EtOAc 9:1); mp 127-129 °C; IR 1662 (C=O), 3376 (NH); ^{1}H NMR (400 MHz, Chloroform-*d*) δ 9.56 (d, *J* = 8.0 Hz, 1H, NH, exch with D_2O), 8.63 (s, 1H), 7.98 (s, 1H), 7.68 (d, J = 8.4 Hz, 1H), 7.55 (d, J = 8.4 Hz, 1H), 7.47 (t, J = 6.4 Hz, 2H), 7.05 (t, J = 7.9 Hz, 2H), 5.43 (s, 2H), 4.25 – 4.04 (m, 1H), 2.06 – 1.91 (m, 2H), 1.79 – 1.48 (m, 10H); ^{13}C NMR (101 MHz, $CDCl_3$) δ 162.93 (CF), 160.47 (CF), 159.01 (C), 158.63 (C), 142.16 (C), 133.22 (C), 132.96 (C), 132.58 (C), 130.98 (C), 130.02 (CH), 130.00 (CH), 129.78 (CH), 129.69 (CH), 129.33 (C), 126.84 (CH), 124.04 (CH), 114.81 (CH), 114.60 (CH), 54.71 (CH_2), 49.93 (CH), 33.68 (CH_2 x2), 27.03 (CH_2 x2), 23.11 (CH_2 x2); MS (ESI): $C_{25}H_{24}FCl_2N_3O_2$ requires m/z 487.1, found 488.1 $[M + 1]^+$; Anal. calcd for $C_{25}H_{24}FCl_2N_3O_2$: C, 61.48; H, 4.95; N, 8.60; Found: C, 61.33; H, 4.94; N, 8.61.

***N*-(Adamantan-1-yl)-6-(3,4-dichlorophenyl)-2-(4-fluorobenzyl)-3-oxo-2,3-dihydropyridazine-4-carboxamide (6):** General procedure A for the synthesis of carboxamides was used to convert acid **45** and 1-adamantylamine into the title products. The mixture of reaction was stirred for 12 h then the crude of reaction was purified by flash chromatography (petroleum ether/EtOAc 85:15) to afford **6** (215 mg, 41%), as a white solid, R_f = 0.47 (petroleum ether/EtOAc 9:1); mp 175-176 °C; IR 1659 (C=O), 3330 (NH); ^{1}H NMR (400 MHz, Chloroform-*d*) δ 9.40 (br s, 1H, NH, exch with D_2O), 8.61 (s, 1H), 7.97 (s, 1H), 7.67 (d, J = 8.4 Hz, 1H), 7.54 (d, J = 8.4 Hz, 1H), 7.47 (t, J = 6.8 Hz, 2H), 7.04 (t, J = 8.3 Hz, 2H), 5.42 (s, 2H), 2.29 – 2.03 (m, 9H), 1.86 – 1.67 (m, 6H); ^{13}C NMR (101 MHz, $CDCl_3$) δ 162.91 (CF), 160.45 (CF), 158.75 (C x2), 142.13 (C), 142.06 (C), 133.17 (C), 133.00 (C), 132.56 (C), 130.16 (C), 130.02 (CH), 129.77 (CH), 129.69 (CH x2), 126.81 (CH), 123.96 (CH), 114.79 (CH), 114.57 (CH), 54.70 (CH_2), 51.46 (C), 40.30 (CH_2 x3), 35.37 (CH_2 x3), 28.40 (CH x3); MS (ESI): $C_{28}H_{26}FCl_2N_3O_2$ requires m/z 525.1, found 526.1 $[M + 1]^+$; Anal. calcd for $C_{28}H_{26}FCl_2N_3O_2$: C, 63.88; H, 4.98; N, 7.98; Found: C, 63.96; H, 4.97; N, 7.96.

***N*-Cyclohexyl-2-(cyclohexylmethyl)-6-(3,4-dichlorophenyl)-3-oxo-2,3-dihydropyridazine-4-carboxamide (9):** General procedure A for the synthesis of carboxamides was used to convert acid **46** and cyclohexylamine into the title products. The mixture of reaction was stirred for 18 h then the crude of reaction was purified by flash chromatography (petroleum ether/EtOAc 9:1) to afford **9** (115 mg, 25%), as a white solid, R_f = 0.35 (petroleum ether/EtOAc 9:1); mp 144-146 °C; IR 1677 (C=O), 3351 (NH); ^{1}H NMR (400 MHz, Chloroform-*d*) δ 9.62 (d, *J* = 8.1 Hz, 1H, NH, exch. with D_2O), 8.63 (s,

1H), 7.98 (s, 1H), 7.69 (d, *J* = 8.4 Hz, 1H), 7.55 (d, *J* = 8.4 Hz, 1H), 4.17 (d, *J* = 7.3 Hz, 2H), 4.06 – 3.91 (m, 1H), 2.07 – 1.93 (m, 4H), 1.82 – 1.58 (m, 7H), 1.51 – 1.03 (m, 10H); ^{13}C NMR (101 MHz, $CDCl_3$) δ 160.60 (C), 160.14 (C), 142.48 (C), 134.24 (C), 134.00 (C), 133.53 (C), 130.98 (CH), 130.54 (CH), 129.69 (C), 127.82 (CH), 125.04 (CH), 58.95 (CH_2), 48.60 (CH), 36.94 (CH), 32.67 (CH_2 x2), 30.58 (CH_2 x2), 26.24 (CH_2 x2), 25.63 (CH_2 x2), 24.64 (CH_2 x2); MS (ESI): $C_{24}H_{29}Cl_2N_3O_2$ requires m/z 461.2, found 462.1 $[M + 1]^+$; Anal. calcd for $C_{24}H_{29}Cl_2N_3O_2$: C, 62.34; H, 6.32; N, 9.09; Found: C, 62.21; H, 6.34; N, 9.06.

***N*-Cycloheptyl-2-(cyclohexylmethyl)-6-(3,4-dichlorophenyl)-3-oxo-2,3-dihydropyridazine-4-carboxamide (10):** General procedure A for the synthesis of carboxamides was used to convert acid **46** and cycloheptylamine into the title products. The mixture of reaction was stirred for 18 h then the crude of reaction was purified by flash chromatography (petroleum ether/EtOAc 93:7) to afford **10** (85 mg, 18%), as a white solid, R_f = 0.25 (petroleum ether/EtOAc 9:1); mp 134-135 °C; IR 1667 (C=O), 3348 (NH); ^{1}H NMR (400 MHz, Chloroform-*d*) δ 9.67 (d, *J* = 8.0 Hz, 1H, NH, exch. with D_2O), 8.63 (s, 1H), 7.98 (s, 1H), 7.69 (d, *J* = 8.5 Hz, 1H), 7.55 (d, *J* = 8.4 Hz, 1H), 4.17 (d, *J* = 7.4 Hz, 3H), 2.08 – 1.95 (m, 3H), 1.81 – 1.54 (m, 14H), 1.33 – 1.06 (m, 6H); ^{13}C NMR (101 MHz, $CDCl_3$) δ 159.35 (C), 159.12 (C), 141.45 (C), 133.24 (C), 132.98 (C), 132.52 (C), 129.97 (CH), 129.47 (CH), 128.71 (C), 126.80 (CH), 124.00 (CH), 57.90 (CH_2), 49.87 (CH), 35.93 (CH), 33.71 (CH_2 x2), 29.56 (CH_2 x2), 27.09 (CH_2), 25.22 (CH_2 x2), 24.61 (CH_2 x2), 23.11 (CH_2 x2); MS (ESI): $C_{25}H_{31}Cl_2N_3O_2$ requires m/z 461.2, found 462.1 $[M + 1]^+$; Anal. calcd for $C_{25}H_{31}Cl_2N_3O_2$: C, 63.02; H, 6.56; N, 8.82; Found: C, 63.16; H, 6.58; N, 8.80.

***N*-(Adamantan-1-yl)-2-(cyclohexylmethyl)-6-(3,4-dichlorophenyl)-3-oxo-2,3-dihydropyridazine-4-carboxamide (11):** General procedure A for the synthesis of carboxamides was used to convert acid **46** and 1-adamantylamine into the title products. The mixture of reaction was stirred for 16 h then the crude of reaction was purified by flash chromatography (petroleum ether/EtOAc 95:5) to afford **11** (210 mg, 41%), as a white solid, R_f = 0.54 (petroleum ether/EtOAc 9:1); mp 179-181 °C; IR 1682 (C=O), 3296 (NH); ^{1}H NMR (400 MHz, Chloroform-*d*) δ 9.51 (br s, 1H, NH, exch. with D_2O), 8.62 (s, 1H), 7.97 (s, 1H), 7.67 (d, *J* = 8.4 Hz, 1H), 7.54 (d, *J* = 8.4 Hz, 1H), 4.16 (d, *J* = 7.2 Hz, 2H), 2.19 – 2.09 (m, 9H), 1.81 – 1.60 (m, 11H), 1.30 – 1.04 (m, 4H); ^{13}C NMR (101 MHz, $CDCl_3$) δ 160.25 (C), 160.08 (C), 142.43 (C), 134.28 (C), 133.95 (C), 133.52 (C), 130.98 (CH), 130.53 (C), 130.17 (CH), 127.78 (CH), 124.93 (CH), 58.92 (CH_2), 52.41 (C), 41.34 (CH_2 x3), 36.91 (CH), 36.41 (CH_2 x3), 30.57 (CH_2 x2), 29.43 (CH x3), 26.25 (CH_2), 25.63 (CH_2 x2); MS (ESI): $C_{28}H_{33}Cl_2N_3O_2$ requires m/z 513.1, found 414.2 $[M + 1]^+$; Anal. calcd for $C_{28}H_{33}Cl_2N_3O_2$: C, 65.37; H, 6.47; N, 8.17; Found: C, 65.44; H, 6.46; N, 8.15.

2-(5-Chloropentyl)-*N*-cyclohexyl-6-(3,4-dichlorophenyl)-3-oxo-2,3-dihydropyridazine-4-carboxamide (14): General procedure A for the synthesis of carboxamides was used to convert acid **47** and cyclohexylamine into the title products. The mixture of reaction was stirred for 24 h then the crude of reaction was purified by flash chromatography (petroleum ether/EtOAc 85:15) to afford **14** (70 mg, 15%), as a yellow oil, R_f = 0.27 (petroleum ether/EtOAc 9:1); IR 1668 (C=O), 3371 (NH); ^{1}H NMR (400 MHz, Chloroform-*d*) δ 9.63 (d, J = 8.2 Hz, 1H, NH, exch. with D_2O), 8.64 (s, 1H), 7.99 (s, 1H), 7.69 (d, *J* = 8.5 Hz, 1H),

7.55 (d, *J* = 9.0 Hz, 1H), 4.33 (t, *J* = 7.2 Hz, 2H), 4.04 – 3.94 (m, 1H), 3.52 – 3.39 (m, 4H), 2.03 – 1.88 (m, 5H), 1.80 – 1.63 (m, 3H), 1.53 – 1.25 (m, 4H), 1.19 (t, *J* = 7.2 Hz, 2H); ^{13}C NMR (101 MHz, $CDCl_3$) δ 160.54 (C), 159.86 (C), 142.85 (C), 134.18 (C), 134.05 (C), 133.55 (C), 130.99 (CH), 130.68 (CH), 129.75 (C), 127.84 (CH), 125.04 (CH), 70.25 (CH_2), 53.08 (CH_2), 48.53 (CH), 32.64 (CH_2 x2), 29.39 (CH_2), 28.31 (CH_2), 25.60 (CH_2), 24.57 (CH_2 x2), 23.44 (CH_2); MS (ESI): $C_{22}H_{26}Cl_3N_3O_2$ requires m/z 469.1, found 470.2 $[M + 1]^+$; Anal. calcd for $C_{22}H_{26}Cl_3N_3O_2$: C, 56.12; H, 5.57; N, 8.93; Found: C, 56.20; H, 5.56; N, 8.95.

2-(5-Chloropentyl)-*N*-cycloheptyl-6-(3,4-dichlorophenyl)-3-oxo-2,3-dihydropyridazine-4-carboxamide (15): General procedure A for the synthesis of carboxamides was used to convert acid **47** and cycloheptylamine into the title products. The mixture of reaction was stirred for 24 h then the crude of reaction was purified by flash chromatography (petroleum ether/EtOAc 9:1) to afford **15** (135 mg, 28%), as a colourless oil, R_f = 0.29 (petroleum ether/EtOAc 9:1); IR 1658 (C=O), 3358 (NH); ^{1}H NMR (400 MHz, Chloroform-*d*) δ 9.68 (d, J = 8.0 Hz, 1H, NH, exch. with D_2O), 8.63 (s, 1H), 7.99 (d, *J* = 2.3 Hz, 1H), 7.69 (d, *J* = 8.5 Hz, 1H), 7.55 (d, *J* = 8.4 Hz, 1H), 4.33 (t, *J* = 7.5 Hz, 2H), 4.22 – 4.13 (m, 1H), 3.51 – 3.39 (m, 4H), 2.06 – 1.86 (m, 4H), 1.74 – 1.44 (m, 10H), 1.23 – 1.14 (m, 2H); ^{13}C NMR (101 MHz, $CDCl_3$) δ 159.29 (C), 158.84 (C), 141.82 (C), 133.17 (C), 133.02 (C), 132.53 (C), 129.97 (CH), 129.62 (CH), 128.76 (C), 126.82 (CH), 124.00 (CH), 69.23 (CH_2), 52.04 (CH_2), 49.79 (CH_2), 33.67 (CH_2 x2), 28.38 (CH_2), 27.30 (CH_2), 27.08 (CH_2 x2), 23.07 (CH_2 x2), 22.43 (CH_2); MS (ESI): $C_{23}H_{28}Cl_3N_3O_2$ requires m/z 483.1, found 484.1 $[M + 1]^+$; Anal. calcd for $C_{23}H_{28}Cl_3N_3O_2$: C, 56.98; H, 5.82; N, 8.67; Found: C, 56.85; H, 5.81; N, 8.70.

***N*-(Adamantan-1-yl)-2-(5-chloropentyl)-6-(3,4-dichlorophenyl)-3-oxo-2,3-dihydropyridazine-4-carboxamide (16):** General procedure A for the synthesis of carboxamides was used to convert acid **47** and 1-adamantylamine into the title products. The mixture of reaction was stirred for 16 h then the crude of reaction was purified by flash chromatography (petroleum ether/EtOAc 9:1) to afford **16** (183 mg, 35%), as a white solid, R_f = 0.35 (petroleum ether/EtOAc 9:1); mp 80-82 °C; IR 1670 (C=O), 3348 (NH); ^{1}H NMR (400 MHz, Chloroform-*d*) δ 9.51 (br s, 1H, NH, exch. with D_2O), 8.61 (s, 1H), 7.98 (s, 1H), 7.67 (d, *J* = 8.3 Hz, 1H), 7.53 (d, *J* = 8.4 Hz, 1H), 4.42 – 4.26 (m, 2H), 3.54 – 3.37 (m, 2H), 2.21 – 2.06 (m, 9H), 2.00 – 1.85 (m, 2H), 1.81 – 1.61 (m, 6H), 1.56 – 1.43 (m, 2H), 1.27 – 1.13 (m, 2H); ^{13}C NMR (101 MHz, $CDCl_3$) δ 158.95 (C), 141.79 (C), 133.26 (C), 133.20 (C), 132.98 (C), 132.52 (C), 129.97 (CH), 129.62 (C), 129.29 (CH), 126.78 (CH), 123.91 (CH), 69.24 (CH_2), 52.07 (CH_2), 51.39 (C), 40.34 (CH_2 x3), 35.39 (CH_2 x3), 28.41 (CH x3), 28.37 (CH_2), 27.29 (CH_2), 22.41 (CH_2); MS (ESI): $C_{26}H_{30}Cl_3N_3O_2$ requires m/z 521.1, found 522.1 $[M + 1]^+$; Anal. calcd for $C_{26}H_{30}Cl_3N_3O_2$: C, 59.72; H, 5.78; N, 8.04; Found: C, 59.64; H, 5.77; N, 8.01.

6-(5-Bromothiophen-2-yl)-*N*-cyclohexyl-2-(4-fluorobenzyl)-3-oxo-2,3-dihydropyridazine-4-carboxamide (19): General procedure B for the synthesis of carboxamides was used to convert acid **48** and cyclohexylamine into the title products. Purified by flash chromatography (petroleum ether/EtOAc 8:2) to afford **19** (240 mg, 49%), as a pale yellow

solid, R_f = 0.23 (petroleum ether/EtOAc 9:1); mp 137-140 °C; IR 1679 (C=O), 3340 (NH); ^{1}H NMR (400 MHz, Chloroform-*d*) δ 9.52 (d, J = 8.2 Hz, 1H, NH, exch with D_2O), 8.50 (s, 1H), 7.54 – 7.42 (m, 2H), 7.24 (d, *J* = 4.0 Hz, 1H), 7.07 – 7.01 (m, 3H), 5.34 (s, 2H), 4.03 – 3.87 (m, 1H), 2.06 – 1.89 (m, 2H), 1.80 – 1.68 (m, 2H), 1.66 – 1.57 (m, 2H), 1.51 – 1.31 (m, 4H); ^{13}C NMR (101 MHz, $CDCl_3$) δ 162.94 (CF), 160.48 (CF), 159.20 (C), 158.41 (C), 140.05 (C), 138.96 (C), 130.01 (C), 129.92 (CH), 129.88 (CH), 129.80 (CH), 129.20 (C), 129.06 (CH), 125.46 (CH), 115.11 (C), 114.76 (CH), 114.55 (CH), 54.18 (CH_2), 47.63 (CH), 31.62 (CH_2 x2), 24.57 (CH_2), 23.62 (CH_2 x2); MS (ESI): $C_{22}H_{21}BrFN_3O_2S$ requires m/z 489.0, found 490.0 $[M + 1]^+$; Anal. calcd for $C_{22}H_{21}BrFN_3O_2S$: C, 53.88; H, 4.32; N, 8.57; Found: C, 53.97; H, 4.31; N, 8.55.

6-(5-Bromothiophen-2-yl)-*N*-cycloheptyl-2-(4-fluorobenzyl)-3-oxo-2,3-dihydropyridazine-4-carboxamide (20): General procedure B for the synthesis of carboxamides was used to convert acid **48** and cycloheptylamine into the title products. Purified by flash chromatography (petroleum ether/EtOAc 9:1) to afford **20** (196 mg, 39%), as a yellow solid, R_f = 0.24 (petroleum ether/EtOAc 9:1); mp 151-152 °C; IR 1672 (C=O), 3331 (NH); ^{1}H NMR (400 MHz, Chloroform-*d*) δ 9.58 (d, J = 8.0 Hz, 1H, NH, exch with D_2O), 8.50 (s, 1H), 7.49 – 7.44 (m, 2H), 7.23 (d, *J* = 4.0 Hz, 1H), 7.07 – 7.01 (m, 3H), 5.34 (s, 2H), 4.30 – 4.01 (m, 1H), 2.04 – 1.93 (m, 2H), 1.79 – 1.43 (m, 10H); ^{13}C NMR (101 MHz, $CDCl_3$) δ 162.93 (CF), 160.48 (CF), 158.97 (C), 158.41 (C), 140.05 (C), 138.97 (C), 130.02 (C), 129.92 (CH), 129.89 (CH), 129.81 (CH), 129.22 (C), 129.01 (CH), 125.43 (CH), 115.10 (C), 114.76 (CH), 114.54 (CH), 54.14 (CH_2), 49.93 (CH), 33.67 (CH_2 x2), 27.03 (CH_2 x2), 23.12 (CH_2 x2); MS (ESI): $C_{23}H_{23}BrFN_3O_2S$ requires m/z 503.0, found 504.1 $[M + 1]^+$; Anal. calcd for $C_{23}H_{23}BrFN_3O_2S$: C, 54.77; H, 4.60; N, 8.33; Found: C, 54.70; H, 4.61; N, 8.31.

***N*-(Adamantan-1-yl)-6-(5-bromothiophen-2-yl)-2-(4-fluorobenzyl)-3-oxo-2,3-dihydropyridazine-4-carboxamide (21):** General procedure B for the synthesis of carboxamides was used to convert acid **48** and 1-adamantylamine into the title products. Purified by flash chromatography (petroleum ether/EtOAc 9:1) to afford **21** (217 mg, 40%), as a white solid, R_f = 0.25 (petroleum ether/EtOAc 95:5); mp 188-190 °C; IR 1664 (C=O), 3297 (NH); ^{1}H NMR (400 MHz, Chloroform-*d*) δ 9.42 (br s, 1H, NH, exch with D_2O), 8.48 (s, 1H), 7.51 – 7.42 (m, 2H), 7.20 (d, *J* = 4.0 Hz, 1H), 7.08 – 6.98 (m, 3H), 5.33 (s, 2H), 2.15 – 2.11 (m, 9H), 1.74 – 1.70 (m, 6H); ^{13}C NMR (101 MHz, $CDCl_3$) δ 162.92 (CF), 160.47 (CF), 158.69 (C), 158.53 (C), 140.04 (C), 139.04 (C), 130.06 (C), 130.02 (C), 129.93 (CH), 129.89 (CH), 129.81 (CH), 128.70 (CH), 125.30 (CH), 115.04 (C), 114.74 (CH), 114.52 (CH), 54.14 (CH_2), 51.45 (C), 40.31 (CH_2 x3), 35.38 (CH_2 x3), 28.41 (CH x3); MS (ESI): $C_{26}H_{25}BrFN_3O_2S$ requires m/z 541.1, found 542.1 $[M + 1]^+$; Anal. calcd for $C_{26}H_{25}BrFN_3O_2S$: C, 57.57; H, 4.65; N, 7.75; Found: C, 57.63; H, 4.64; N, 7.77.

6-(4-Chloro-3-methylphenyl)-*N*-cyclohexyl-3-oxo-2-pentyl-2,3-dihydropyridazine-4-carboxamide (23): General procedure A for the synthesis of carboxamides was used to convert acid **44** and cyclohexylamine into the title product. The mixture of reaction was stirred for 16 h, then the crude of reaction was purified by flash chromatography (petroleum ether/EtOAc 9:1) to afford **23** (99 mg, 24%) as a colourless oil. R_f = 0.74 (petroleum ether/EtOAc 8:2); IR 1676 (C=O), 3295 (NH); ^{1}H NMR (400 MHz, Chloroform-

d) δ 9.69 (d, *J* = 8.1 Hz, 1H, NH, exch. with D_2O), 8.64 (s, 1H), 7.73 (s, 1H), 7.63 (d, J = 8.3 Hz, 1H), 7.43 (d, J = 8.3 Hz, 1H), 4.31 (t, J = 7.6 Hz, 2H), 4.09 – 3.92 (m, 1H), 2.45 (s, 3H), 2.06 – 1.83 (m, 4H), 1.82 – 1.57 (m, 4H), 1.52 – 1.25 (m, 8H), 0.92 (t = J = 6.3 Hz, 3H); ^{13}C NMR (101 MHz, $CDCl_3$) δ 159.79 (C), 158.89 (C), 143.24 (C), 135.84 (C), 135.06 (C), 131.78 (C), 130.03 (CH), 128.67 (CH), 128.46 (C), 127.35 (CH), 123.63 (CH), 52.03 (CH_2), 47.48 (CH), 31.64 (CH_2 x2), 27.78 (CH_2), 27.16 (CH_2), 24.60 (CH_2), 23.59 (CH_2 x2), 21.30 (CH_2), 19.19 (CH_3), 12.93 (CH_3); MS (ESI): $C_{23}H_{30}ClN_3O_2$ requires m/z 415.2, found 416.2 $[M + 1]^+$; Anal. calcd for $C_{23}H_{30}ClN_3O_2$: C, 66.41; H, 7.27; N, 10.10; Found: C, 66.50; H, 7.25; N, 10.13.

6-(4-Chloro-3-methylphenyl)-*N*-cycloheptyl-3-oxo-2-pentyl-2,3-dihydropyridazine-4-carboxamide (24): General procedure A for the synthesis of carboxamides was used to convert acid **44** and cycloheptylamine into the title product. The mixture of reaction was stirred for 18 h, then the crude of reaction was purified by flash chromatography (petroleum ether/EtOAc 9:1) to afford **24** (115 mg, 27%) as a colourless oil. R_f = 0.75 (petroleum ether/EtOAc 8:2); IR 1681 (C=O), 3290 (NH); ^{1}H NMR (400 MHz, Chloroform-*d*) δ 9.75 (d, *J* = 8.1 Hz, 1H, NH, exch. with D_2O), 8.65 (s, 1H), 7.73 (s, 1H), 7.63 (d, J = 8.3 Hz, 1H), 7.43 (d, J = 8.3 Hz, 1H), 4.31 (t, J = 7.5 Hz, 2H), 4.22 – 4.12 (m, 1H), 2.45 (s, 3H), 2.05 – 1.96 (m, 2H), 1.95 – 1.85 (m, 2H), 1.80 – 1.48 (m, 10H), 1.45 – 1.35 (m, 4H), 0.93 (t, J = 6.4 Hz, 3H); ^{13}C NMR (101 MHz, $CDCl_3$) δ 160.57 (C), 159.90 (C), 144.25 (C), 136.85 (C), 136.08 (C), 132.80 (C), 131.00 (CH), 129.70 (CH), 129.50 (C), 128.37 (CH), 124.63 (CH), 53.04 (CH_2), 50.78 (CH), 34.71 (CH_2 x2), 28.80 (CH_2), 28.18 (CH_2 x2), 28.11 (CH_2 x2), 24.10 (CH_2), 22.33 (CH_2), 20.21 (CH_3), 13.96 (CH_3).; MS (ESI): $C_{24}H_{32}ClN_3O_2$ requires m/z 429.2, found 430.3 $[M + 1]^+$; Anal. calcd for $C_{24}H_{32}ClN_3O_2$: C, 67.04; H, 7.50; N, 9.77; Found: C, 67.01; H, 7.49; N, 9.75.

Figure S1. ^{1}H-NMR ($CDCl_3$, 400 MHz): Compound **2**

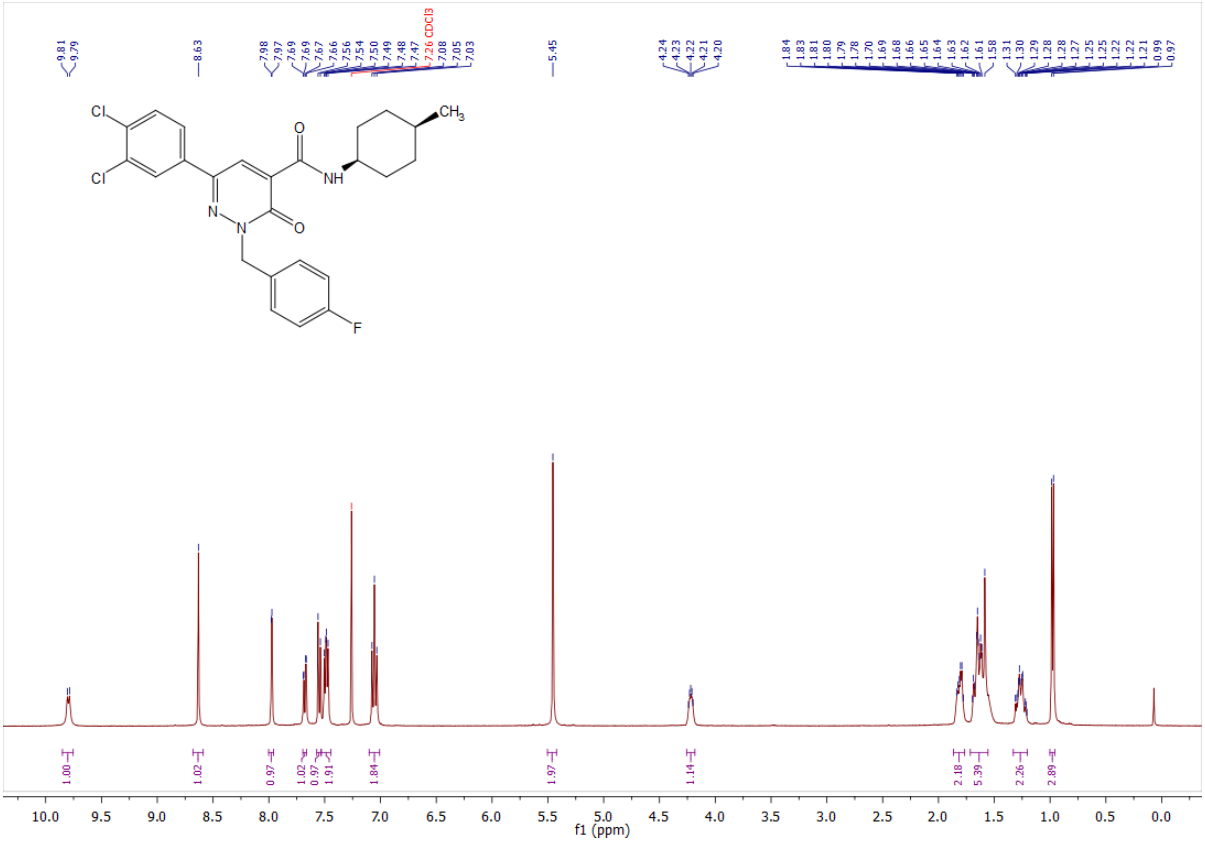

Figure S2. ^{13}C-APT ($CDCl_3$, 101 MHz): Compound **2**

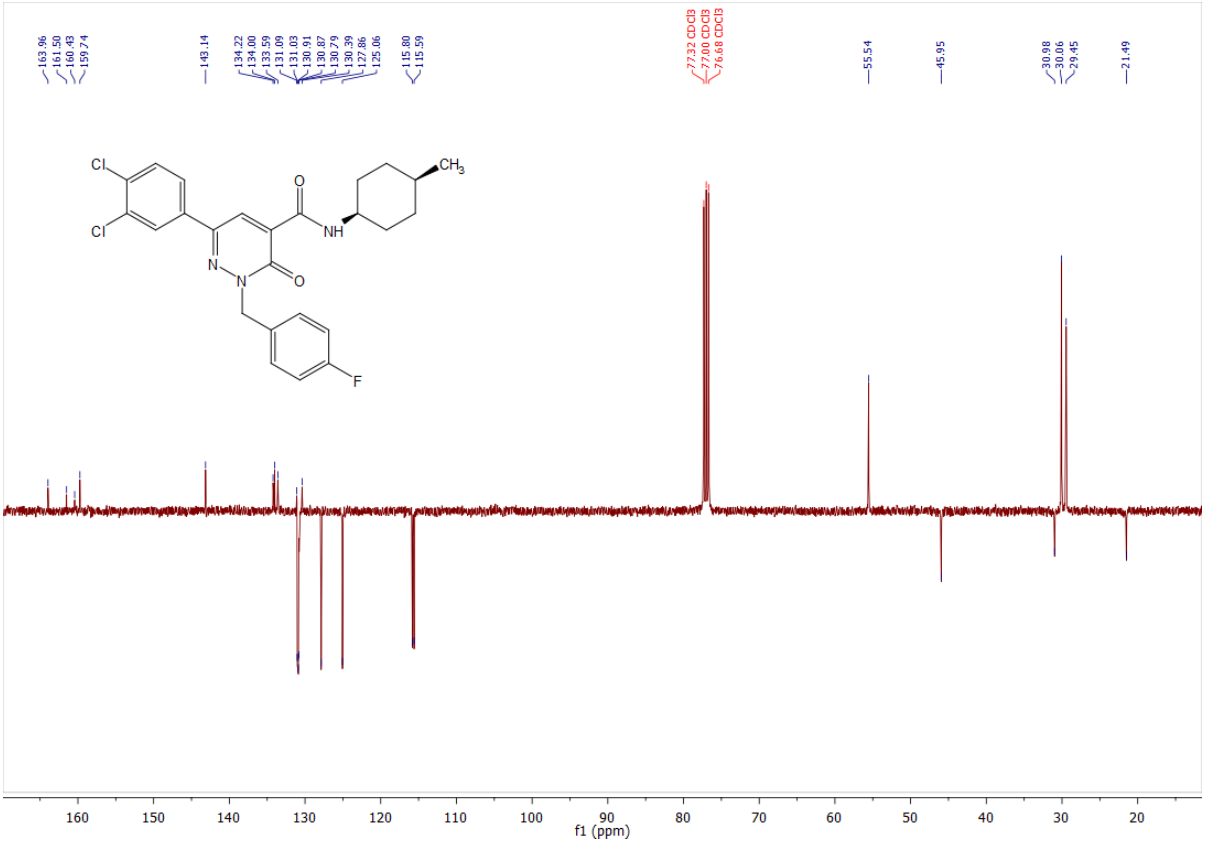

Figure S3. ^{1}H-NMR ($CDCl_3$, 400 MHz): Compound **3**

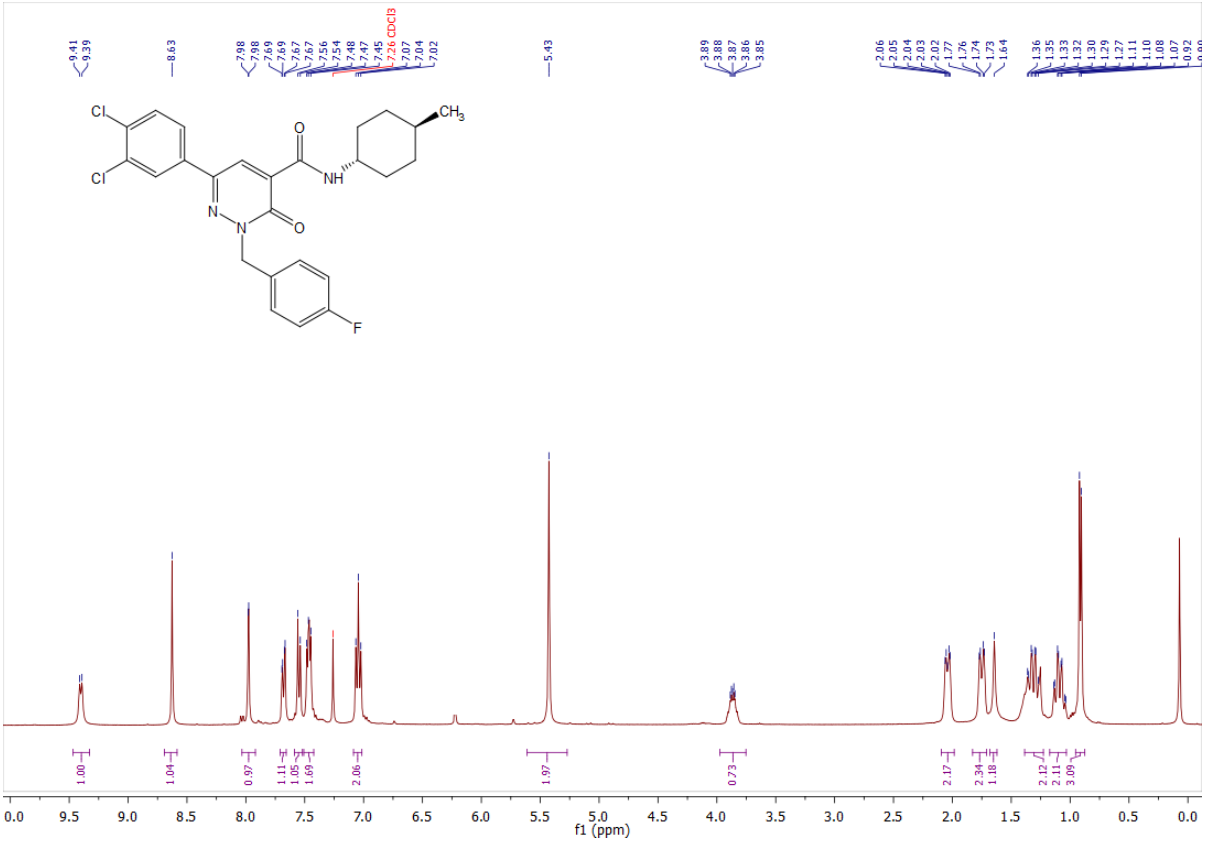

Figure S4. ^{13}C-APT ($CDCl_3$, 101 MHz): Compound **3**

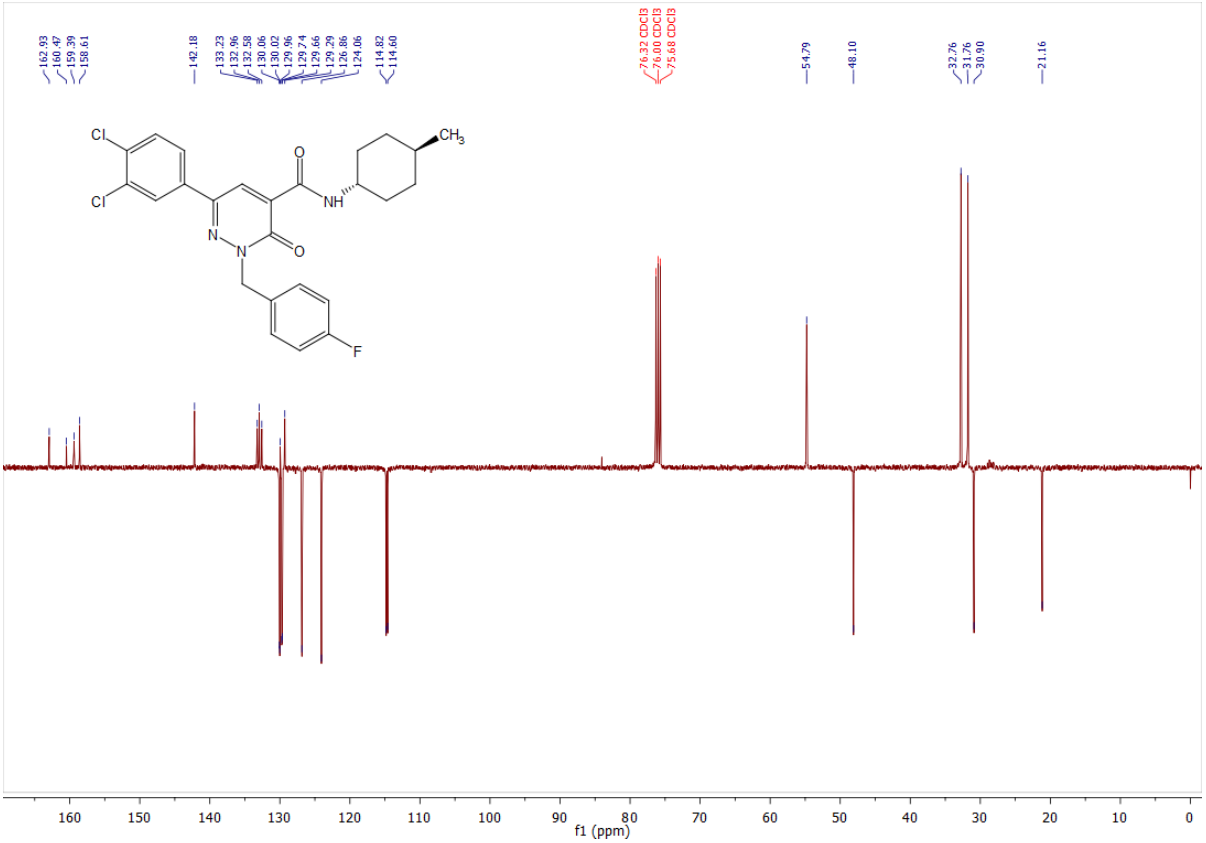

Figure S5. ^{1}H-NMR ($CDCl_3$, 400 MHz): Compound **4**

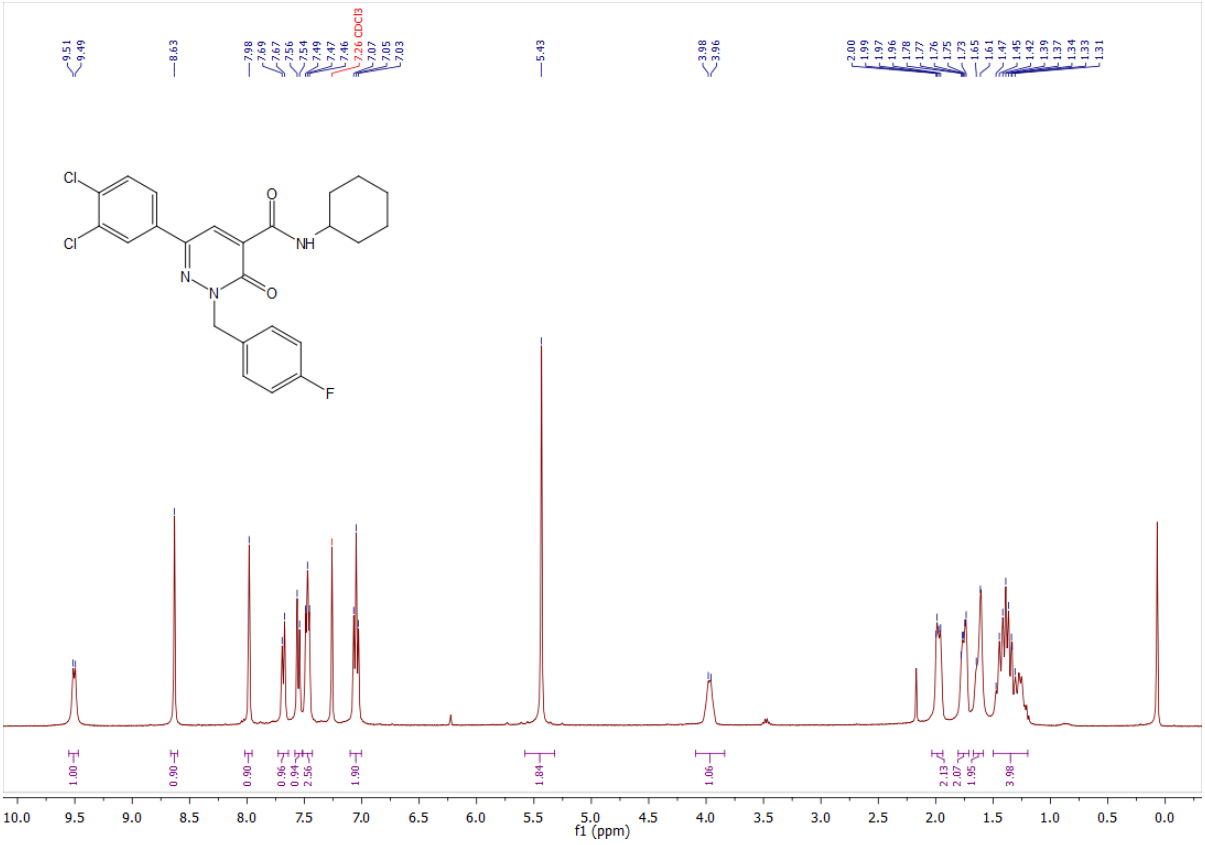

Figure S6. ^{13}C-APT ($CDCl_3$, 101 MHz): Compound **4**

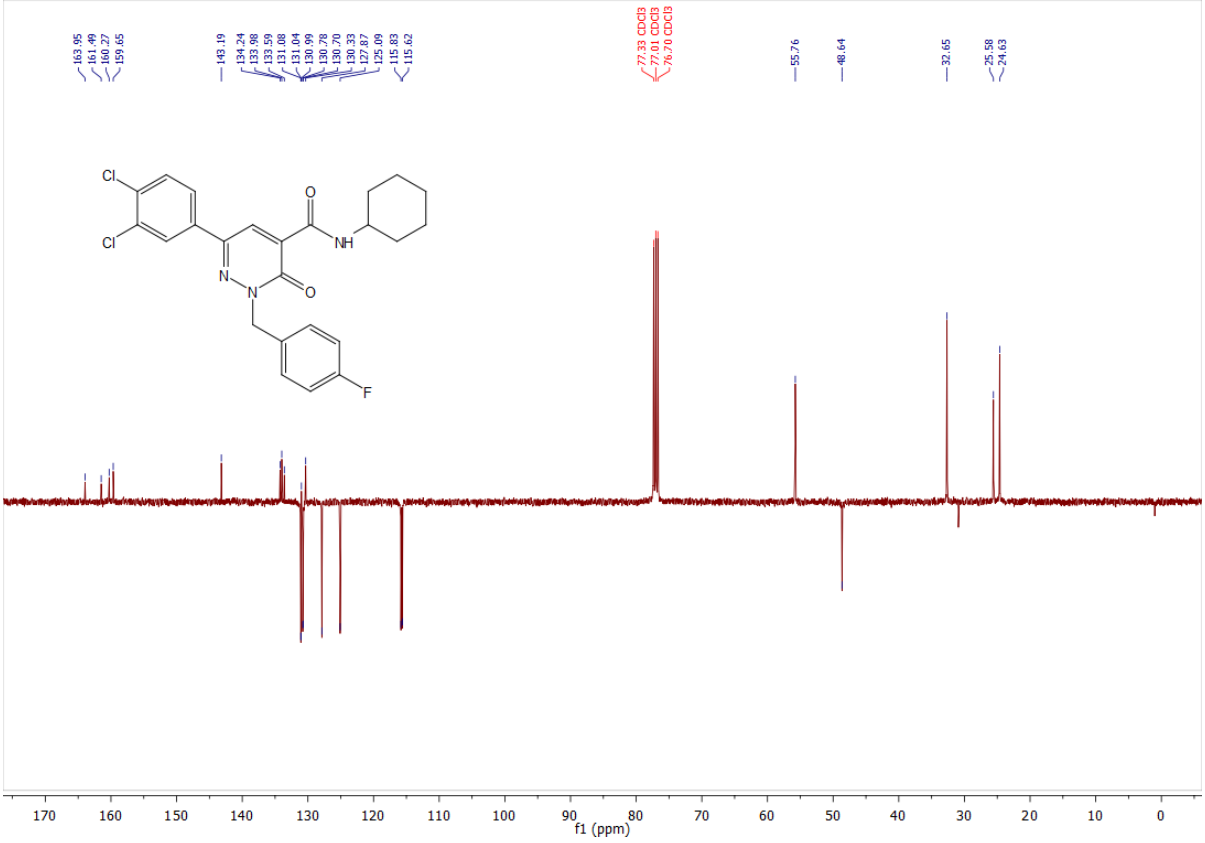

Figure S7. ^{1}H-NMR ($CDCl_3$, 400 MHz): Compound **5**

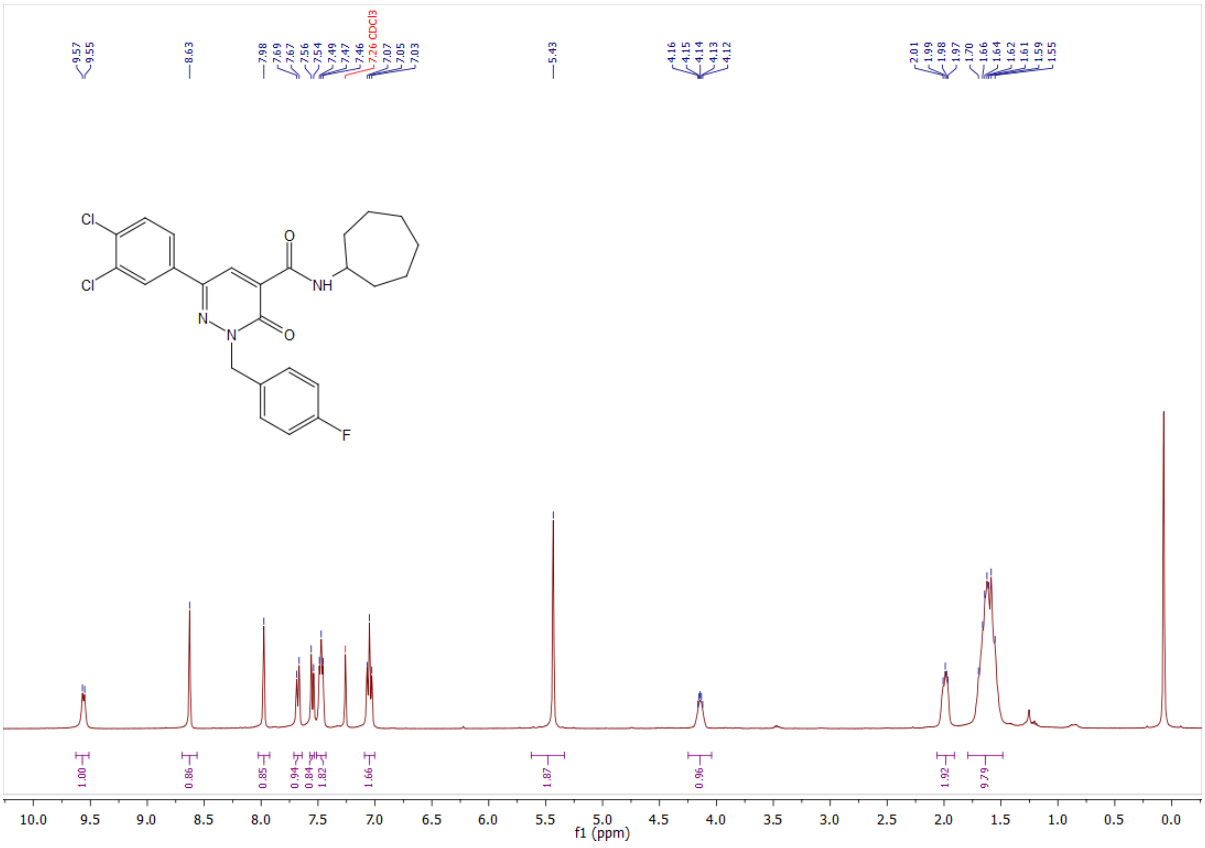

Figure S8. ^{13}C-APT ($CDCl_3$, 101 MHz): Compound **5**

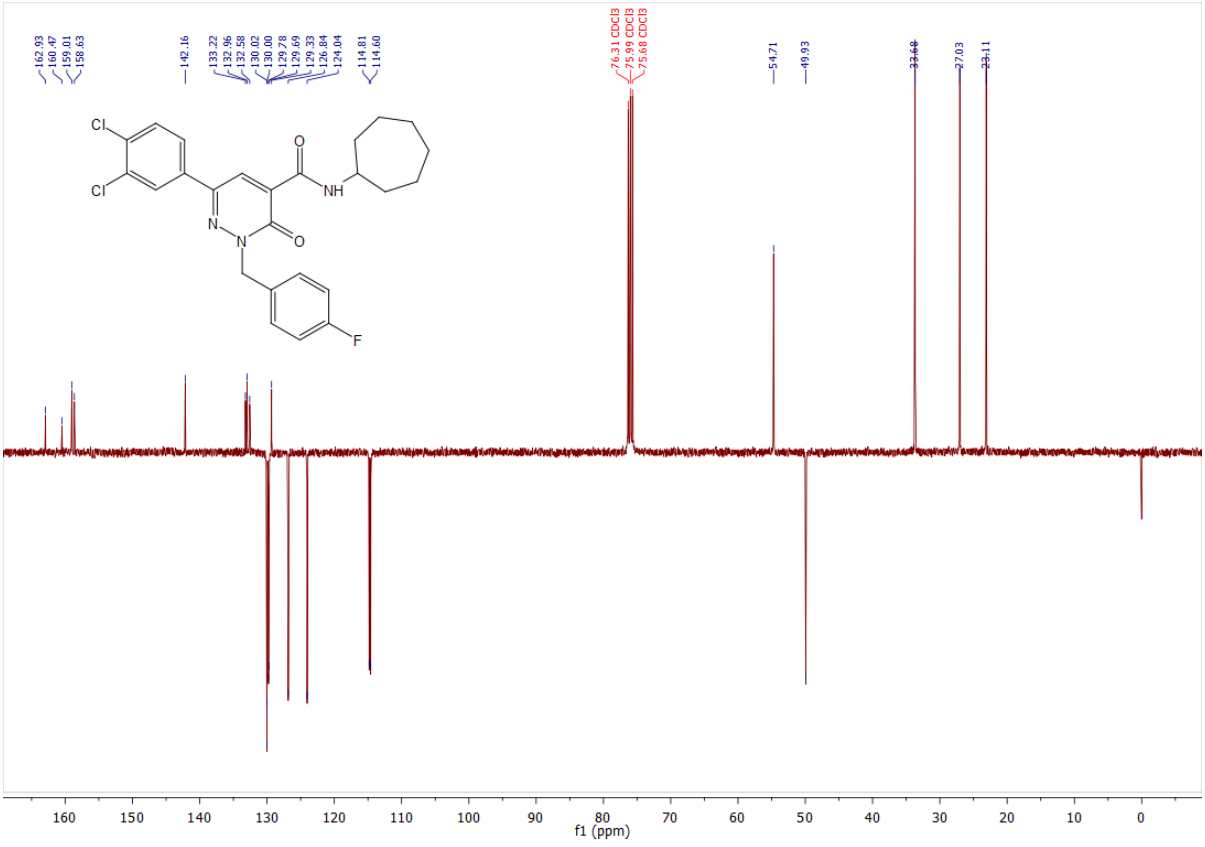

Figure S9. ^{1}H-NMR ($CDCl_3$, 400 MHz): Compound **6**

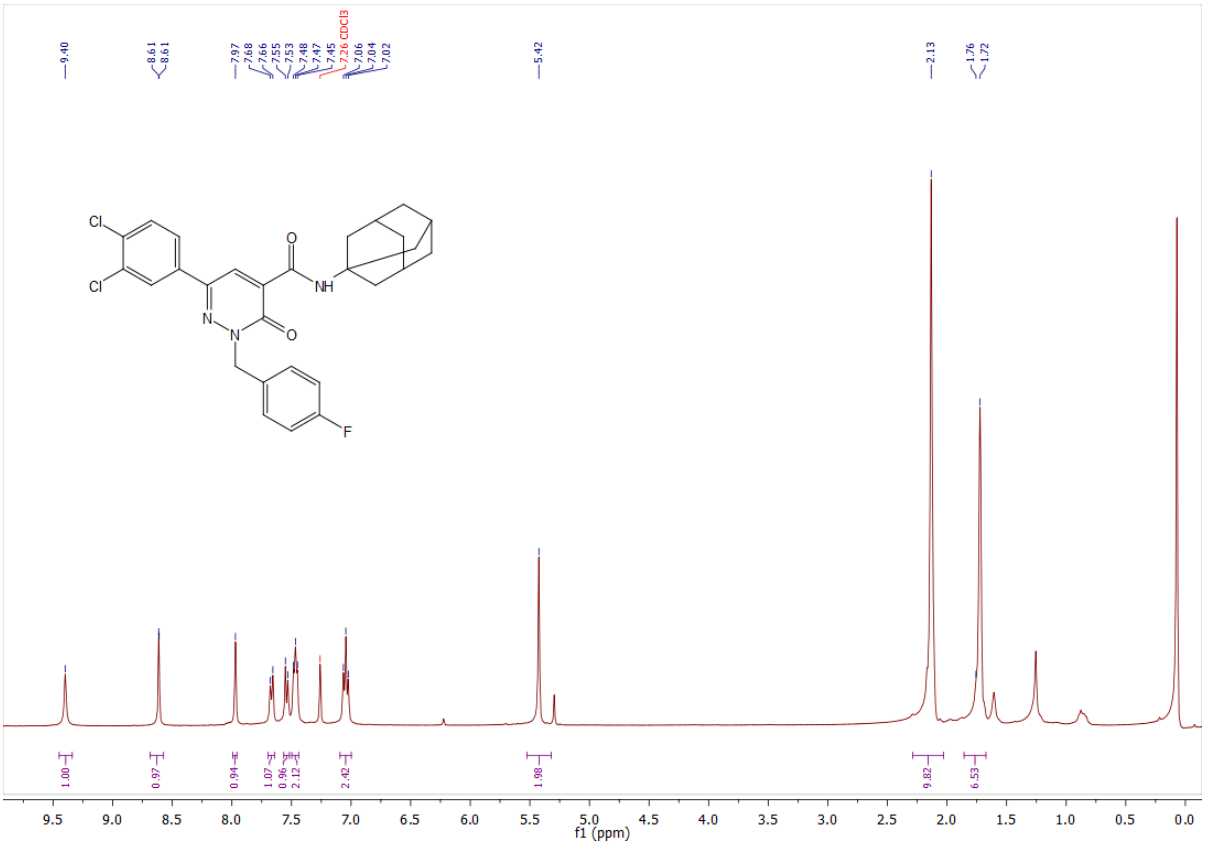

Figure S10. ^{13}C-APT ($CDCl_3$, 101 MHz): Compound **6**

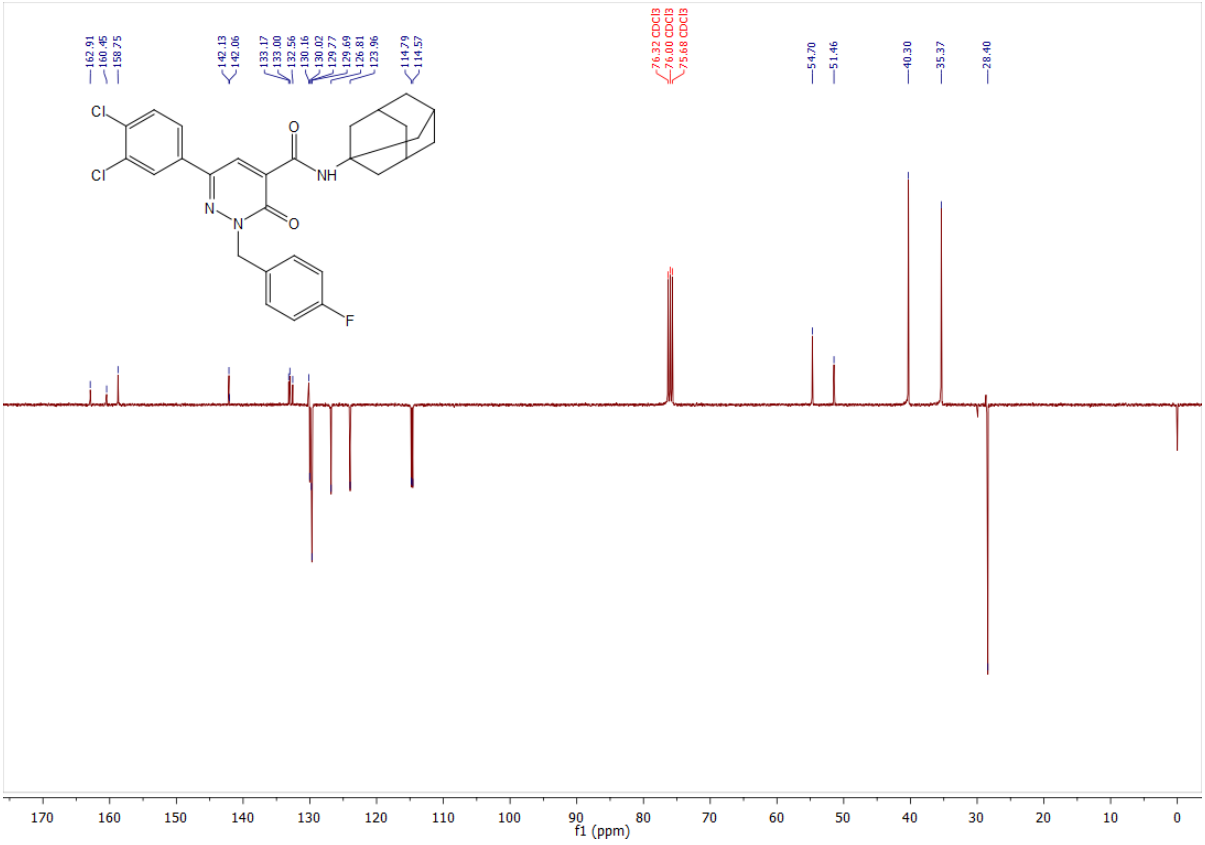

Figure S11. ^{1}H-NMR ($CDCl_3$, 400 MHz): Compound **7**

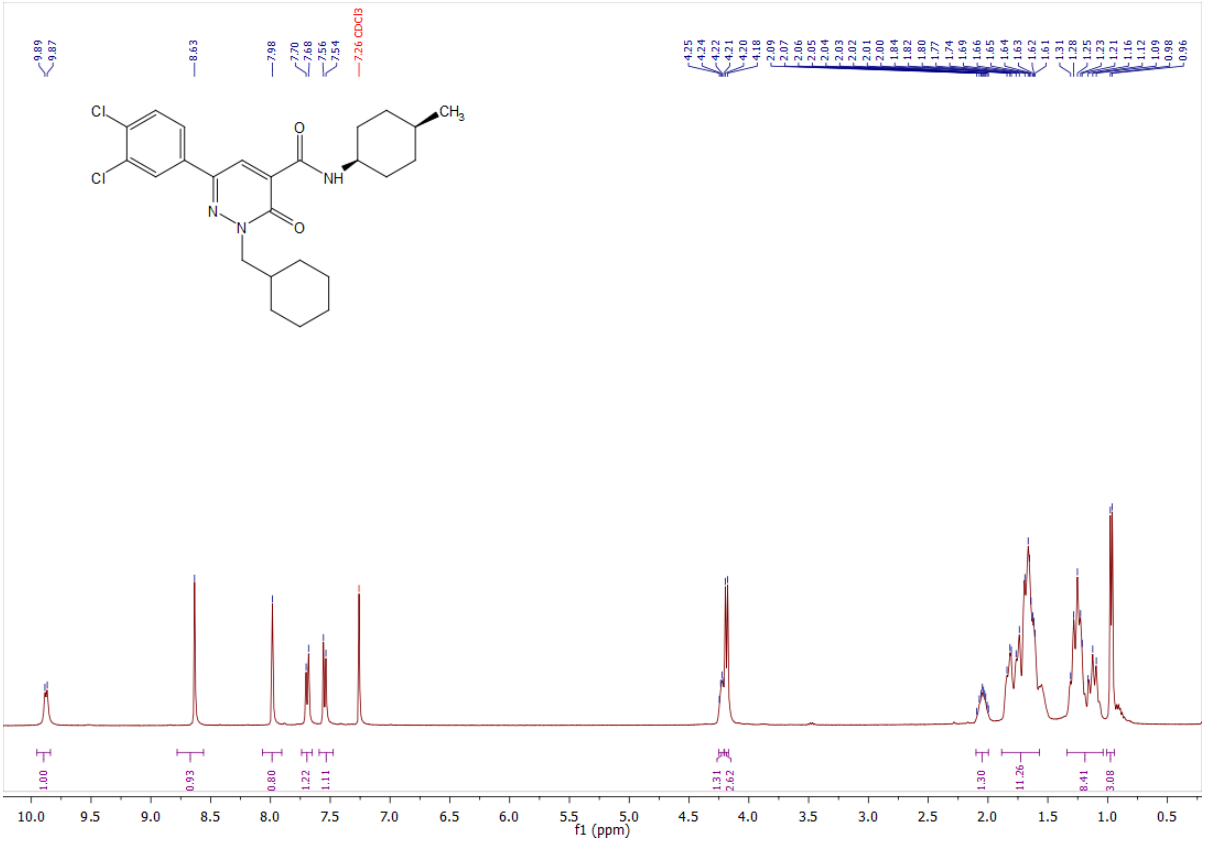

Figure S12. ^{13}C-APT ($CDCl_3$, 101 MHz): Compound **7**

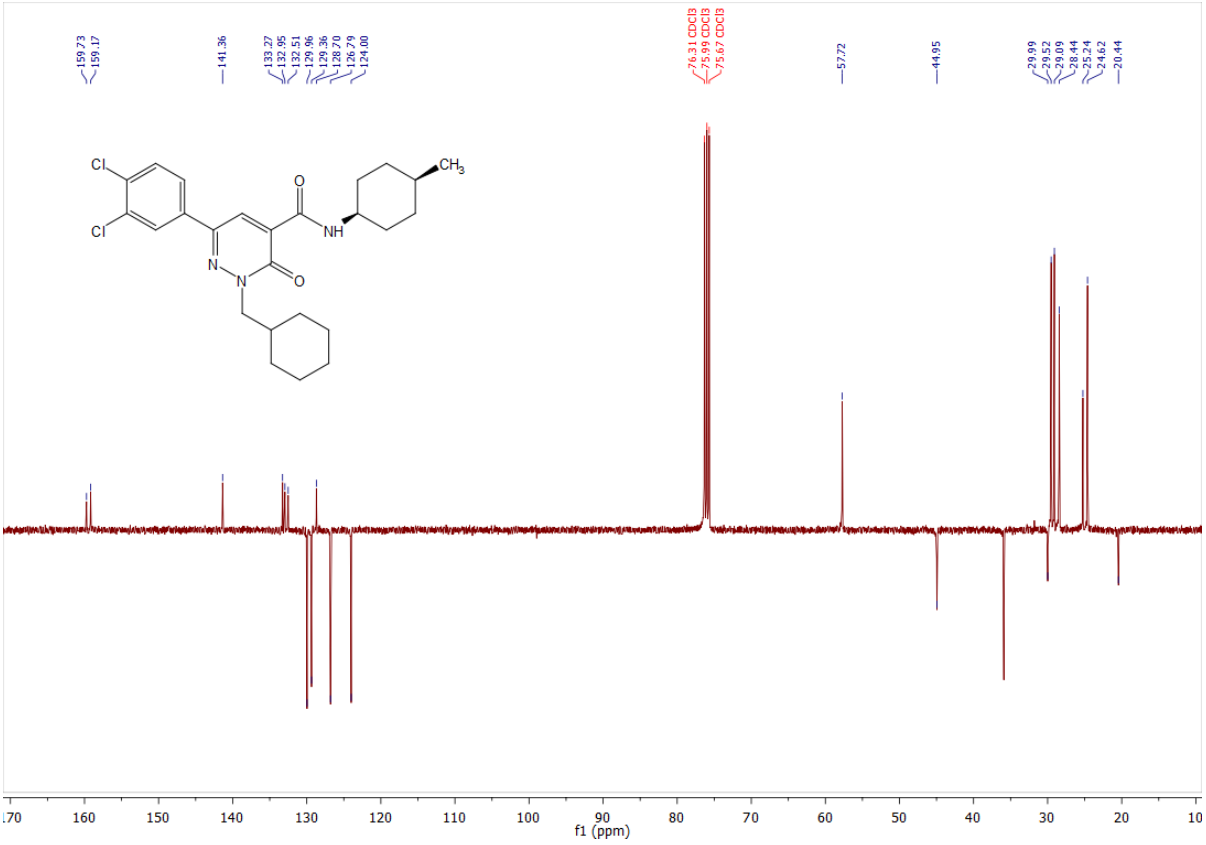

Figure S13. ^{1}H-NMR ($CDCl_3$, 400 MHz): Compound **8**

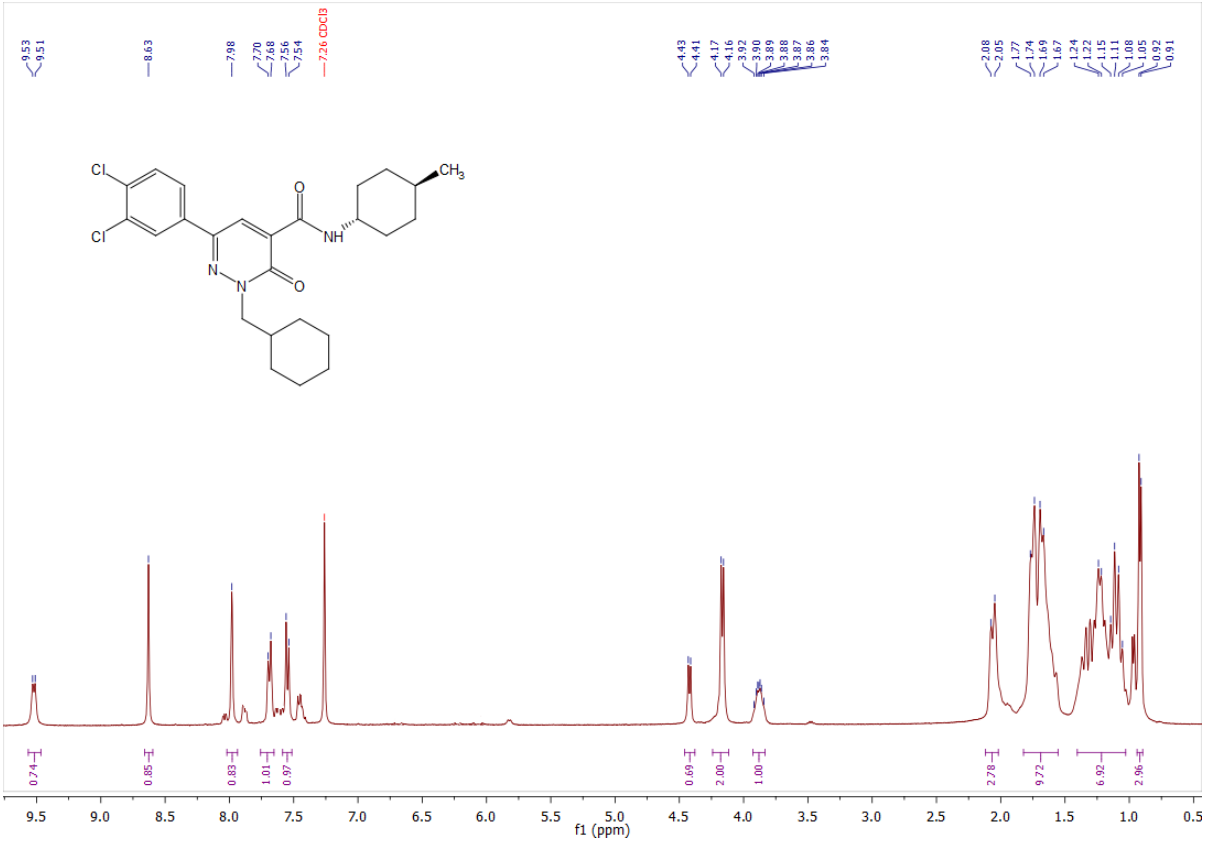

Figure S14. ^{13}C-APT ($CDCl_3$, 101 MHz): Compound **8**

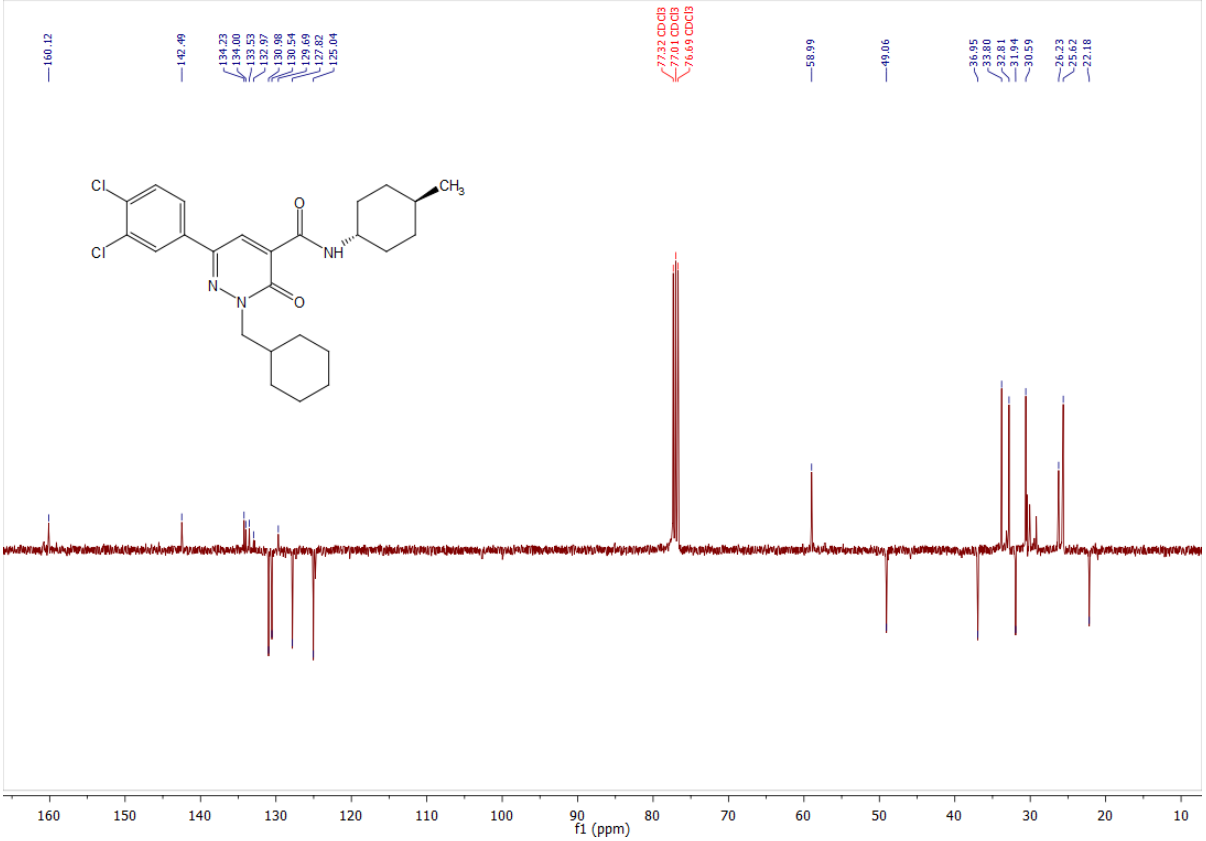

Figure S15. ^{1}H-NMR ($CDCl_3$, 400 MHz): Compound **9**

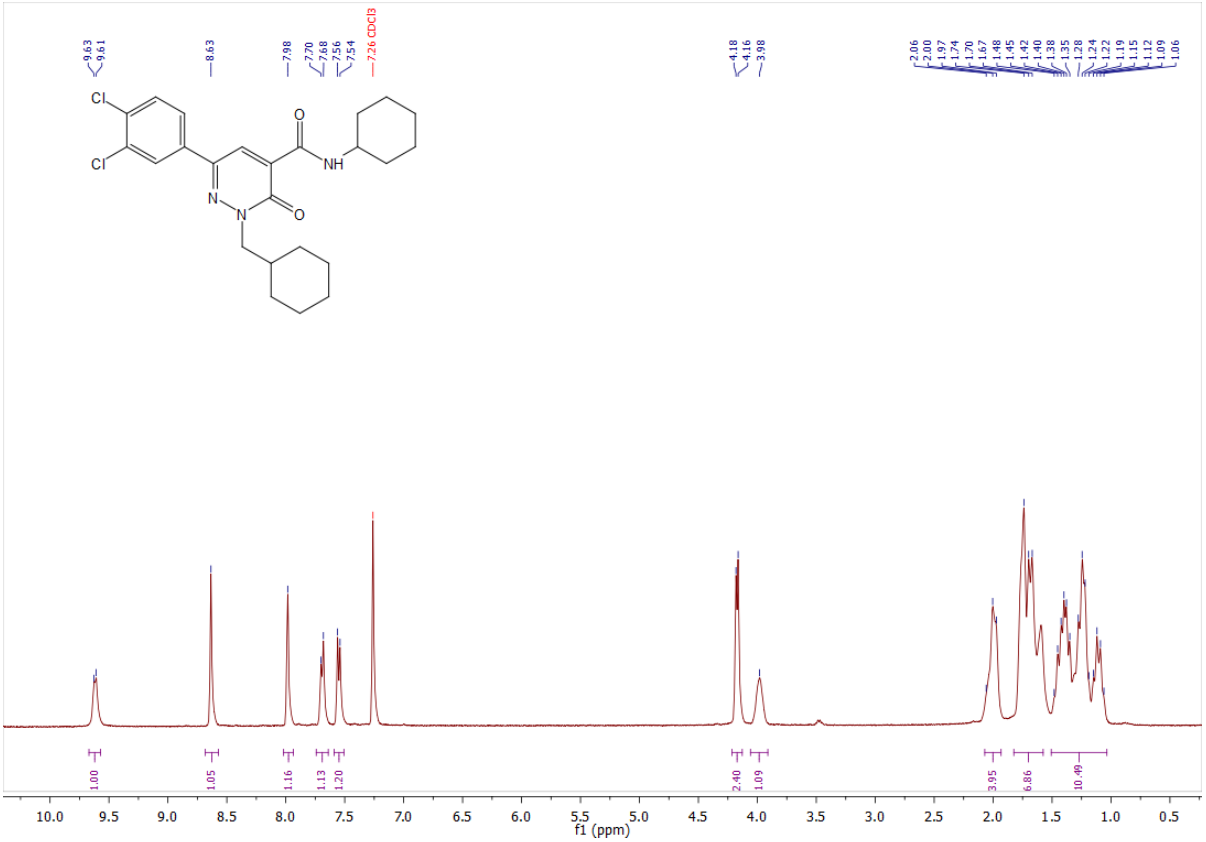

Figure S16. ^{13}C-APT ($CDCl_3$, 101 MHz): Compound **9**

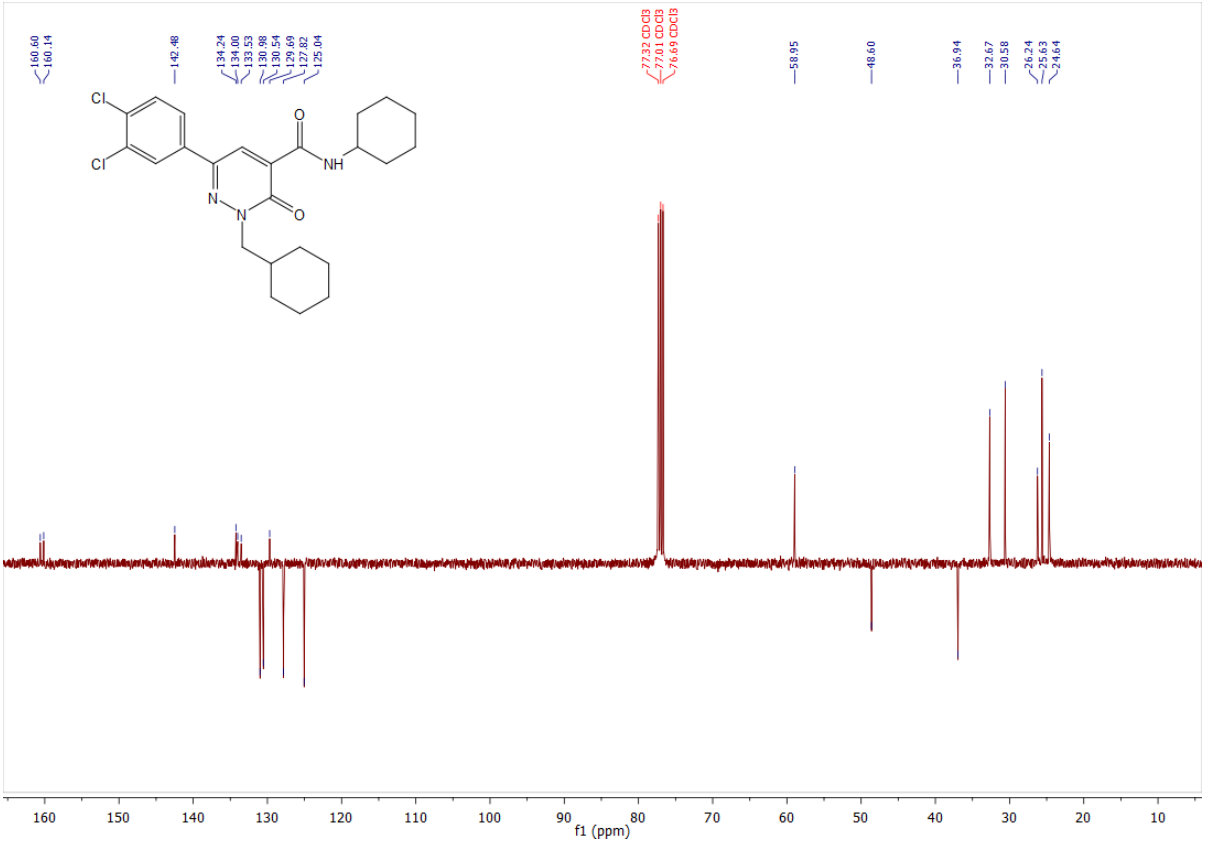

Figure S17. ^{1}H-NMR ($CDCl_3$, 400 MHz): Compound **10**

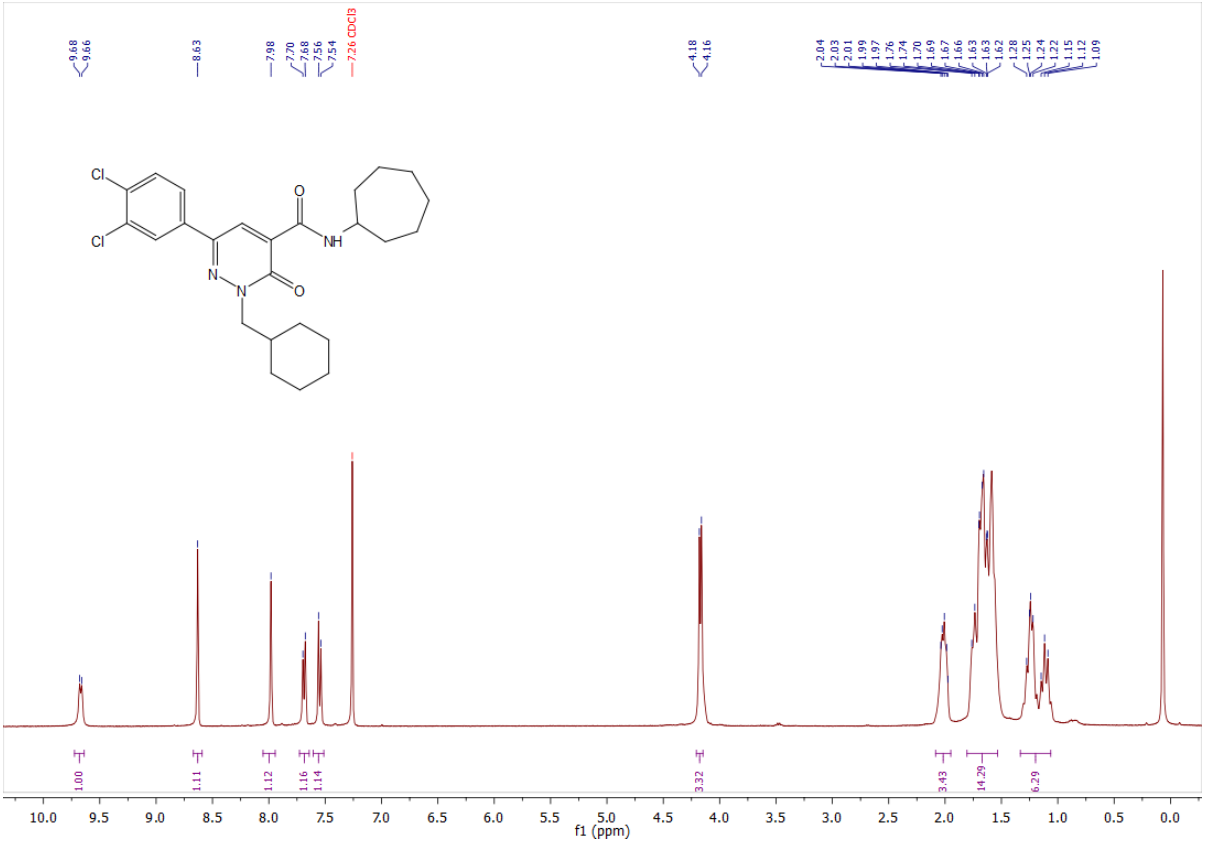

Figure S18. ^{13}C-APT ($CDCl_3$, 101 MHz): Compound **10**

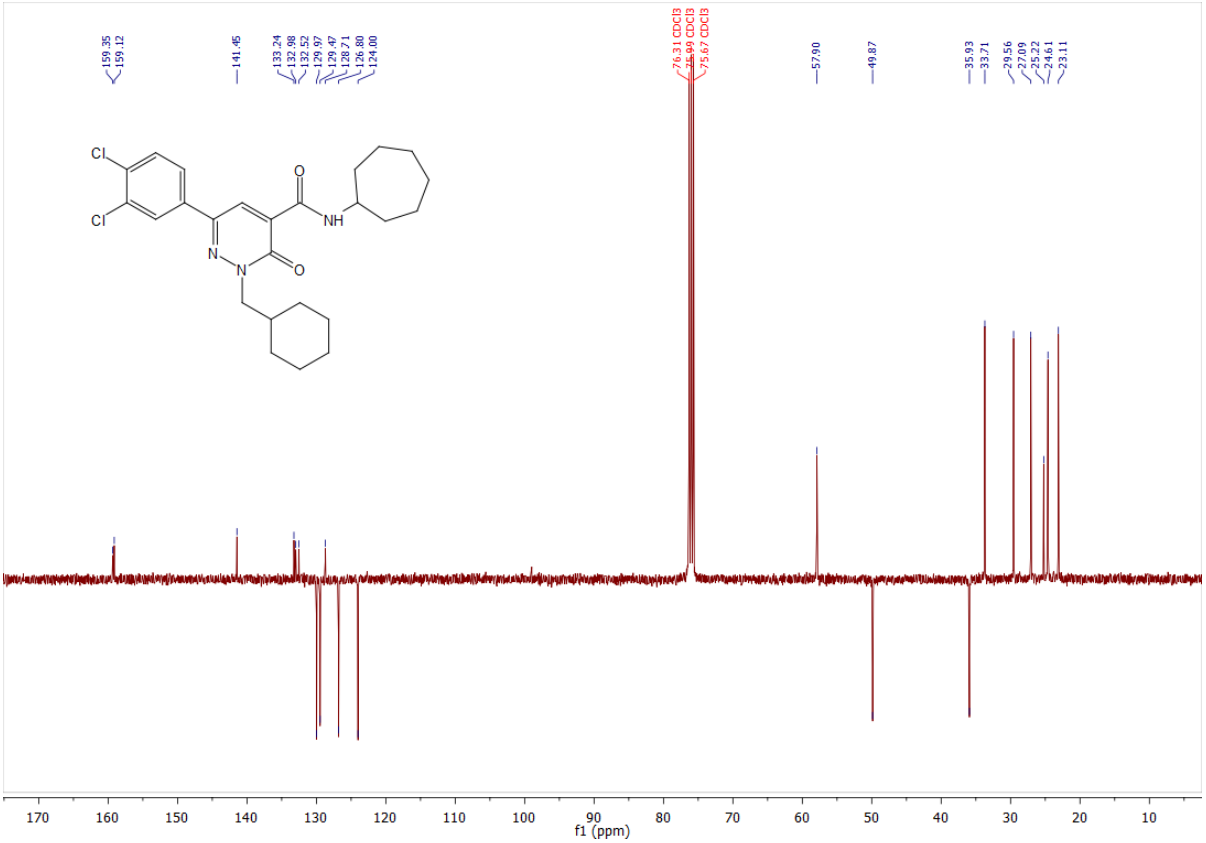

Figure S19. ^{1}H-NMR ($CDCl_3$, 400 MHz): Compound **11**

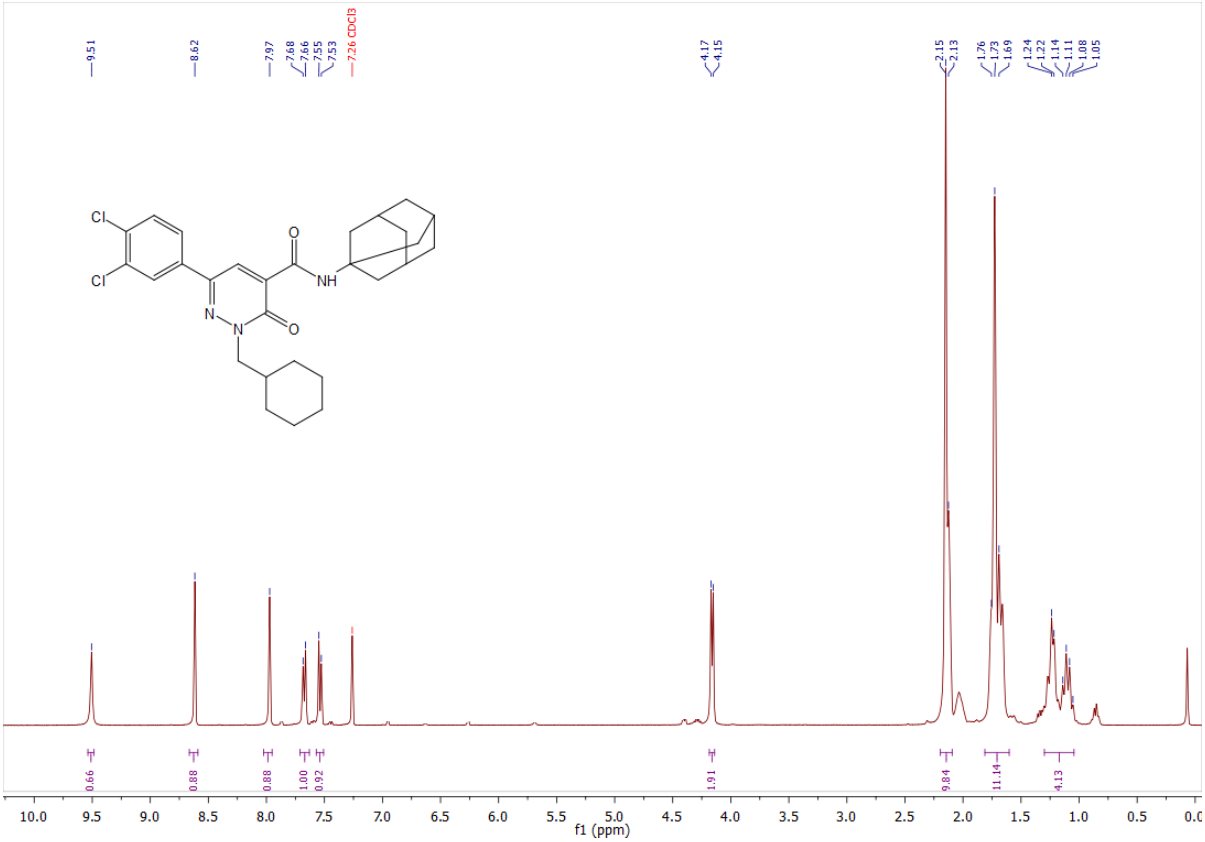

Figure S20. ^{13}C-APT ($CDCl_3$, 101 MHz): Compound **11**

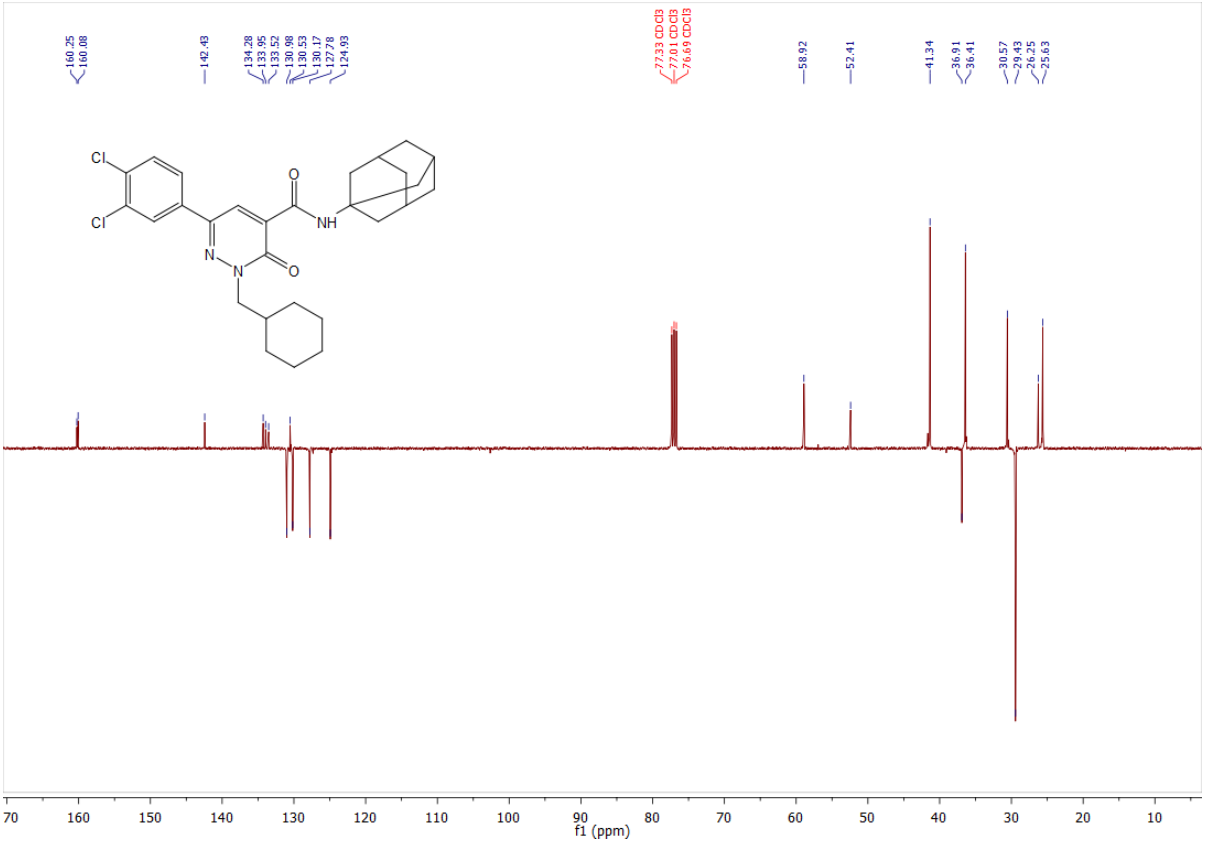

Figure S21. ^{1}H-NMR ($CDCl_3$, 400 MHz): Compound **12**

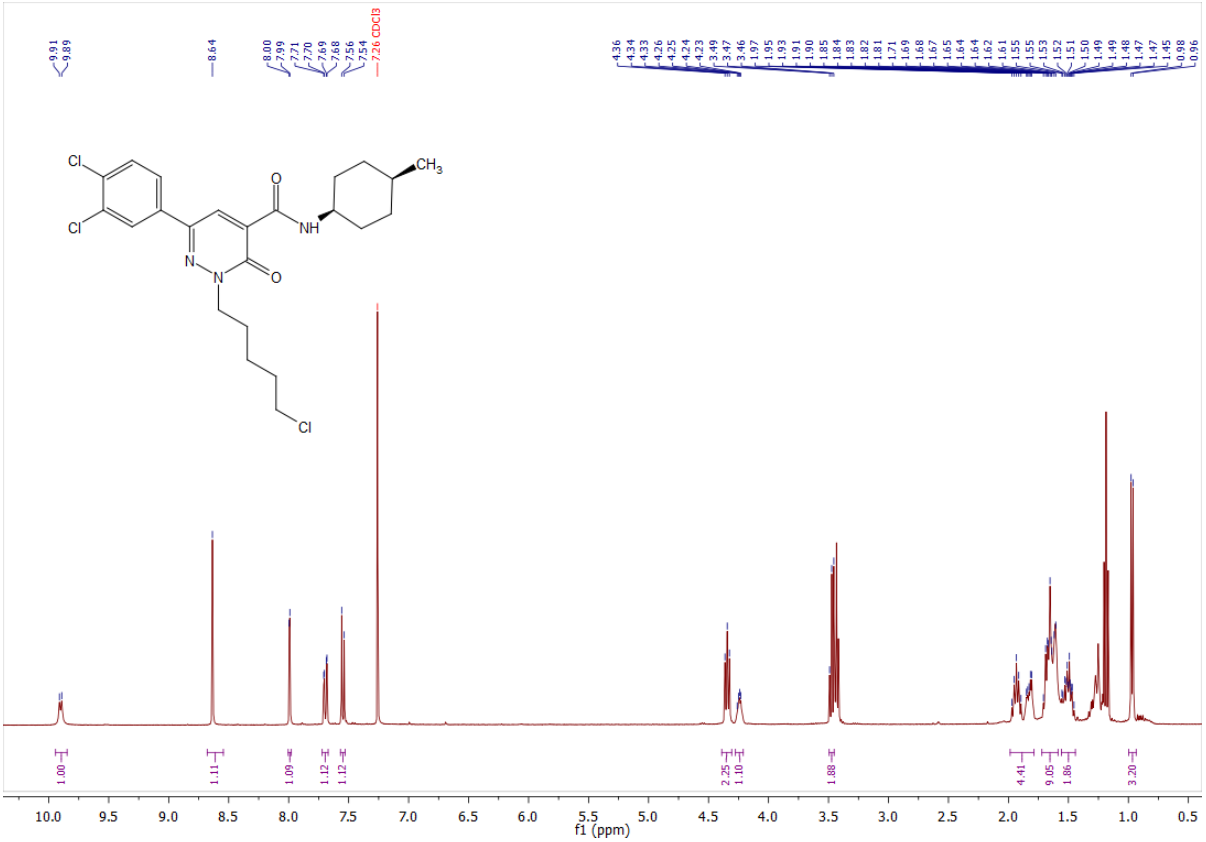

Figure S22. ^{13}C-APT ($CDCl_3$, 101 MHz): Compound **12**

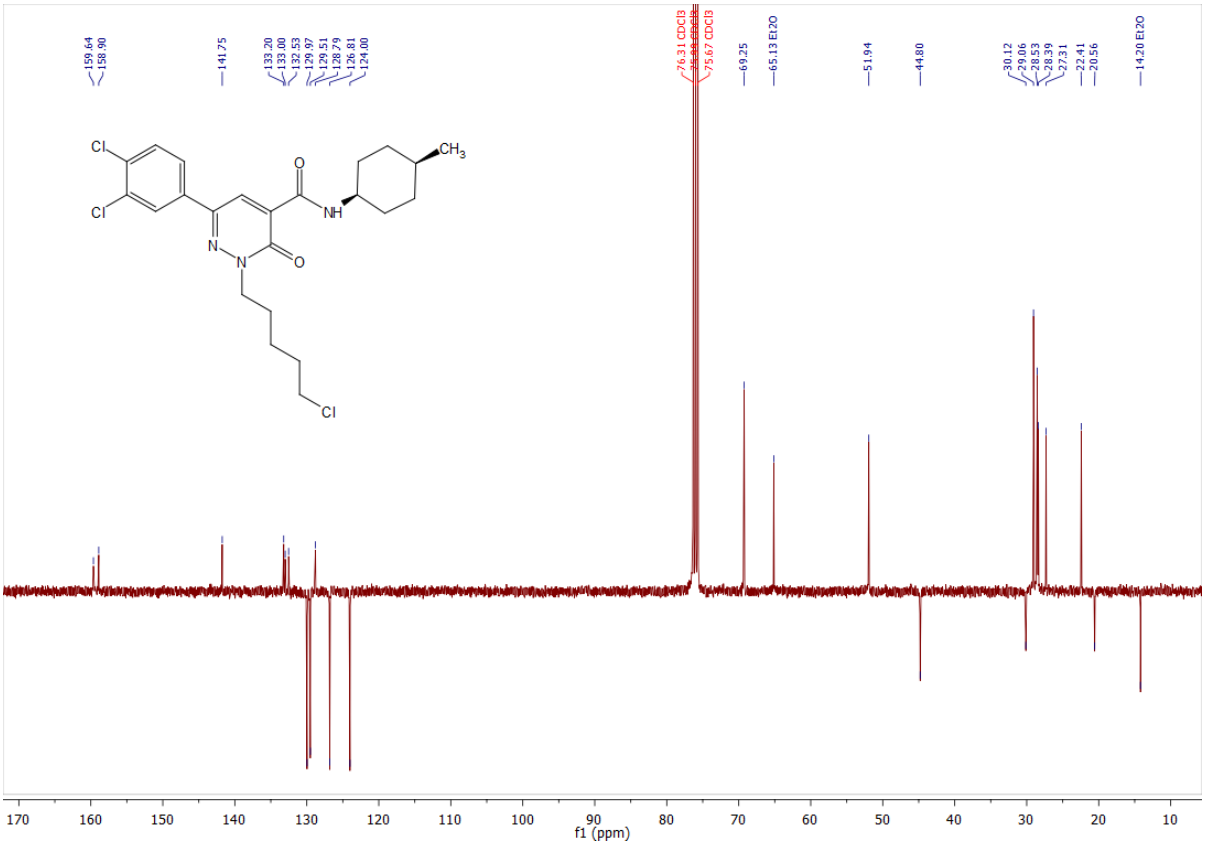

Figure S23. ^{1}H-NMR ($CDCl_3$, 400 MHz): Compound **14**

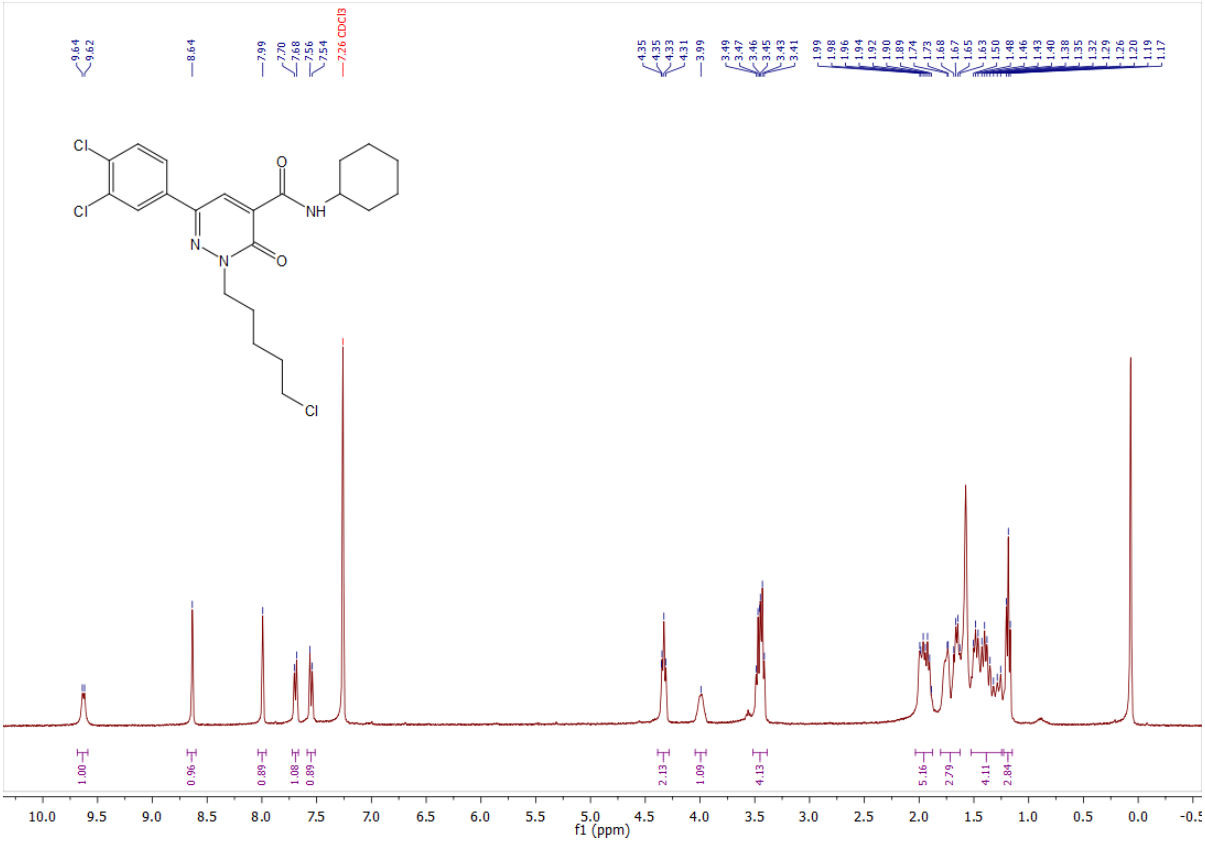

Figure S24. ^{13}C-APT ($CDCl_3$, 101 MHz): Compound **14**

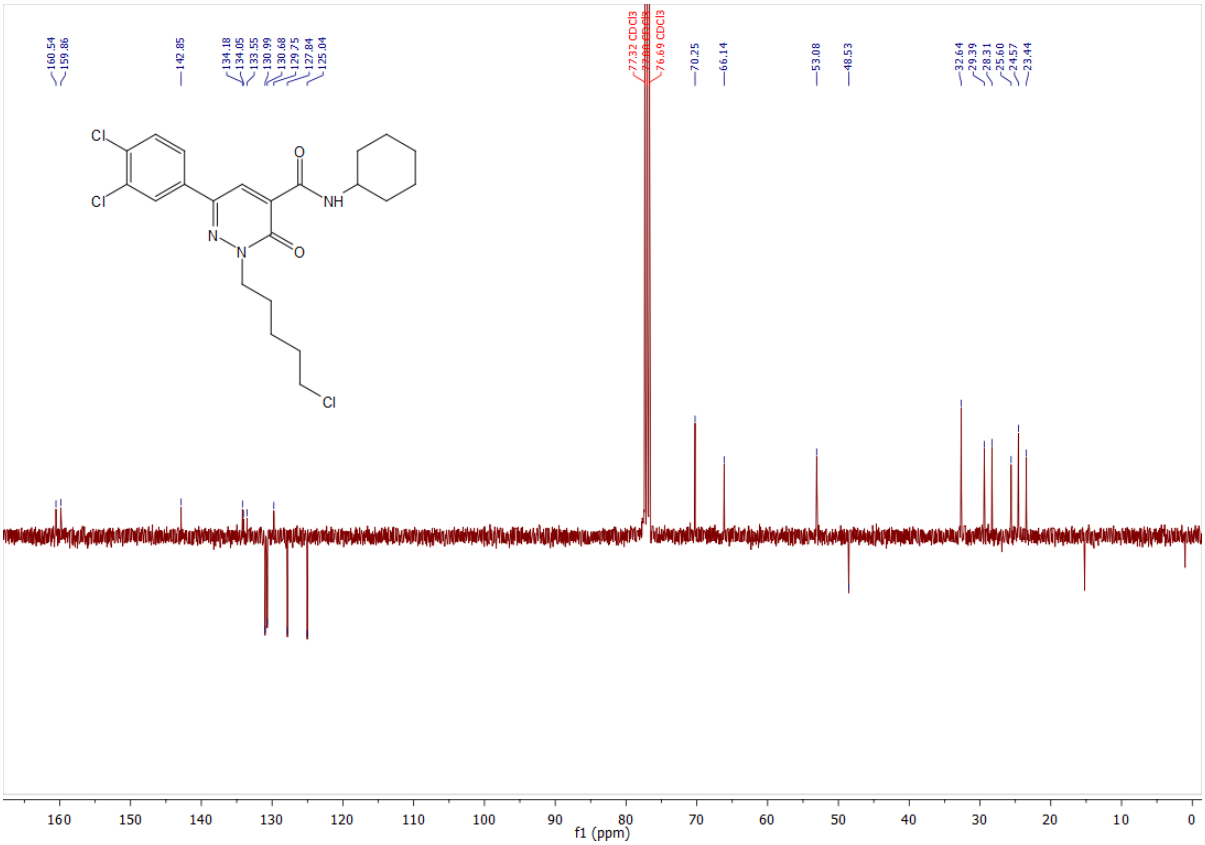

Figure S25. ^{1}H-NMR ($CDCl_3$, 400 MHz): Compound **15**

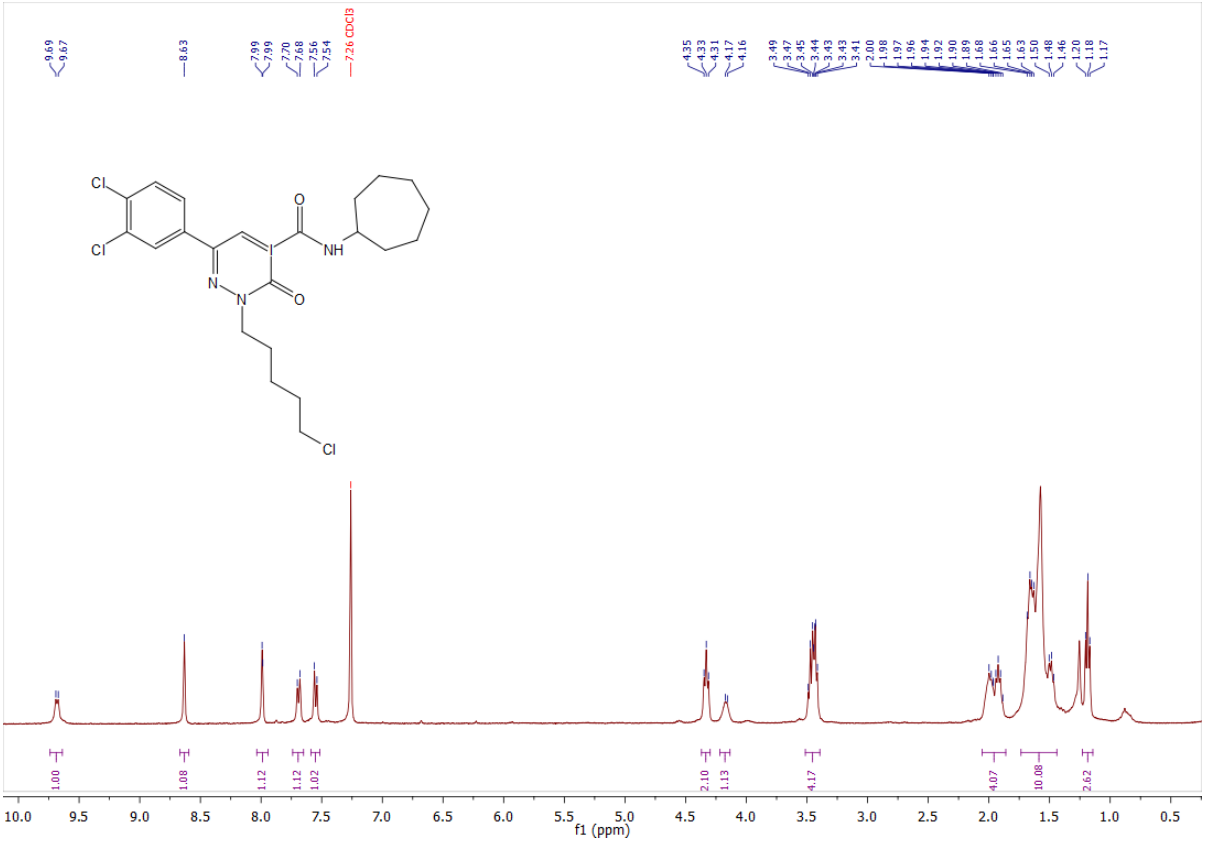

Figure S26. ^{13}C-APT ($CDCl_3$, 101 MHz): Compound **15**

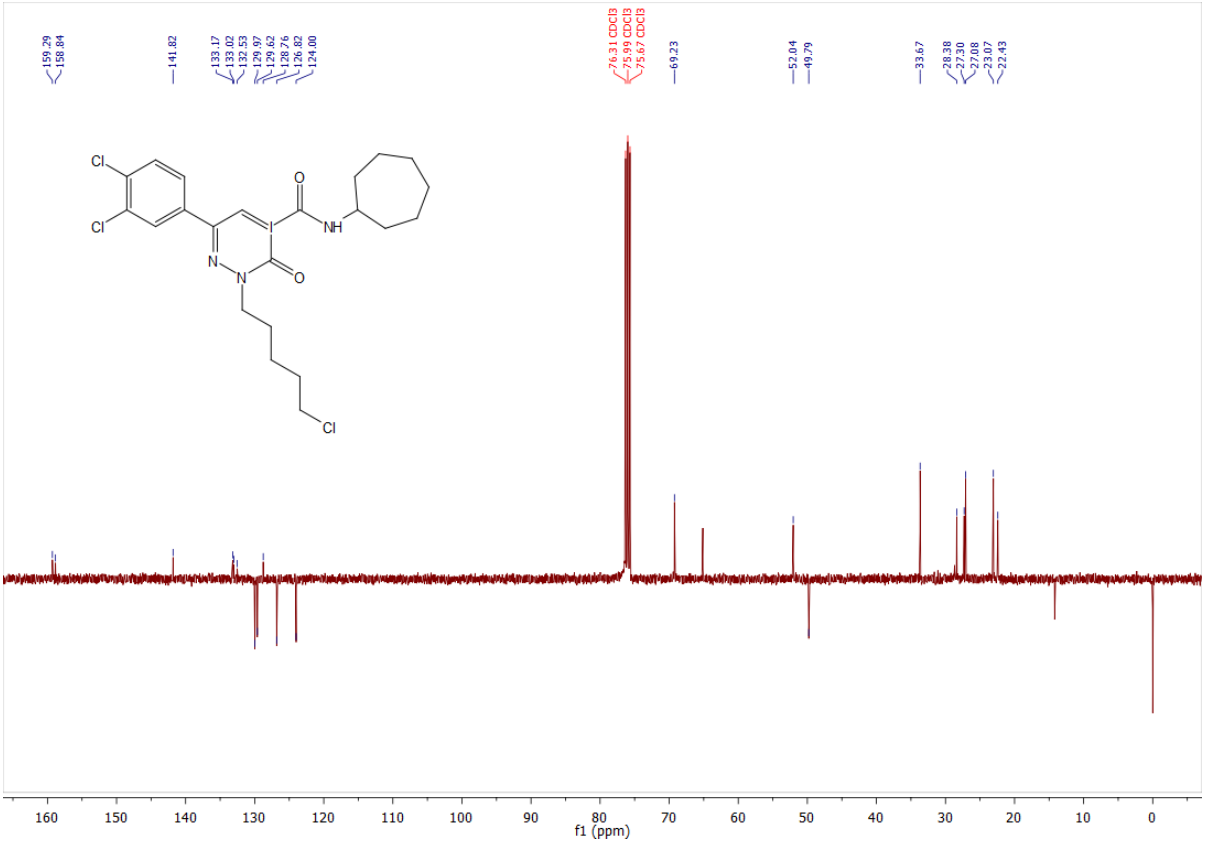

Figure S27. ^{1}H-NMR ($CDCl_3$, 400 MHz): Compound **16**

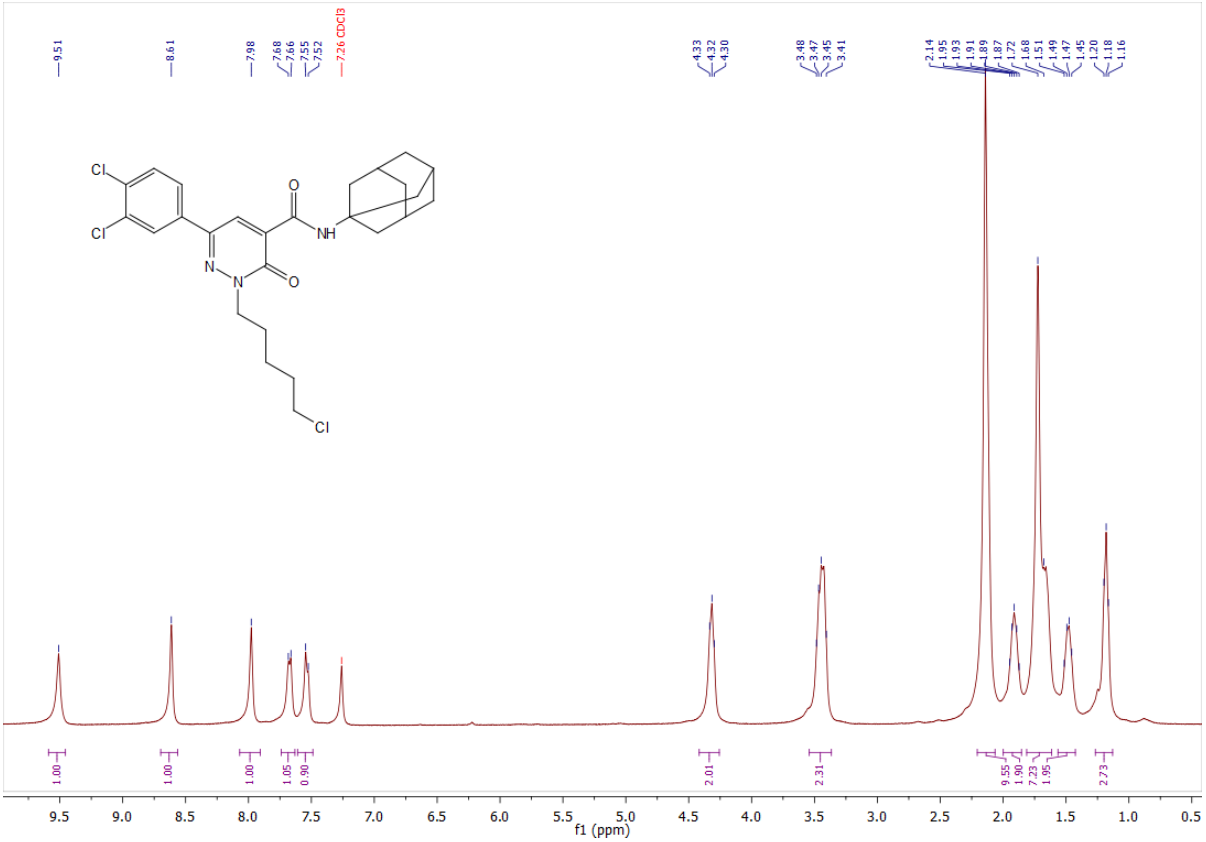

Figure S28. ^{13}C-APT ($CDCl_3$, 101 MHz): Compound **16**

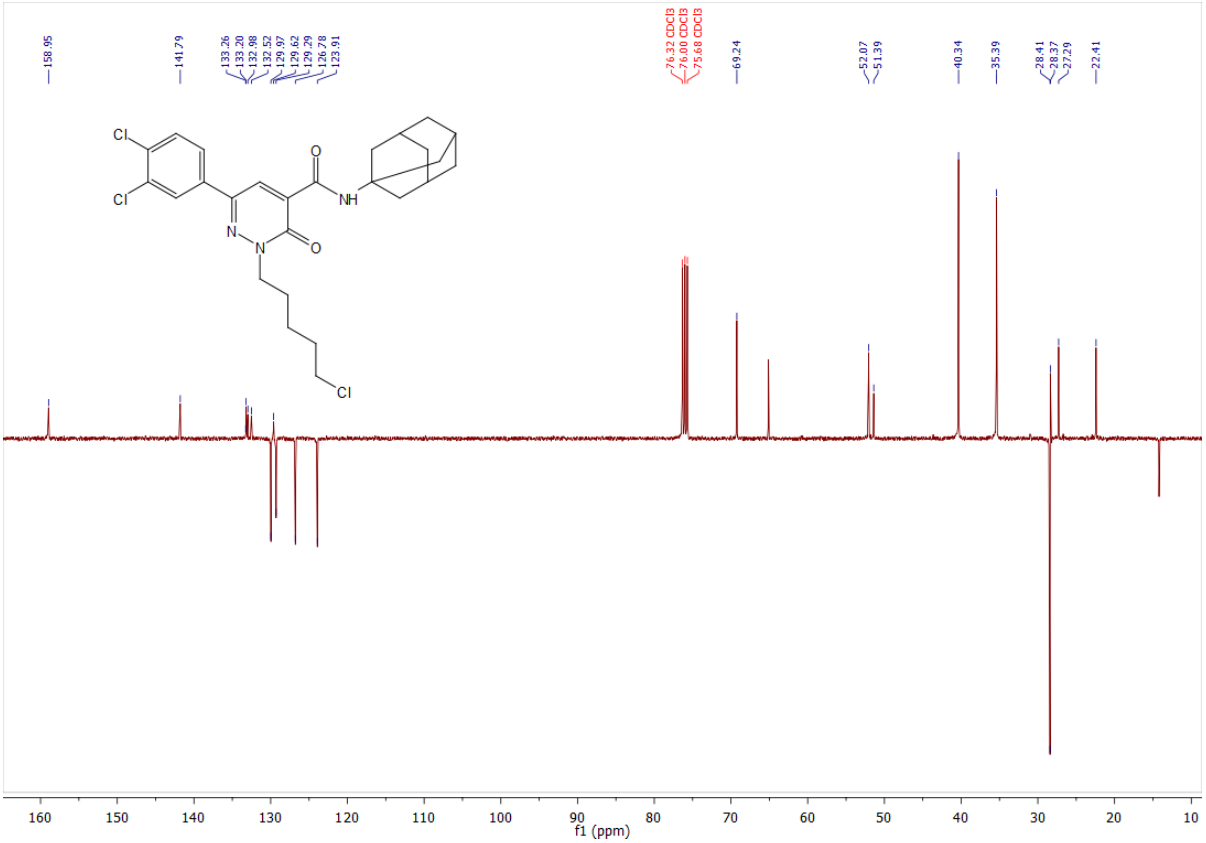

Figure S29. ^{1}H-NMR ($CDCl_3$, 400 MHz): Compound **17**

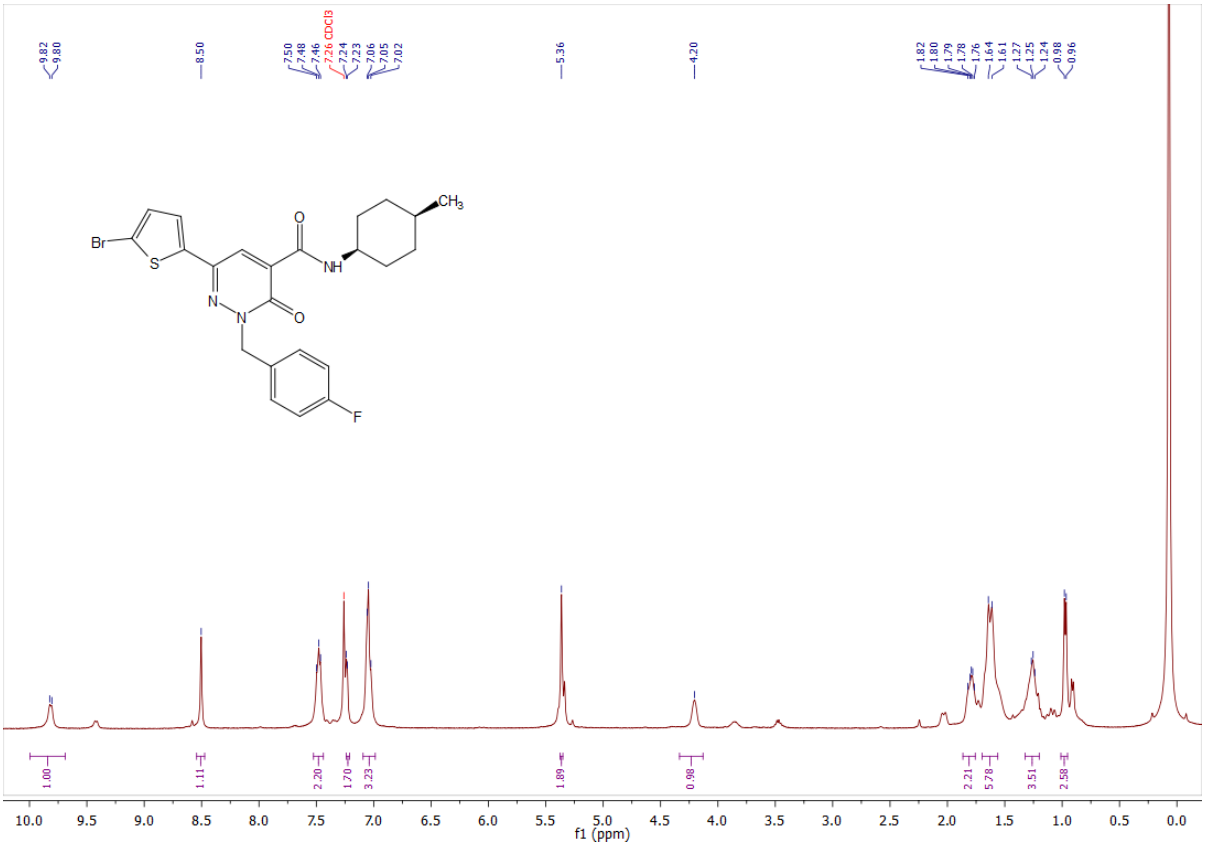

Figure S30. ^{13}C-APT ($CDCl_3$, 101 MHz): Compound **17**

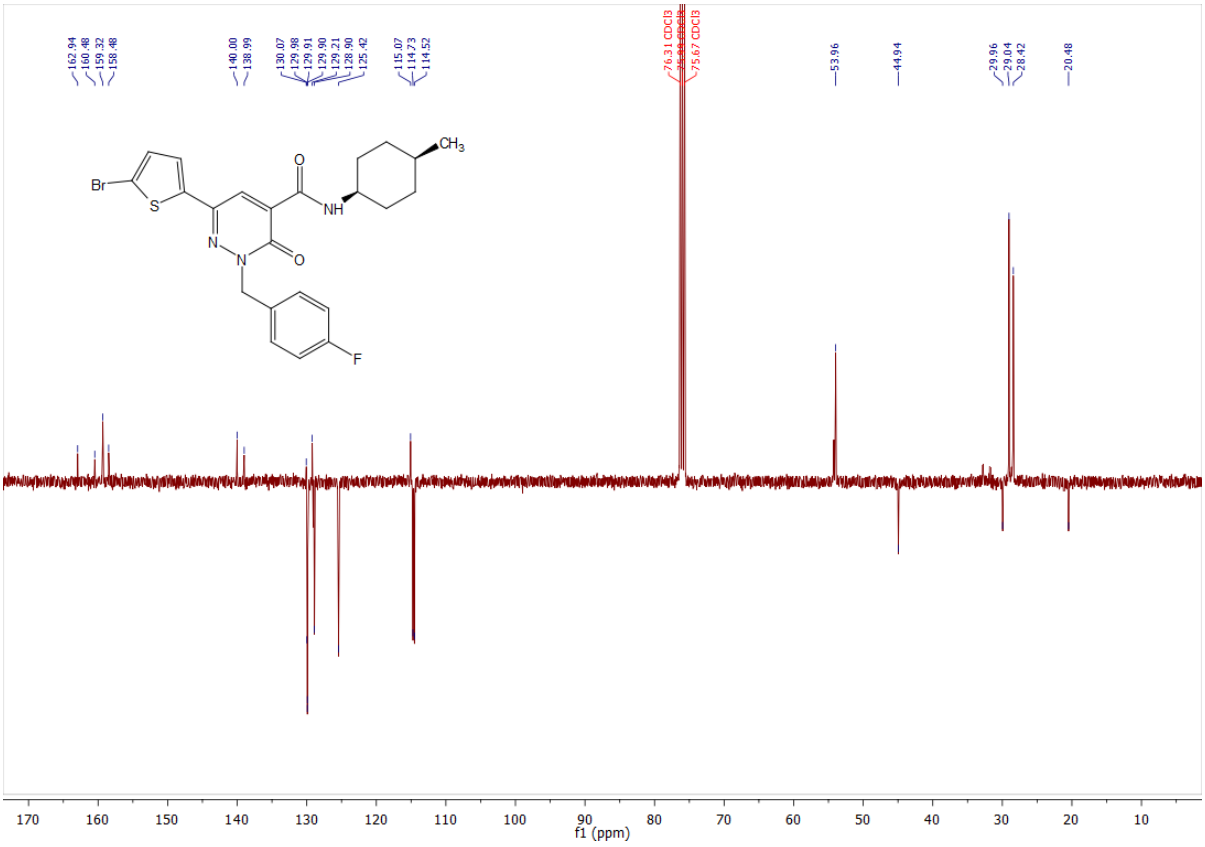

Figure S31. ^{1}H-NMR ($CDCl_3$, 400 MHz): Compound **18**

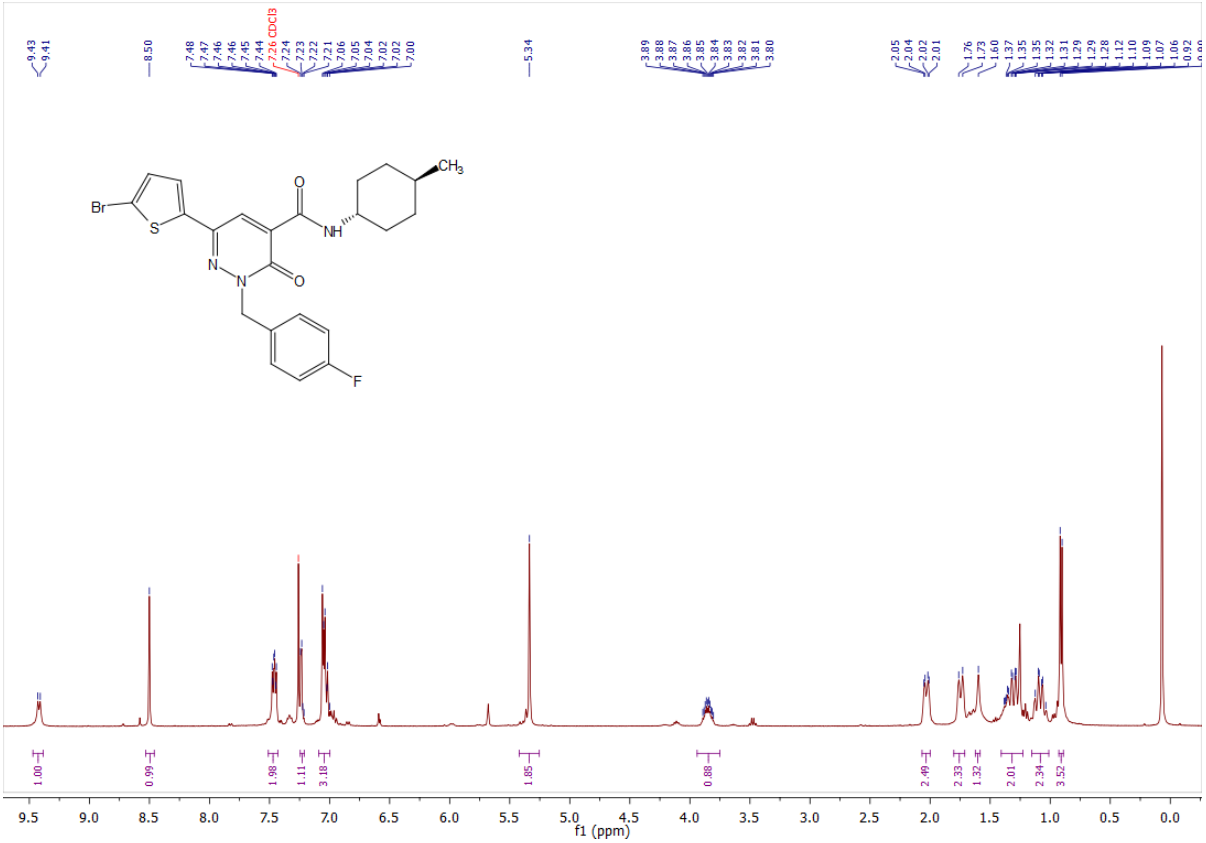

Figure S32. ^{13}C-APT ($CDCl_3$, 101 MHz): Compound **18**

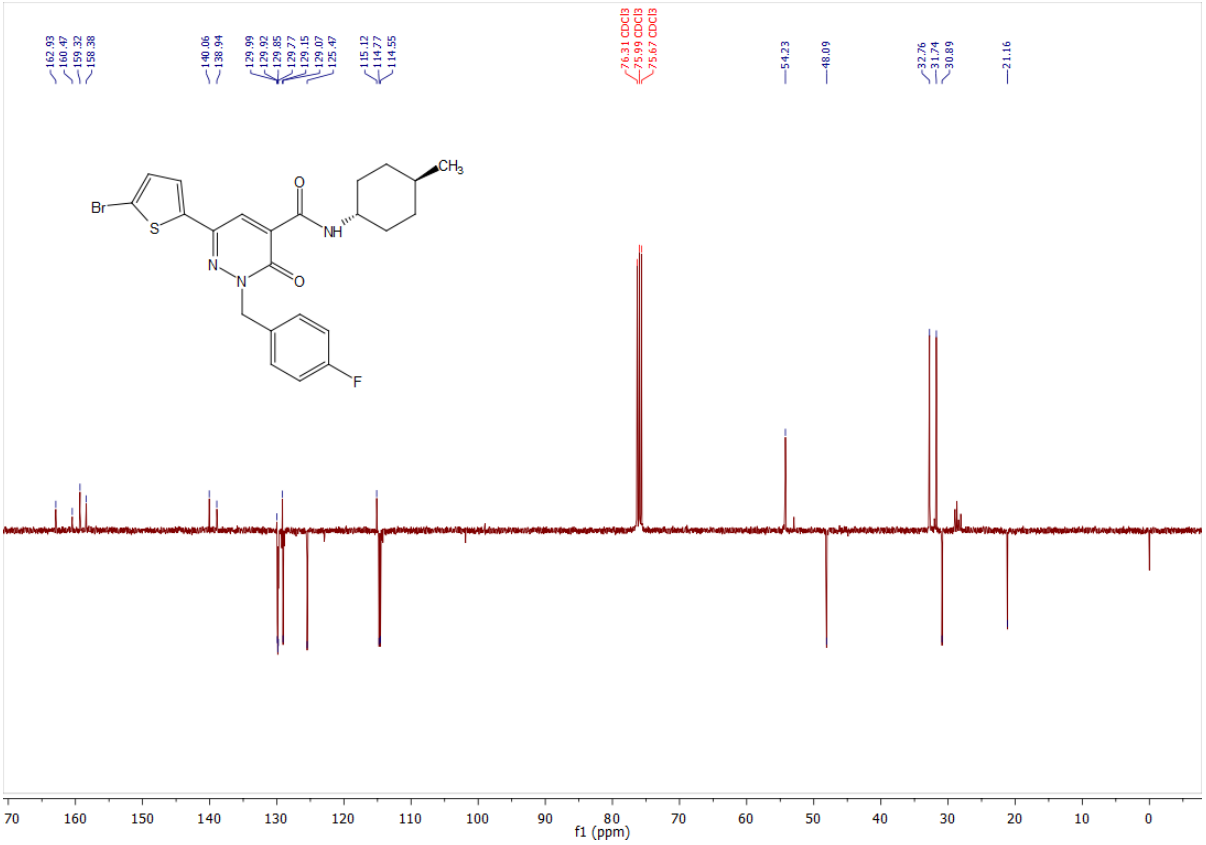

Figure S33. ^{1}H-NMR ($CDCl_3$, 400 MHz): Compound **19**

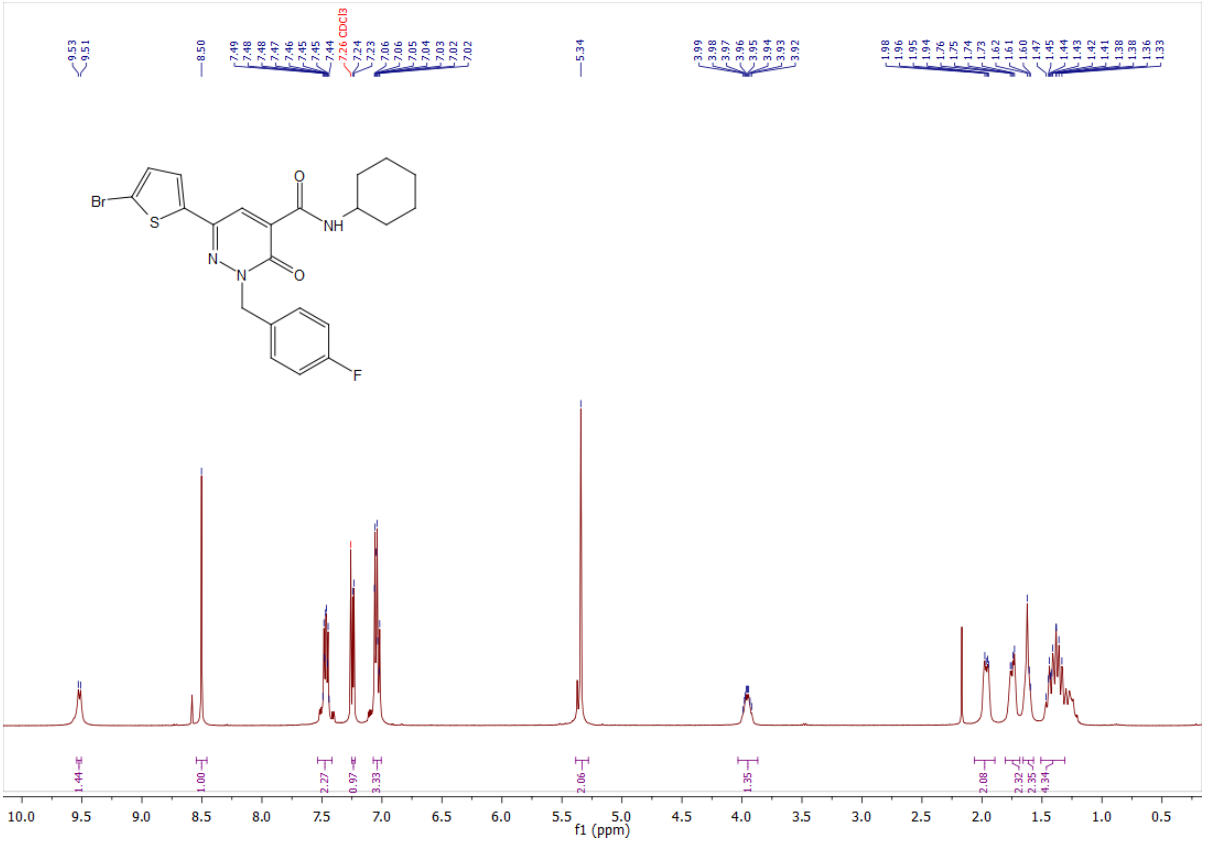

Figure S34. ^{13}C-APT ($CDCl_3$, 101 MHz): Compound **19**

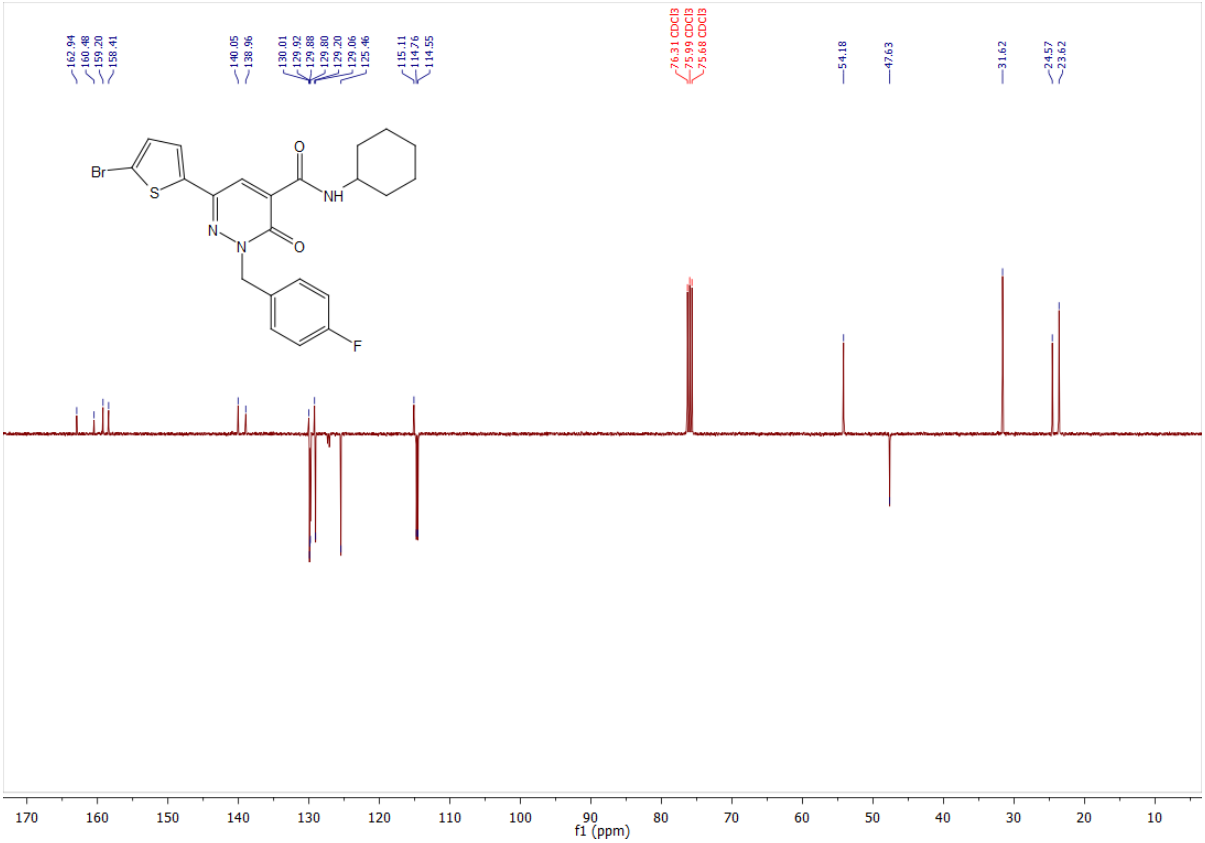

Figure S35. ^{1}H-NMR ($CDCl_3$, 400 MHz): Compound **20**

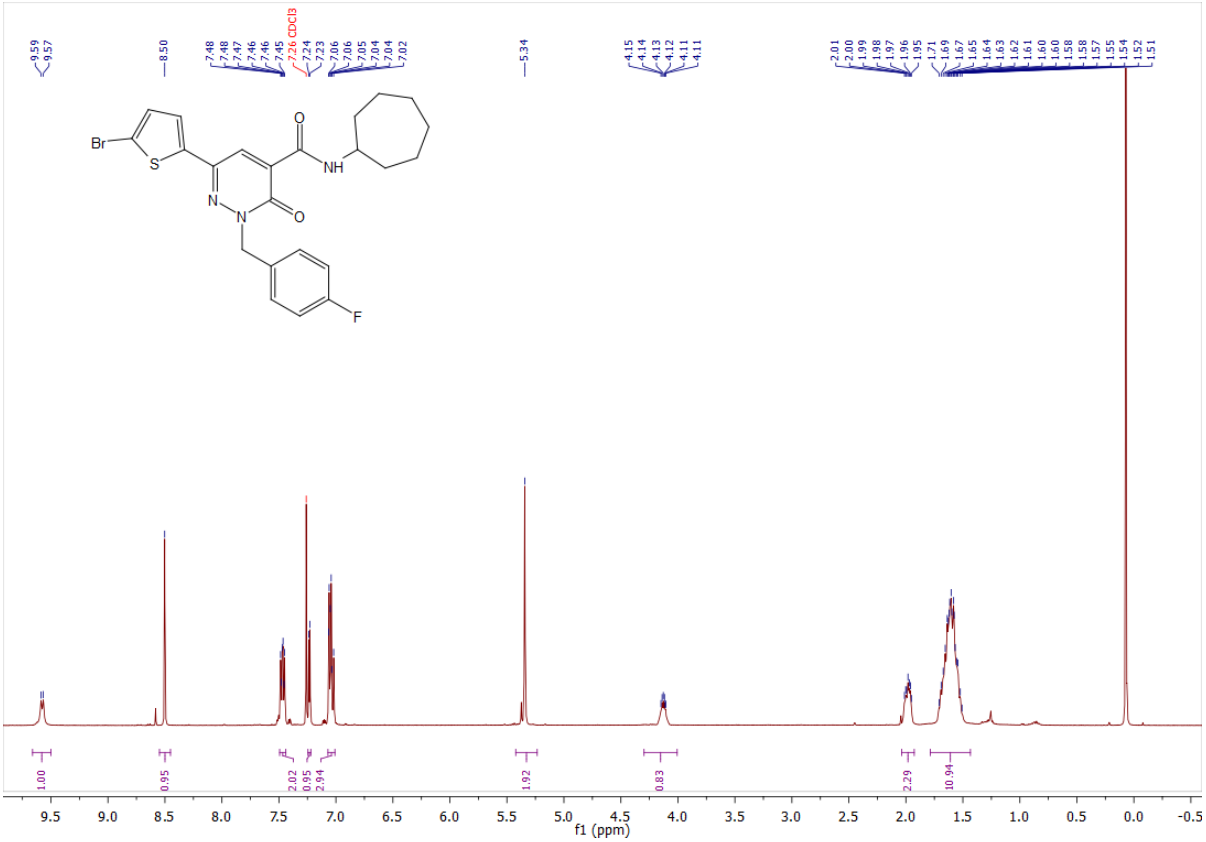

Figure S36. ^{13}C-APT ($CDCl_3$, 101 MHz): Compound **20**

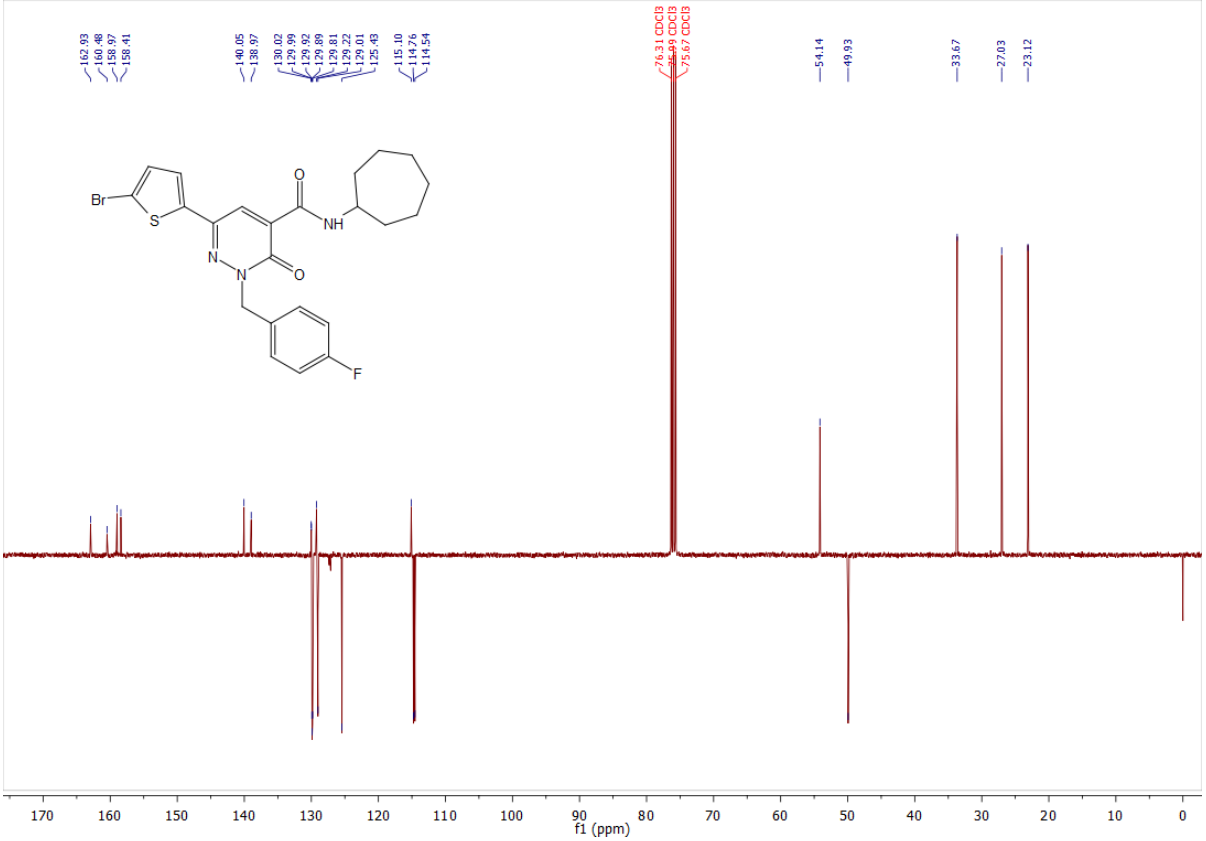

Figure S37. ^{1}H-NMR ($CDCl_3$, 400 MHz): Compound **21**

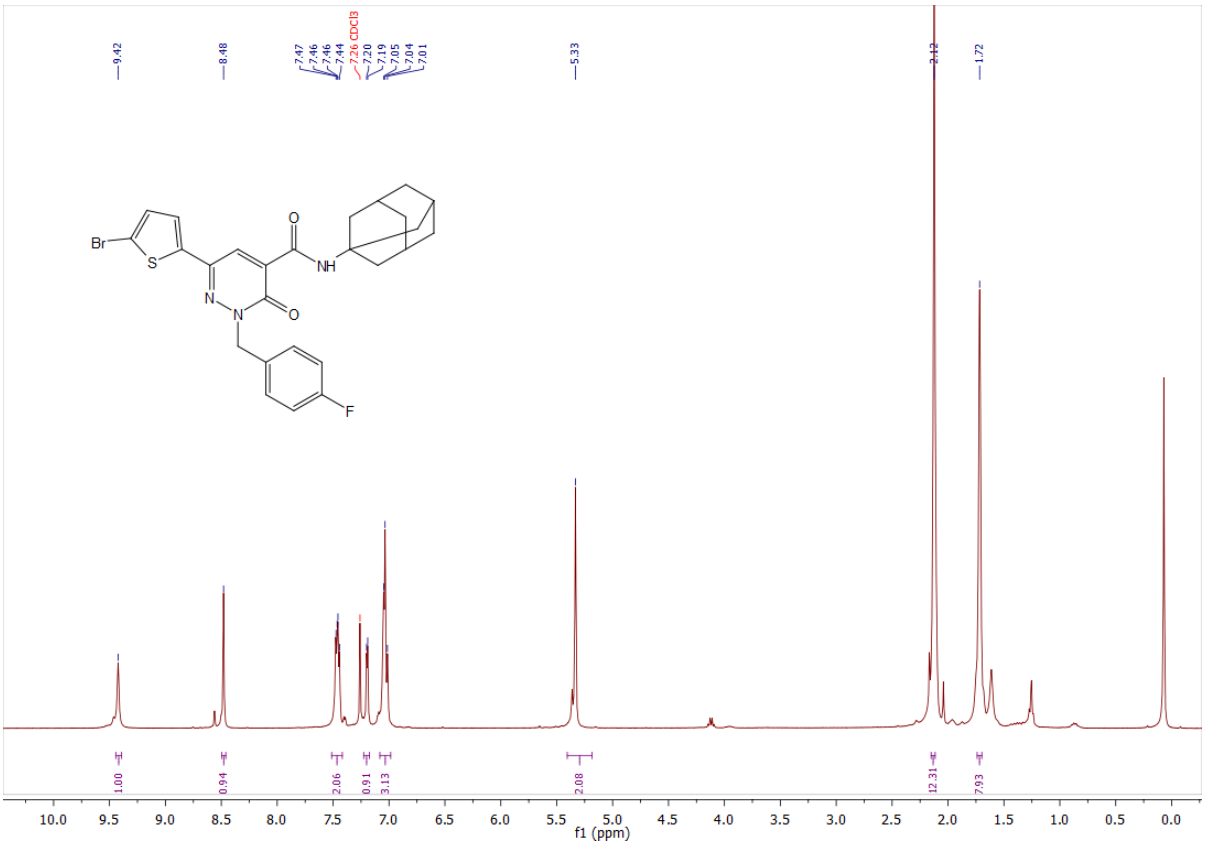

Figure S38. ^{13}C-APT ($CDCl_3$, 101 MHz): Compound **21**

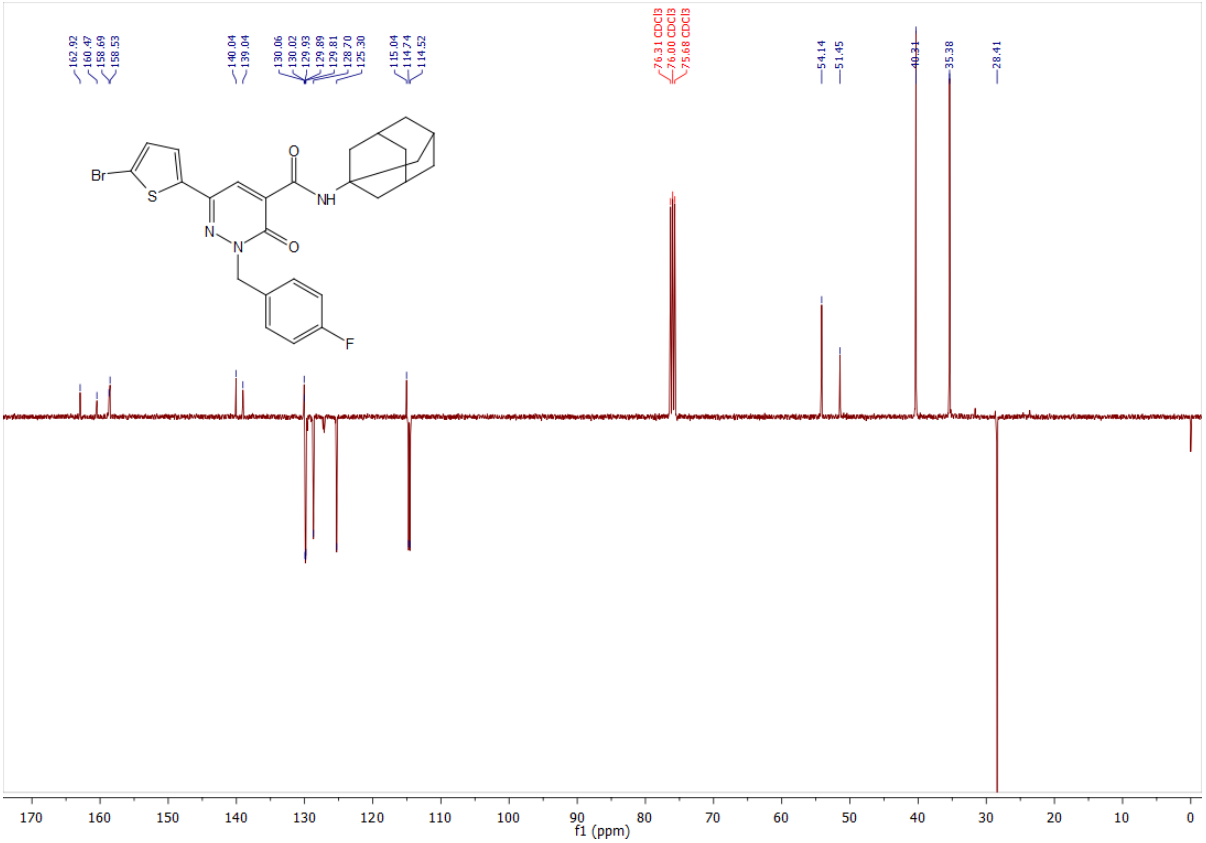

Figure S39. ^{1}H-NMR ($CDCl_3$, 400 MHz): Compound **22**

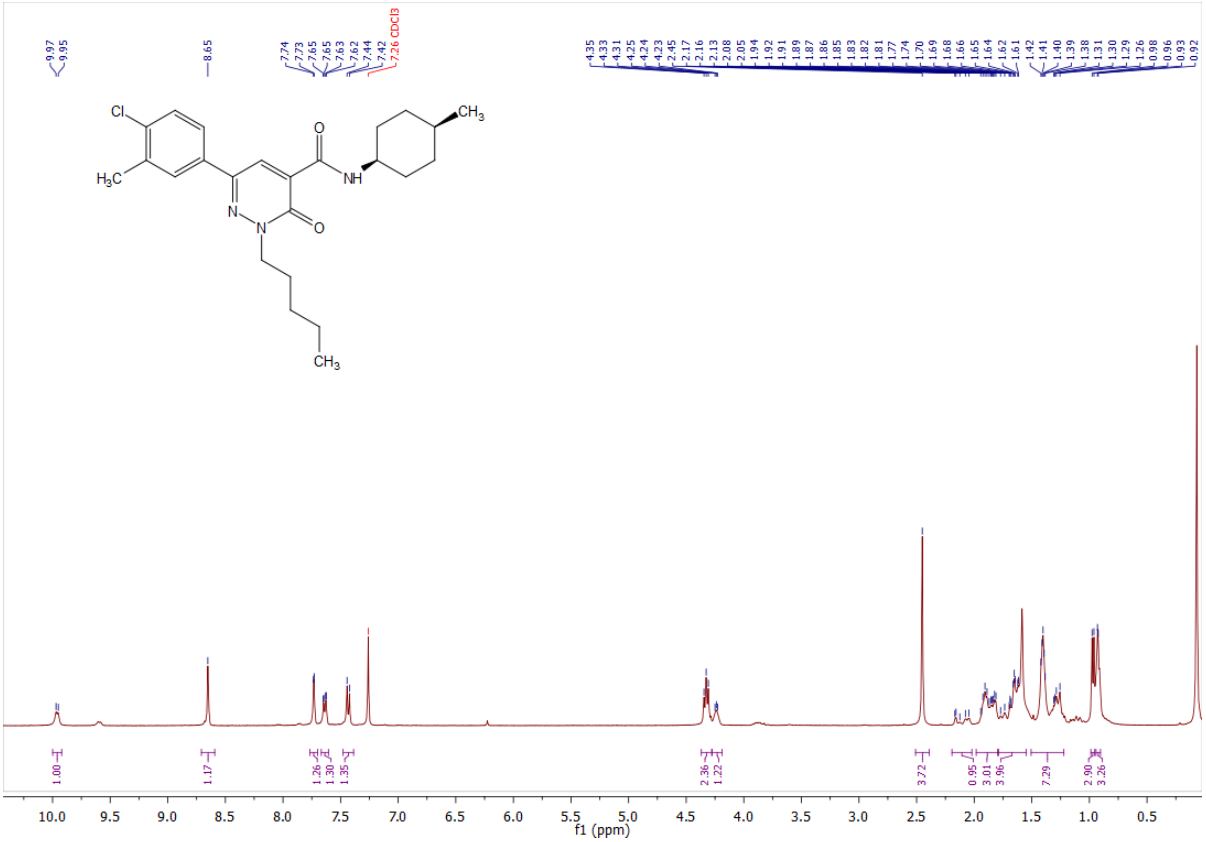

Figure S40. ^{13}C-APT ($CDCl_3$, 101 MHz): Compound **22**

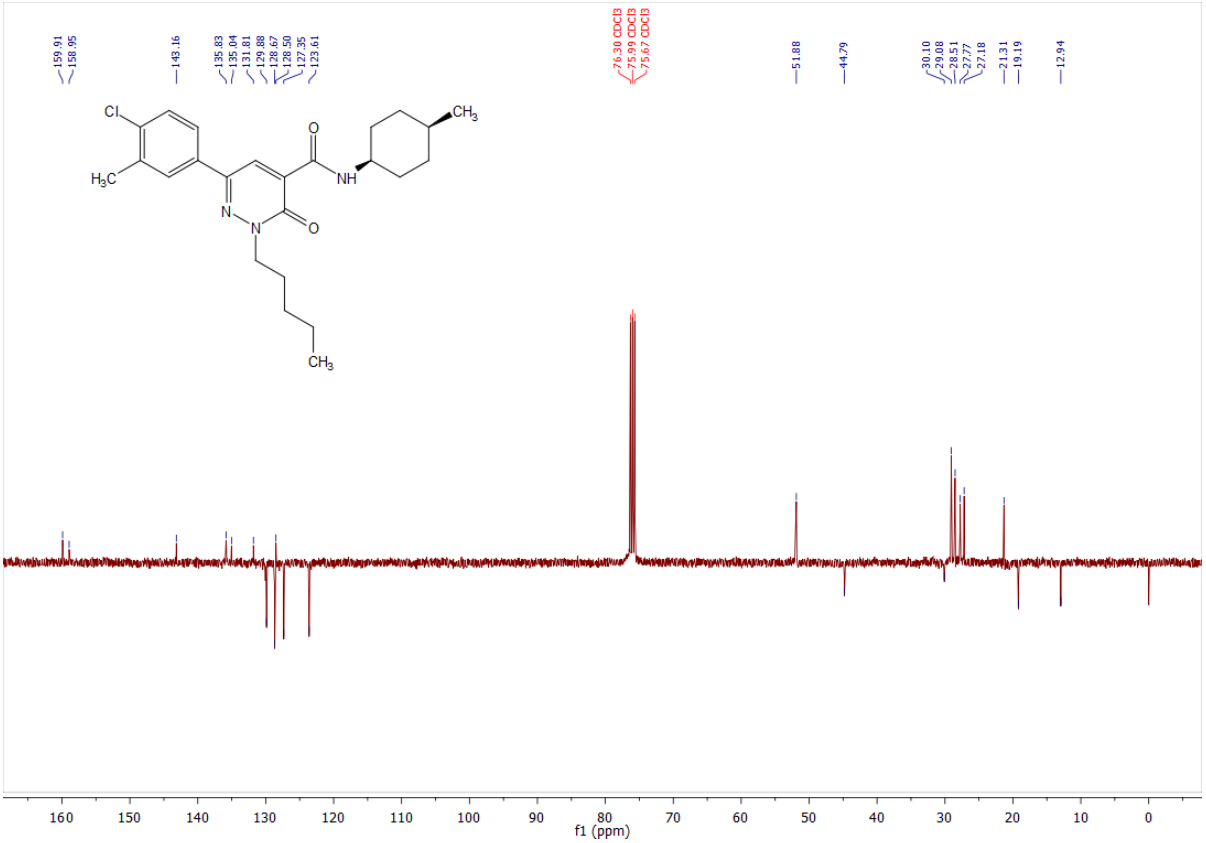

Figure S41. ^{1}H-NMR ($CDCl_3$, 400 MHz): Compound **23**

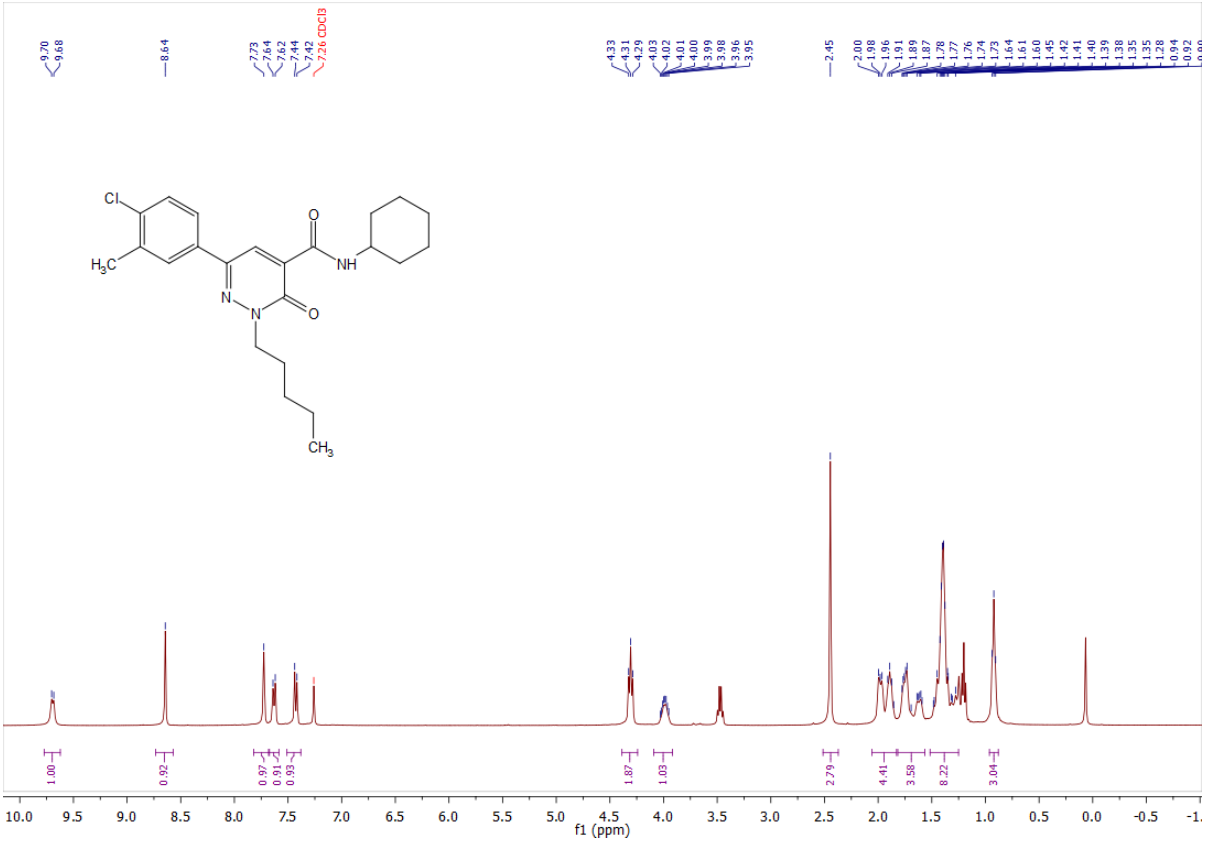

Figure S42. ^{13}C-APT ($CDCl_3$, 101 MHz): Compound **23**

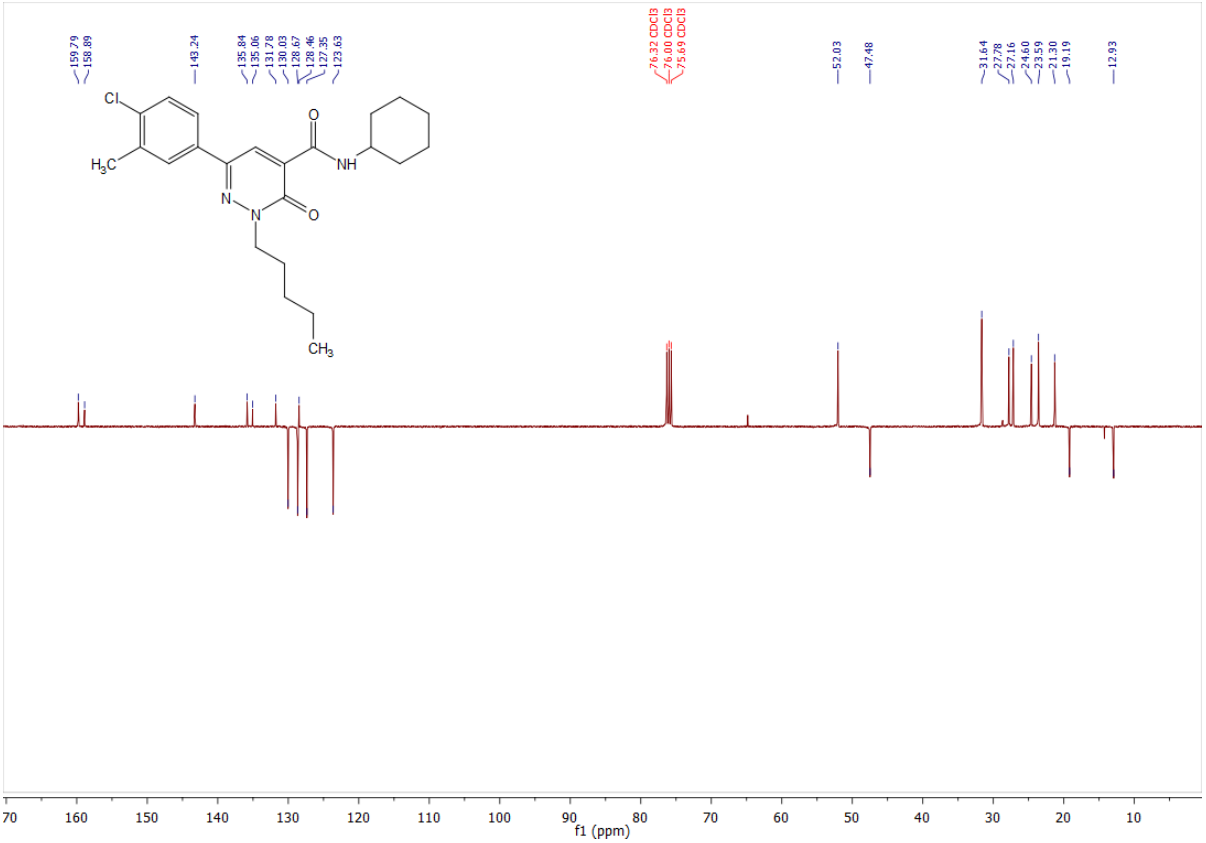

SR144528 docked at the CB_2R

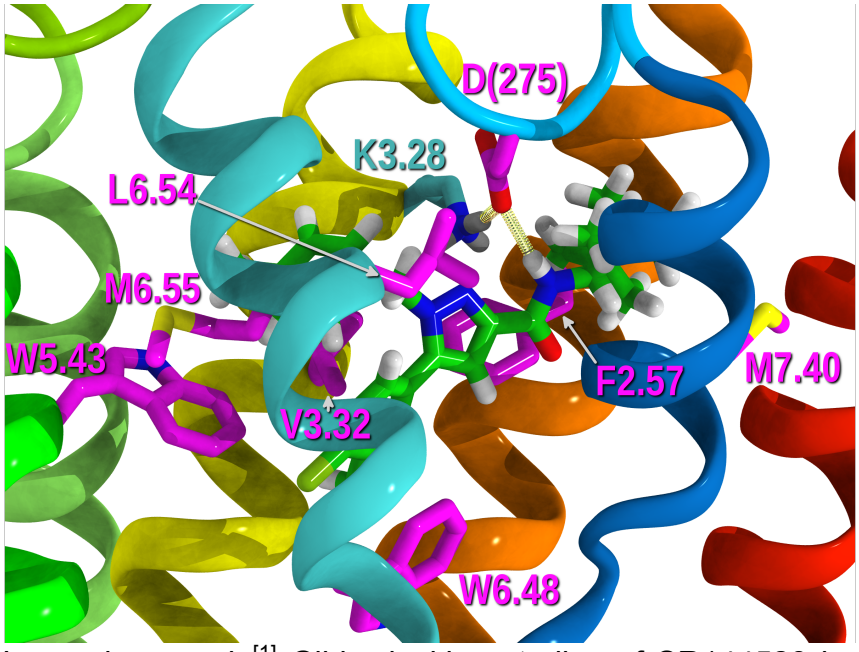

Figure S43. In previous work,[1] Glide docking studies of SR144528 in our CB_2 inactive state model suggested that this ligand spans the CB_2 binding pocket and uses the EC-3 loop residue, D275, as its primary interaction site. These results are consistent with CB_2 mutation and modeling studies (see Discussion in[1]). SR144528 also has favorable electrostatic and van der Waals interactions with K3.28(109) and forms a number of aromatic stacking interactions at CB_2. The chloromethylphenyl ring forms an offset parallel stack with W6.48(258) and also forms a T-stack with W5.43(194). Additionally, the methylbenzyl ring forms a tilted-T aromatic stack with W5.43(194). SR144528 has favorable van der Waals interactions with F2.57(87). V3.32(113), M6.55(265), L6.54(264), M7.40(286), and V6.51(261) (not shown).

Pairwise Interaction Energies for Compound 22 at CB_2R State Model

Table S1. Compound 22/CB_2R Complex			
Residue	**VdW (kcal/mol)**	**Electrostatic (kcal/mol)**	**Total Energy (kcal/mol)**
M6.55	-0.40	-7.43	-7.82
K3.28	-5.61	-2.08	-7.69
F2.57	-0.19	-7.28	-7.47
S7.39	-3.16	-4.04	-7.20
S6.58	0.47	-4.12	-3.65
I3.29	-0.06	-3.23	-3.28
L6.54	0.21	-3.06	-2.85
V6.51	-0.09	-2.50	-2.59
F2.61	0.03	-2.40	-2.38
Q(276)	0.03	-2.25	-2.23
L6.59	0.13	-2.33	-2.20
V3.32	0.06	-2.23	-2.17
W5.43	-0.18	-1.83	-2.01
L7.43	0.01	-2.00	-1.99
C7.42	0.12	-2.05	-1.93
M7.40	-0.04	-1.57	-1.61
P(178)	-0.08	-1.25	-1.34
W6.48	0.04	-1.26	-1.22
S2.60	0.09	-1.17	-1.07
A7.36	0.00	-0.83	-0.83
F2.64	-0.03	-0.64	-0.67
D(275)	0.04	-0.54	-0.49
R(177)	-0.03	-0.38	-0.41
T3.33	-0.01	-0.35	-0.36
C7.38	-0.05	-0.21	-0.26
T(272)	-0.07	-0.18	-0.25
L4.61	-0.02	-0.23	-0.25
A2.58	-0.01	-0.22	-0.23
I7.44	0.03	-0.17	-0.14
Y5.39	0.39	-0.39	0.00
Conf Expense			0.89
Grand Total			**-65.70**

In silico ADMET parameters

Table S2. Metabolism parameters of compounds **2**-**24**, SR144528 and HU308 calculated with the admetSAR prediction tool.

Compound	*CYP substrate/ inhibition* [a]		
	CYP3A4	**CYP2C9**	**CYP2D6**
2	substrate/ inhibitor	non-substrate/ non-inhibitor	non-substrate/ non-inhibitor
3	substrate/ inhibitor	non-substrate/ non-inhibitor	non-substrate/ non-inhibitor
4	substrate/ inhibitor	non-substrate/ non-inhibitor	non-substrate/ non-inhibitor
5	substrate/ inhibitor	non-substrate/ non-inhibitor	non-substrate/ non-inhibitor
6	substrate/ inhibitor	non-substrate/ non-inhibitor	non-substrate/ non-inhibitor
7	substrate/ inhibitor	non-substrate/ non-inhibitor	non-substrate/ non-inhibitor
8	substrate/ inhibitor	non-substrate/ non-inhibitor	non-substrate/ non-inhibitor
9	substrate/ inhibitor	non-substrate/ non-inhibitor	non-substrate/ non-inhibitor
10	substrate/ inhibitor	non-substrate/ non-inhibitor	non-substrate/ non-inhibitor
11	substrate/ inhibitor	non-substrate/ non-inhibitor	non-substrate/ non-inhibitor
12	substrate/ inhibitor	non-substrate/ non-inhibitor	non-substrate/ non-inhibitor
13	substrate/ inhibitor	non-substrate/ non-inhibitor	non-substrate/ non-inhibitor
14	substrate/ inhibitor	non-substrate/ non-inhibitor	non-substrate/ non-inhibitor
15	substrate/ inhibitor	non-substrate/ non-inhibitor	non-substrate/ non-inhibitor
16	substrate/ inhibitor	non-substrate/ non-inhibitor	non-substrate/ non-inhibitor
17	substrate/ inhibitor	non-substrate/ non-inhibitor	non-substrate/ non-inhibitor
18	substrate/ inhibitor	non-substrate/ non-inhibitor	non-substrate/ non-inhibitor
19	substrate/ inhibitor	non-substrate/ non-inhibitor	non-substrate/ non-inhibitor
20	substrate/ inhibitor	non-substrate/ non-inhibitor	non-substrate/ non-inhibitor

21	substrate/ inhibitor	non-substrate/ non-inhibitor	non-substrate/ non-inhibitor
22	substrate/ non-inhibitor	non-substrate/ non-inhibitor	non-substrate/ non-inhibitor
23	substrate/ non-inhibitor	non-substrate/ non-inhibitor	non-substrate/ non-inhibitor
24	substrate/ non-inhibitor	non-substrate/ non-inhibitor	non-substrate/ non-inhibitor
HU308	substrate/ inhibitor	non-substrate/ non-inhibitor	non-substrate/ non-inhibitor
SR144528	substrate/ inhibitor	non-substrate/ non-inhibitor	non-substrate/ non-inhibitor

[a] Molecules were classified as substrate or non-substrate, and inhibitor or non-inhibitor of the different CYP450 isoforms according to the previously published classification.[2,3]

Table S3. Toxicity parameters of compounds **2**-**24**, SR144528 and HU308 calculated with the admetSAR prediction tool.

Compound	*hERG blockage*[a]	*AMES toxicity*[b]	*Carcinogenicity*[c]	*Acute oral toxicity*[d]	*LD_{50} in rat*[d]
2	weak inhibitor	nontoxic	noncarcinogenic	III	2.4069
3	weak inhibitor	nontoxic	noncarcinogenic	III	2.4069
4	weak inhibitor	nontoxic	noncarcinogenic	III	2.4055
5	weak inhibitor	nontoxic	noncarcinogenic	III	2.4057
6	weak inhibitor	nontoxic	noncarcinogenic	III	2.4241
7	weak inhibitor	nontoxic	noncarcinogenic	III	2.3635
8	weak inhibitor	nontoxic	noncarcinogenic	III	2.3635
9	weak inhibitor	nontoxic	noncarcinogenic	III	2.3485
10	weak inhibitor	nontoxic	noncarcinogenic	III	2.3573
11	weak inhibitor	nontoxic	noncarcinogenic	III	2.4033
12	weak inhibitor	nontoxic	noncarcinogenic	III	2.4032
13	weak inhibitor	nontoxic	noncarcinogenic	III	2.4032
14	weak inhibitor	nontoxic	noncarcinogenic	III	2.4107
15	weak inhibitor	nontoxic	noncarcinogenic	III	2.4138
16	weak inhibitor	nontoxic	noncarcinogenic	III	2.4413
17	weak inhibitor	nontoxic	noncarcinogenic	III	2.4397
18	weak inhibitor	nontoxic	noncarcinogenic	III	2.4397
19	weak inhibitor	nontoxic	noncarcinogenic	III	2.3862
20	weak inhibitor	nontoxic	noncarcinogenic	III	2.3977
21	weak inhibitor	nontoxic	noncarcinogenic	III	2.4819
22	weak inhibitor	nontoxic	noncarcinogenic	III	2.5119
23	weak inhibitor	nontoxic	noncarcinogenic	III	2.5182
24	weak inhibitor	nontoxic	noncarcinogenic	III	2.5259
HU308	weak inhibitor	nontoxic	noncarcinogenic	III	2.4010
SR144528	weak inhibitor	nontoxic	noncarcinogenic	III	2.5354

[a]Predicted hERG blockade: compounds are classified according to the previously published approach[4] as: strong inhibitors (IC_{50}<1 mM), 'non-blockers' exhibiting moderate (1– 10 mM) and weak (IC_{50}>10 mM) inhibitors. [b] AMES mutagenicity predictions are based on the previously published benchmark data set.[5,6] [c] Carcinogenic potency is divided into three classes, labeled as "Danger", "Warning" and "Non-required", according to the TD_{50} (median toxic dose) values. Carcinogenic compounds with TD_{50} ≤ 10 mg/kg body wt/day were assigned as "Danger", those with TD_{50} > 10 mg/kg body wt/day were assigned as "Warning", and non-carcinogenic chemicals were assigned as "Non-required".[7,8] [d] Compounds are classified into four categories based on the criterion of US EPA (Category I contains compounds with LD_{50} values less than or equal to 50 mg/kg. Category II contains compounds with LD_{50} values greater than 50 mg/kg but less than 500 mg/kg. Category III includes compounds with LD_{50} values greater than 500 mg/kg but less than 5000 mg/kg. Category IV consisted of compounds with LD_{50} values greater than 5000 mg/kg).[9] [e] Predicted median lethal dose (LD_{50}) in rat model (Acute Toxicity in mol/kg).[10]

References:

[1] E. Kotsikorou, F. Navas, 3rd, M. J. Roche, A. F. Gilliam, B. F. Thomas, H. H. Seltzman, P. Kumar, Z. H. Song, D. P. Hurst, D. L. Lynch, P. H. Reggio, *J. Med. Chem.* **2013**, *56*, 6593-6612.

[2] F. Cheng, Y. Yu, J. Shen, L. Yang, W. Li, G. Liu, P. W. Lee, Y. Tang, *J. Chem. Inf. Mod.* **2011**, *51*, 996-1011.

[3] M. Carbon-Mangels, M. C. Hutter, *Mol. Inform.* **2011**, *30*, 885-895.

[4] R. L. Marchese Robinson, R. C. Glen, J. B. O. Mitchell, *Mol. Inform.* **2011**, *30*, 443-458.

[5] C. Xu, F. Cheng, L. Chen, Z. Du, W. Li, G. Liu, P. W. Lee, Y. Tang, *J. Chem. Inf. Mod.* **2012**, *52*, 2840-2847.

[6] K. Hansen, S. Mika, T. Schroeter, A. Sutter, A. T. Laak, S. H. Thomas, N. Heinrich, K. R. Müller, *J. Chem. Inf. Mod.* **2009**, *49*, 2077-2081.

[7] X. Li, Z. Du, J. Wang, Z. Wu, W. Li, G. Liu, X. Shen, Y. Tang, *Mol. Inform.* **2015**, *34*, 228-235.

[8] A. Lagunin, D. Filimonov, A. Zakharov, W. Xie, Y. Huang, F. Zhu, T. Shen, J. Yao, V. Poroikov, *QSAR Comb. Sci.* **2009**, *28*, 806-810.

[9] X. Li, L. Chen, F. Cheng, Z. Wu, H. Bian, C. Xu, W. Li, G. Liu, X. Shen, Y. Tang, *J. Chem. Inf. Mod.* **2014**, *54*, 1061-1069.

[10] H. Zhu, T. M. Martin, L. Ye, A. Sedykh, D. M. Young, A. Tropsha, *Chem. Res. Toxicol.* **2009**, *22*, 1913-1921.